



**Defense Threat Reduction Agency
8725 John J. Kingman Road, MS 6201
Fort Belvoir, VA 22060-6201**



DTRA-TR-12-002

TECHNICAL REPORT

Probabilistic Analysis of Radiation Doses for Shore-Based Individuals in Operation Tomodachi

Approved for public release: distribution is unlimited.

May 2013

Prepared by:

Operation Tomodachi Registry,
Dose Assessment and Recording Working Group



For:

Assistant Secretary of Defense for Health Affairs

This page intentionally left blank.

REPORT DOCUMENTATION PAGE				Form Approved OMB No. 0704-0188	
<small>Public reporting burden for this collection of information is estimated to average 1 hour per response, including the time for reviewing instructions, searching data sources, gathering and maintaining the data needed, and completing and reviewing the collection of information. Send comments regarding this burden estimate or any other aspect of this collection of information, including suggestions for reducing this burden to Washington Headquarters Service, Directorate for Information Operations and Reports, 1215 Jefferson Davis Highway, Suite 1204, Arlington, VA 22202-4302, and to the Office of Management and Budget, Paperwork Reduction Project (0704-0188) Washington, DC 20503.</small>					
PLEASE DO NOT RETURN YOUR FORM TO THE ABOVE ADDRESS.					
1. REPORT DATE (DD-MM-YYYY) 21-05-2013		2. REPORT TYPE Technical report		3. DATES COVERED (From - To)	
4. TITLE AND SUBTITLE Probabilistic Analysis of Radiation Doses for Shore-Based Individuals in Operation Tomodachi				5a. CONTRACT NUMBER HDTRA1-07-C-0015	
				5b. GRANT NUMBER	
				5c. PROGRAM ELEMENT NUMBER	
6. AUTHOR(S) Chehata, Mondher; Dunavant, Jason D.; Mason, Carol; McKenzie-Carter, Michael; Singer, Harvey.				5d. PROJECT NUMBER	
				5e. TASK NUMBER	
				5f. WORK UNIT NUMBER	
7. PERFORMING ORGANIZATION NAME(S) AND ADDRESS(ES) Science Applications International Corporation (SAIC), 1710 SAIC Drive McLean, VA 22102				8. PERFORMING ORGANIZATION REPORT NUMBER DTRA-TR-12-002	
9. SPONSORING/MONITORING AGENCY NAME(S) AND ADDRESS(ES) Nuclear Technology Department, Attn: Dr. Paul Blake Defense Threat Reduction Agency 8725 John J. Kingman Road, Mail Stop 6201 Fort Belvoir, VA 22060-6201				10. SPONSOR/MONITOR'S ACRONYM(S) DTRA J9-NTSN	
				11. SPONSORING/MONITORING AGENCY REPORT NUMBER	
12. DISTRIBUTION AVAILABILITY STATEMENT Approved for public release: distribution is unlimited.					
13. SUPPLEMENTARY NOTES					
14. ABSTRACT Department of Defense affiliated individuals were potentially exposed to radioactive materials as a result of the Fukushima Daiichi Nuclear Power Station radiological releases that followed the earthquake and tsunami on March 11, 2011. This report presents the findings of the probabilistic analysis for the radiation dose assessment of the DoD shore-based population. The main objective of this analysis was to assess whether the doses calculated using deterministic methods as reported in DTRA-TR-12-001 "Radiation Dose Assessments for Shore-Based Individuals in Operation Tomodachi" (Cassata et al., 2012) met the goal of being sufficiently conservative to apply to all or nearly all shore-based individuals.					
15. SUBJECT TERMS Operation Tomodachi, Radiation Dose, Department of Defense, Japan, Fukushima, Earthquake, Tsunami					
16. SECURITY CLASSIFICATION OF:			17. LIMITATION OF ABSTRACT U	18. NUMBER OF PAGES 156	19a. NAME OF RESPONSIBLE PERSON Dr. Paul K. Blake
a. REPORT U	b. ABSTRACT U	c. THIS PAGE U			19b. TELEPHONE NUMBER (Include area code) 703 767-3384

UNIT CONVERSION TABLE
U.S. customary units to and from international units of measurement*

U.S. Customary Units	<div> <div>Multiply by </div> <div> Divide by[†]</div> </div>	International Units
Length/Area/Volume		
inch (in)	2.54 $\times 10^{-2}$	meter (m)
foot (ft)	3.048 $\times 10^{-1}$	meter (m)
mile (mi, international)	1.609 344 $\times 10^3$	meter (m)
micron (μ)	1 $\times 10^{-6}$	meter (m)
angstrom (\AA)	1 $\times 10^{-10}$	meter (m)
barn (b)	1 $\times 10^{-28}$	square meter (m^2)
gallon (gal, U.S. liquid)	3.785 412 $\times 10^{-3}$	cubic meter (m^3)
Mass/Density/Force		
pound (lb)	4.535 924 $\times 10^{-1}$	kilogram (kg)
atomic mass unit (AMU)	1.660 539 $\times 10^{-27}$	kilogram (kg)
pound-mass per cubic foot (lb ft^{-3})	1.601 846 $\times 10^1$	kilogram per cubic meter (kg m^{-3})
pound-mass-square foot (lb ft^2)	4.214 011 $\times 10^{-2}$	kilogram-square meter (kg m^2)
pound-force (lbf avoirdupois)	4.448 222	newton (N)
pound-force inch (lbf in)	1.129 848 $\times 10^{-1}$	newton-meter (N m)
pound-force per inch (lbf in^{-1})	1.751 268 $\times 10^2$	newton per meter (N m^{-1})
Energy/Power		
electronvolt (eV)	1.602 177 $\times 10^{-19}$	joule (J)
erg	1 $\times 10^{-7}$	joule (J)
kiloton (kT) (TNT equivalent)	4.184 $\times 10^{12}$	joule (J)
British thermal unit (Btu) (thermochemical)	1.054 350 $\times 10^3$	joule (J)
foot-pound-force (ft lbf)	1.355 818	joule (J)
calorie (cal) (thermochemical)	4.184	joule (J)
Pressure		
kip per square inch (ksi)	6.894 757 $\times 10^6$	pascal (Pa)
atmosphere (atm)	1.013 250 $\times 10^5$	pascal (Pa)
bar	1 $\times 10^5$	pascal (Pa)
torr (Torr)	1.333 224 $\times 10^2$	pascal (Pa)
pound-force per square inch (psi)	6.894 757 $\times 10^3$	pascal (Pa)
Angle/Temperature/Time		
hour (h)	3.6 $\times 10^3$	second (s)
degree of arc ($^\circ$)	1.745 329 $\times 10^{-2}$	radian (rad)
degree Fahrenheit ($^\circ\text{F}$)	$[\text{T}(^\circ\text{F}) - 32]/1.8$	degree Celsius ($^\circ\text{C}$)
degree Fahrenheit ($^\circ\text{F}$)	$[\text{T}(^\circ\text{F}) + 459.67]/1.8$	kelvin (K)
Radiation[`]		
curie (Ci) (activity of radionuclides)	3.7 $\times 10^{10}$	per second ($\text{s}^{-1\dagger}$)
roentgen (R) (air exposure)	2.579 760 $\times 10^{-4}$	coulomb per kilogram (C kg^{-1})
absorbed dose (rad)	1 $\times 10^{-2}$	joule per kilogram (J kg^{-1**})
equivalent dose (rem)	1 $\times 10^{-2}$	joule per kilogram ($\text{J kg}^{-1\dagger\dagger}$)

*Specific details regarding the implementation of SI units may be viewed at <http://www.bipm.org/en/si/>.

[†]Multiply U.S. customary unit by factor to get international unit. Divide international unit by factor to get U.S. customary unit.

[‡]The special name for the SI unit of activity of a radionuclide is the becquerel (Bq). (1 Bq = 1 s^{-1}).

**The special name for the SI unit of absorbed dose is the gray (Gy). (1 Gy = 1 J kg^{-1}).

^{††}The special name for the SI unit of equivalent and effective dose is the sievert (Sv). (1 Sv = 1 J kg^{-1}).

**DTRA-TR-12-002: Probabilistic Analysis of Radiation Doses for Shore-Based Individuals
in Operation Tomodachi**

Table of Contents

List of Figures	4
List of Tables	8
Acknowledgements.....	10
Executive Summary	11
Section 1. Introduction.....	15
1.1 Background	15
1.2 Purpose and Objectives	16
Section 2. Modeling of Uncertainty.....	18
2.1 Definitions.....	18
2.1.1 Central Estimates of Doses	18
2.1.2 Doses Estimated by Deterministic Methods	18
2.1.3 Doses Estimated Using Probabilistic Analysis	19
2.2 Uncertainty Modeling	19
2.2.1 Monte Carlo Method.....	19
2.2.2 Quantifying Uncertainty	20
Section 3. Selected Locations and Populations of Concern.....	21
3.1 General Approach to Selection of Populations of Concern	21
3.2 Description of Selected Locations	23
3.2.1 Yokosuka Naval Base	23
3.2.2 Yokota Air Base.....	23
3.2.3 Sendai Airport and Camp Sendai.....	24
Section 4. Radiation Dose Estimation and Parameter Distributions.....	27
4.1 Exposure to External Radiation	27
4.1.1 Net Dose Rate from Gamma Radiation for Presence Outdoors	28
4.1.2 Indoor Dose Reduction Factor	37
4.1.3 Time Spent Outdoors	38

4.1.4	Protection Factor	39
4.2	Exposure to Internally-Deposited Radioactive Materials	45
4.2.1	Inhalation Intakes	45
4.2.2	Ingestion of Drinking Water	58
4.2.3	Incidental Ingestion of Soil and Dust.....	62
Section 5.	Results of Probabilistic Analyses and Comparison with Doses Estimated by Deterministic Methods	69
5.1	Results of Probabilistic Analyses.....	69
5.2	Comparison of the Doses Using Probabilistic Analysis with Doses Estimated by Deterministic Methods.....	71
5.3	Discussion of Results	79
Section 6.	Sensitivity Analysis for the Dose Models.....	80
6.1	Technical Approach and Methodology.....	80
6.2	Sensitivity Analysis for the Total Effective Dose Model	82
6.3	Sensitivity Analysis for the Total Equivalent Dose to the Thyroid Model.....	83
Section 7.	Conclusions.....	91
Section 8.	References.....	94
Appendix A.	Overview of Probability Distributions	98
A-1	Uniform Distribution	98
A-2	Gaussian Distribution.....	99
A-3	Log-normal Distribution	100
A-4	Triangular Distribution	101
A-5	Log-triangular Distribution.....	102
Appendix B.	Summary of Dose Parameters Values and Distributions	104
Appendix C.	Correlations and Dependencies	112
Appendix D.	Air Activity Concentration Model for Sendai Locations	116
D-1	Step 1: Air Activity Concentration Model for Yokota Air Base	116
D-2	Step 2: Model for Sendai Locations during the “Early Period” (March 11-21, 2011)	117
D-3	Step 3: Model for Sendai Locations during the “Late Period” (March 21 to May 11, 2011).....	118

Appendix E. Time-Activity Patterns.....	125
Appendix F. Inhalation and Ingestion Dose Coefficients	131
Data Compendium	134
DC-1 Air Activity Concentration	134
DC-2 Water Activity Concentration	141
DC-3 Soil Activity Concentration	145
Abbreviations, Acronyms, and Unit Symbols	151

List of Figures

Figure 1. Locations of DoD-Affiliated Populations of Concern on the Islands of Honshu and Kyushu, Japan	22
Figure 2. Yokosuka Naval Base.....	23
Figure 3. Loading of a C-17 Globemaster III with relief supplies at Yokota Air Base.....	24
Figure 4. A tent camp set up for about 200 service members at Sendai Airport	25
Figure 5. Aerial view of Camp Sendai, Miyagi Prefecture.....	25
Figure 6. Temporary barracks at Camp Sendai	26
Figure 7. Yokosuka Naval Base - locations of radiation monitoring stations in Kanagawa Prefecture	30
Figure 8. Radiation dose rates in Kanagawa Prefecture near Yokosuka Naval Base.....	30
Figure 9. Dose rates for MEXT station and mean of the two SPEEDI stations closest to Yokosuka Naval Base.....	31
Figure 10. Yokota Air Base—locations of radiation monitoring stations in Tokyo and Saitama Prefectures	32
Figure 11. Dose rates from MEXT data at Tokyo and Saitama (stations closest to Yokota Air Base).....	32
Figure 12. Kanto Plain shown between the mountains and the ocean.....	33
Figure 13. Dose rates at 1 meter above the ground derived from airborne monitoring surveys	34
Figure 14. Location of the radiation monitoring stations in Sendai City and Yamagata City	36
Figure 15. Dose rates from MEXT monitoring stations at Sendai City and Yamagata City.....	36
Figure 16. Combined measured and modeled dose rates for Sendai locations.....	37
Figure 17. Example of a two-story townhouse at Yokosuka Naval Base.....	41
Figure 18. Probability density and cumulative distribution functions of the protection factor for a residential structure	41
Figure 19. Example of non-residential building at Yokosuka Naval Base.....	42
Figure 20. Probability density and cumulative distribution functions of the protection factor for a non-residential structure.....	42
Figure 21. Protection factors for a variety of building types and locations (from Buddemeier and Dillon, 2009)	43
Figure 22. Military personnel spending time inside a tent at the camp erected at Sendai Airport.....	43

Figure 23. Tents used by service members in the camp erected at Sendai Airport	44
Figure 24. Probability density and cumulative distribution functions of the protection factor for a tent.....	44
Figure 25. Air activity concentrations measured at Yokota Air Base for selected radionuclide	48
Figure 26. Sendai air activity concentration model based on daily dose rates and activity measurements at Yokota Air Base.....	49
Figure 27. Relative frequency distribution of I-131 gas-to-aerosol air activity concentration ratios at U.S. Embassy (Tokyo) and Yokota Air Base	52
Figure 28. Fitted distributions and statistical data of the ratios of I-131 gas-to-aerosol air activity concentration collected at U.S. Embassy (Tokyo) and Yokota Air Base.....	53
Figure 29. Log-normal (LN) cumulative probability functions of inhalation rates for adults (age > 17 years).....	55
Figure 30. Relative frequency distribution of the composite daily inhalation rate for adults (age > 17 years) and humanitarian field workers.....	56
Figure 31. Relative frequency distribution of the daily inhalation rate for 1-to-2 year-old children	57
Figure 32. Water activity concentration of I-131 for Yokosuka Naval Base	59
Figure 33. Water activity concentrations for Yokota Air Base	60
Figure 34. Cumulative probability distribution functions fitted to the published statistical data for water ingestion rate of adults.....	61
Figure 35. Cumulative probability distribution functions fitted to the published statistical data for water ingestion rate of 1-to-2 year-old children	61
Figure 36. Modeled and measured soil activity concentrations at Yokosuka Naval Base	64
Figure 37. Modeled and measured soil activity concentrations at Yokota Air Base	66
Figure 38. Modeled and measured soil activity concentrations for Sendai locations.....	68
Figure 39. Total effective dose distribution using probabilistic analysis and range of doses estimated by deterministic methods for adults at Yokosuka Naval Base	74
Figure 40. Total equivalent dose to the thyroid distribution using probabilistic analysis and range of doses estimated by deterministic methods for adults at Yokosuka Naval Base.....	74
Figure 41. Total effective dose distribution using probabilistic analysis and range of doses estimated by deterministic methods for adults at Yokota Air Base.....	75
Figure 42. Total equivalent dose to the thyroid distribution using probabilistic analysis and range of doses estimated by deterministic methods for adults at Yokota Air Base	75

Figure 43. Total effective dose distribution using probabilistic analysis and range of doses estimated by deterministic methods for 1-to-2 year-old children at Yokota Air Base	76
Figure 44. Total equivalent dose to the thyroid distribution using probabilistic analysis and range of doses estimated by deterministic methods for 1-to-2 year-old children at Yokota Air Base	76
Figure 45. Total effective dose distribution using probabilistic analysis and range of doses estimated by deterministic methods at Camp Sendai	77
Figure 46. Total equivalent dose to the thyroid distribution using probabilistic analysis and range of doses estimated by deterministic methods at Camp Sendai	77
Figure 47. Total effective dose distribution using probabilistic analysis and range of doses estimated by deterministic methods for humanitarian field workers at Sendai Airport.....	78
Figure 48. Total equivalent dose to the thyroid distribution using probabilistic analysis and range of doses estimated by deterministic methods for humanitarian field workers at Sendai Airport.....	78
Figure 49. Sensitivity score SS1 for model parameters to total effective dose at Yokosuka Naval Base.....	85
Figure 50. Sensitivity score SS2 for model parameters to total effective dose at Yokosuka Naval Base.....	86
Figure 51. Sensitivity score SS3 for model parameters to total effective dose at Yokosuka Naval Base.....	87
Figure 52. Sensitivity score SS1 for model parameters to total equivalent dose to the thyroid at Yokosuka Naval Base	88
Figure 53. Sensitivity score SS2 for model parameters to total equivalent dose to the thyroid at Yokosuka Naval Base	89
Figure 54. Sensitivity score SS3 for model parameters to total equivalent dose to the thyroid at Yokosuka Naval Base	90
Figure A-1. Probability density function of a uniform distribution.....	98
Figure A-2. Probability density function of a Gaussian distribution	99
Figure A-3. Probability density functions of the log-normal distribution for various values of σ	101
Figure A-4. Probability density functions of a triangular distribution (1) skewed right, (2) symmetric, and (3) skewed left	101
Figure A-5. A right-skewed log-triangular distribution.....	103
Figure D-1. I-131 air activity concentration model for Yokota Air Base.....	120
Figure D-2. I-131 air activity concentration model for Sendai (early period).....	121
Figure D-3. I-131 air activity concentration model for Sendai (late period)	122

Figure D-4. I-131 combined air activity concentration model for Sendai	123
Figure D-5. I-131, Cs-134, and Cs-137 air activity concentration models for Sendai	124

List of Tables

Table 1. Locations selected for probabilistic analysis with selection rationale	21
Table 2. Age groups and locations of potentially exposed populations addressed by probabilistic and deterministic methods	22
Table 3. Dose rate data sources and characteristics	29
Table 4. Distributions of the amount of time spent outdoors	39
Table 5. Radionuclides and chemical forms considered for air activity and inhalation pathway.....	47
Table 6. Measured air activity concentrations at Sendai locations	49
Table 7. Inhalation rate log-normal distributions for four activity levels.....	56
Table 8. Log-normal distributions selected for the water ingestion rate	62
Table 9. Measured soil activity concentrations at Yokosuka Naval Base	64
Table 10. Measured soil activity concentrations at Yokota Air Base.....	65
Table 11. Measured soil activity concentrations at Sendai.....	67
Table 12. Triangular distributions selected for soil and dust ingestion rates.....	68
Table 13. Dose results for adults at Yokosuka Naval Base using probabilistic analysis.....	69
Table 14. Dose results for adults at Yokota Air Base using probabilistic analysis	70
Table 15. Dose results for 1-to-2 year-old children at Yokota Air Base using probabilistic analysis	70
Table 16. Dose results for support personnel at Camp Sendai using probabilistic analysis.....	71
Table 17. Dose results for the humanitarian field workers at Sendai Airport using probabilistic analysis	71
Table 18. Population exposure factors for PEPs with doses estimated by deterministic methods and the corresponding factors used in the probabilistic analysis	72
Table 19. Comparison of doses estimated by deterministic methods with doses from probabilistic analysis	73
Table 20. Model parameter and variable names that apply to each exposure pathway.....	82
Table 21. Sensitivity scores for input parameters to the total effective dose model	84
Table 22. Sensitivity scores for input parameters to the committed equivalent dose to the thyroid model.....	84
Table 23. Summary and comparison of doses estimated using probabilistic analysis and by deterministic methods	93

Table B-1. Parameter values and distributions used in external and internal dose calculations	104
Table C-1. Correlations and dependencies among dose model input parameters	112
Table D-1. Air activity concentration model parameters for Yokota Air Base	118
Table D-2. Air activity concentration model parameters for Sendai (early period)	118
Table D-3. Air activity concentration model parameters for Sendai (late period)	119
Table E-1. Fraction of time indoor and outdoor workers spend in each inhalation activity level.....	128
Table E-2. Fraction of time indoor and outdoor children spend in each inhalation activity level.....	130
Table F-1. Inhalation 50-year committed dose coefficients for adults	131
Table F-2. Ingestion 50-year committed dose coefficients for adults	132
Table F-3. Inhalation committed dose coefficients to age 70 for 1 year-old children	132
Table F-4. Ingestion committed dose coefficients to age 70 for 1 year-old children	133
Table DC-1. Air activity concentration measurement data at Yokota Air Base.....	135
Table DC-2. Modeled air activity concentrations used for Sendai Airport and Camp Sendai	138
Table DC-3. Water activity concentration measurement data at Yokosuka Naval Base.....	141
Table DC-4. Water activity concentration measurement data at Yokota Air Base	143
Table DC-5. Modeled soil activity concentrations used for Yokosuka Naval Base.....	145
Table DC-6. Modeled soil activity concentrations used for Yokota Air Base	147
Table DC-7. Modeled soil activity concentrations used for Sendai locations	149

Acknowledgements

The authors gratefully acknowledge the support of the following individuals:

- Operation Tomodachi Dose Assessment and Recording Working Group members who provided critical information and/or useful reviews including CDR Ralph J. Marro, Armed Forces Radiobiology Research Institute; Dr. Gerald Falo, Army Institute of Public Health; LCDR Terry Miles, Navy Marine Corps Public Health Center; Dr. Steven Rademacher, U.S. Air Force Safety Center; Mr. Richard Ranellone, Engility, Inc., and Dr. Paul Blake, Defense Threat Reduction Agency.
- Dr. Daniel Blumenthal, National Nuclear Security Administration, who shared DOE's radiological monitoring results.
- Veterans' Advisory Board on Dose Reconstruction, Subcommittee No. 1 members (Mr. Harold Beck, Mr. Paul Voilleque, and Dr. Gary Zeman), who provided a preliminary peer review.
- National Council on Radiation Protection and Measurements, Scientific Committee No. 6-8 members (Dr. John Till, Dr. John Boice, Dr. Iulian Apostoaei, and Mr. William Kennedy, Jr.) who provided peer review of this report.
- Major Mark J. Allen and Master Gunnery Sergeant Gregory Clemenson, 3rd Marine Expeditionary Brigade, who provided background information on activities at Sendai.
- Dr. Morino Yu, National Institute for Environmental Studies, Tsukuba-City, Japan, who provided modeling results for review.
- Mr. Chris Ziemniak, Dr. David Case, Dr. Ronald Weitz, and Dr. Stephen Egbert, SAIC, who provided editorial and technical assistance in preparing the report.
- Dr. David Kocher of SENES Oak Ridge, Inc., who provided peer review.
- Ms. Hilda Maier, Mr. Hanson Gaugler, Ms. Debra Gross of L-3 Services, Inc., who provided logistics and computing support for this effort.
- Dr. Craig Postlewaite and Mr. Scott Gordon of the Office of the Assistant Secretary of Defense for Health Affairs, who provided critical guidance and support.

Executive Summary

This report describes a probabilistic method and analyses developed to estimate distributions of total effective doses and total equivalent doses to the thyroid gland from ionizing radiation for persons affiliated with the U.S. Department of Defense who were in Japan following the nuclear accident at the Fukushima Daiichi Nuclear Power Station during the 60-day period from March 12, 2011, to May 11, 2011. The probabilistic analyses were performed to provide a basis for comparison with the doses estimated by deterministic methods and reported in Cassata et al. (2012), and to assess whether the latter doses are sufficiently conservative (high-sided). These probabilistic analyses were carried out to determine if the doses estimated in Cassata et al. (2012) met the goal of being conservative at or above the 95-percent confidence level. In addition, sensitivity analyses were conducted to study how the output of probabilistic dose calculations is affected by the magnitude and broadness of uncertainty distributions of input parameters, qualitatively or quantitatively.

Total doses from ionizing radiation were previously estimated by deterministic methods using highly conservative assumptions for 13 shore locations in Japan where potentially exposed populations were known to have lived, worked, or been deployed (Cassata et al., 2012). These doses were calculated for adults and several age groups of children. In this report, the doses estimated by deterministic methods are compared with the 95th percentile of the dose distributions calculated by probabilistic analyses for five selected potentially exposed populations. These analyses used realistic input parameter values and corresponding uncertainties in the dose models, which represent the current state of knowledge. Estimates of external and internal dose distributions were performed by Monte Carlo simulation, a common technique in probabilistic analysis.

Probabilistic analyses were performed for four locations including Yokota Air Base, Yokosuka Naval Base, Camp Sendai, and Sendai Airport. The locations were selected based on the size of the populations of concern or proximity to the nuclear power station. Doses were estimated for adults for the first three locations and for humanitarian field workers at Sendai Airport. Doses for children in the 1-to-2 year-old group were estimated for Yokota Air Base. The exposure pathways considered were external radiation, inhalation of airborne radioactive material, ingestion of contaminated drinking water, and incidental ingestion of contaminated soil and dust.

Model input parameters and uncertainty distributions were developed based on radiation exposure data collected from published sources, e.g., the Japanese Ministry of Education, Culture, Sports, Science and Technology; U.S. Department of Defense; and U.S. Department of Energy. In addition, recent exposure and radiation dose assessment literature was used as the basis for selected statistical data and models, including the Environmental Protection Agency Exposure Factors Handbook (EPA, 2011) and Defense Threat Reduction Agency technical reports (Weitz et al., 2009; DTRA, 2010; Cassata et al., 2012). The type of correlations among all input parameters of the total dose models were evaluated and applied in the probabilistic models.

The dose comparisons show that for all potentially exposed Department of Defense-affiliated populations that are evaluated in this report, the total effective doses and total equivalent doses to the thyroid estimated in Cassata et al. (2012) were higher than the 95th percentile doses determined by the probabilistic methods. This finding demonstrates that the estimated doses reported in Cassata et al. (2012) are sufficiently conservative. Moreover, all the total doses estimated by deterministic methods are higher than the 95.8th percentile values calculated using probabilistic analyses. Finally, the total effective doses and total equivalent doses to the thyroid estimated by deterministic methods exceed their corresponding 95th percentile probabilistic values by a factor of about 1.1 or more. A summary and comparison of doses resulting from deterministic and probabilistic methods are presented in Table ES-1.

Furthermore, uncertainty factors derived from the probabilistic analyses, which are defined as the ratio of the 95th percentile and the central estimate values, range from 1.9 to 2.4 for external dose distributions. The uncertainty factors for the internal doses due to the intake of radioactive materials by inhalation, ingestion of water, and incidental ingestion of soil range from 4.4 to 8.2. The uncertainty factors for the total effective doses and total equivalent doses to the thyroid from the probabilistic analyses range from 3.0 to 7.2. The magnitude of the uncertainty factors for the total effective doses and total equivalent doses to the thyroid depends on the contributions from the external versus internal doses, with the higher uncertainty factors being associated with higher contributions from internal doses.

To evaluate how the output of probabilistic dose calculations is affected by the magnitude and broadness of uncertainty distributions of the input parameters, sensitivity analyses were performed using the dose models developed for adults at Yokosuka Naval Base. The results of these analyses indicate that the model for the total effective dose is most sensitive to the uncertainty in inhalation and ingestion dose coefficients and least sensitive to uncertainties in parameters that are used in the calculation of the soil ingestion dose. The total effective doses showed an extremely low sensitivity to the ratio of strontium radionuclides to cesium-137. As expected, the dose model results are much more sensitive to input parameters that present broader uncertainty distributions and are used in the calculation of dose components with larger contributions to total doses.

The sensitivity analysis carried out for the Yokosuka Naval Base location indicate that the model for the total equivalent dose to the thyroid is most sensitive to the uncertainty in inhalation and ingestion dose coefficients and least sensitive to uncertainties in parameters that are included in the calculation of the external dose or soil ingestion dose. The total equivalent doses to the thyroid showed an extremely low sensitivity to the ratio of strontium radionuclides to cesium-137. As expected, the dose model results are much more sensitive to input parameters that present broader uncertainty distributions and are used in the calculation of dose components with greater contributions to total doses.

Finally, the first draft of this report was peer reviewed by Scientific Committee 6-8 of the National Council on Radiation Protection and Measurements, which provided detailed feedback and recommendations to expand on the description of the technical bases employed in the analysis. The committee concluded that “in general, the analysis was well done and confirms that doses to adults estimated using the deterministic methodology meet the objective of the dose estimation process in Cassata et al. (2012).” Doses for children in the 1-to-2 year-old group were not included in the peer-reviewed draft. However, these dose distributions were estimated and are included in this report based on a recommendation by the review committee. The doses to

children were calculated and are compared to the deterministic analysis doses using the same methodology and environmental data as those used for adults.

Table ES-1. Summary and comparison of doses estimated using probabilistic analysis and by deterministic methods

Dose Type	Geometric Mean (mSv)	Arithmetic Mean Dose (mSv)	Dose Estimated by Deterministic Methods* (mSv)	Probabilistic 95th Percentile Dose (mSv)	Dose Estimated by Deterministic Methods as Percentile of the Probabilistic Distribution	Ratio of Deterministic Analysis to 95th Percentile Dose
Yokosuka Naval Base (Adults)						
Total effective dose	0.024	0.031	0.32	0.077	99.8	4.1
Total equivalent dose to thyroid	0.24	0.40	3.6	1.3	99.7	2.9
Yokota Air Base (Adults)						
Total effective dose	0.048	0.060	0.51	0.15	99.9	3.6
Total equivalent dose to thyroid	0.48	0.69	4.5	2.0	99.4	2.4
Yokota Air Base (1-to-2 Year-Old Children)						
Total effective dose	0.093	0.12	0.99	0.31	99.8	3.2
Total equivalent dose to thyroid	1.4	1.9	14	5.4	99.6	2.6
Camp Sendai (Adults)						
Total effective dose	0.074	0.12	1.0	0.36	99.6	2.9
Total equivalent dose to thyroid	0.87	1.8	9.8	6.3	98.6	1.6
Sendai Airport (Humanitarian Field Workers)						
Total effective dose	0.17	0.23	1.2	0.67	98.4	1.9
Total equivalent dose to thyroid	1.7	3.2	13	12	95.8	1.1

*Doses estimated by deterministic methods are those reported in Cassata et al. (2012).

Section 1.

Introduction

1.1 Background

The earthquake and the tsunami that occurred in Japan on March 11, 2011, led to releases of radioactive materials into the environment from the Tokyo Electric Power Company's Fukushima Daiichi Nuclear Power Station (FDNPS). Immediately after these events, Operation Tomodachi was initiated by the U.S. Department of Defense (DOD) to provide humanitarian assistance and disaster relief in support the government of Japan (GOJ). Shortly after the end of Operation Tomodachi, the Dose Assessment and Recording Working Group (DARWG) was established to carry out radiation dose assessments for military personnel and other DOD-affiliated persons who were in Japan during the 60-day period from March 12, 2011, to May 11, 2011. DARWG carried out the dose assessment for shore-based individuals who were potentially exposed during Operation Tomodachi. The radiation doses for shore-based individuals are estimated by deterministic methods with conservative assumptions and are reported in Cassata et al. (2012).

The DARWG shore-based dose assessment represents one part of a process to estimate radiation doses and health risks to potentially exposed populations (PEPs) that form the population of interest (POI). The POI is composed of DOD-affiliated individuals who were present in Japan, on-shore, at sea, and in the air during the 60-day period following the accident at the FDNPS. A PEP is a group of persons who have a similar exposure scenario and are characterized by the same set of dose model parameter values. The dose assessment for shore-based individuals constitutes the technical basis for doses recorded in the Operation Tomodachi Registry (OTR). The OTR is a database of the estimated radiation doses and dosimetry records for military service personnel, DOD civilians, DOD contractors, and their family members who were in or deployed to Japan during the 60 days after the earthquake and tsunami. The [OTR website](#) provides public access to the estimated doses for groups and locations that are reported in Cassata et al. (2012).

The DARWG shore-based radiation assessment as well as the probabilistic analysis presented in this document was based on measured environmental data such as external radiation dose rates and activity concentrations of radioactive materials in air, water, and soil. The approach used to estimate doses was based on dose calculation methods and dose coefficients (DC) published by the International Commission on Radiological Protection (ICRP), the National Council on Radiation Protection and Measurements (NCRP), and the U.S. Environmental Protection Agency (USEPA). In addition, the dose assessments in Cassata et al. (2012) and in the current study relied on guidance and standardized procedures from U.S. government programs, with decades-long record of experience in radiation dose assessments, such as the Nuclear Test Personnel Review (NTPR) Program of DOD's Defense Threat Reduction Agency (DTRA). Furthermore, the Veterans' Advisory Board on Dose Reconstruction (VBDR) provides technical peer review and quality assurance oversight through audits of the NTPR Program (VBDR, 2013).

This report is part of a series of reports undertaken by DOD to assess radiation doses to DOD-affiliated individuals or characterizing the radiological environment at J-Village. This series of reports provides the technical basis for the assessment of doses that will be posted on the Operation Tomodachi Registry (OTR) website. These doses and information about the possible health effects from them will be accessible to all members of the POI, members of the medical community, and the public at large. This series of reports include:

- Radiation Dose Assessments for Shore-Based Individuals in Operation Tomodachi, Revision 1 (DTRA-TR-12-001).
- Probabilistic Analysis of Radiation Doses for Shore-Based Individuals in Operation Tomodachi (DTRA-TR-12-002).
- Radiation Internal Monitoring by In Vivo Scanning in Operation Tomodachi (DTRA-TR-12-004).
- Radiation Doses for Embryo and Fetus, and Nursing Infants from Operation Tomodachi (DTRA-TR-12-017).
- Radiation Doses for Fleet-Based Individuals in Operation Tomodachi (DTRA-TR-12-041).
- Characterization and Assessment of Radiological Environment at J-Village during Operation Tomodachi (DTRA-TR-12-045).
- Comparison of Radiation Dose Studies of the 2011 Fukushima Nuclear Accident Prepared by the World Health Organization and the U.S. Department of Defense (DTRA-TR-12-048).
- Army Institute of Public Health (AIPH) Standard Methods (SM) and Standard Operating Procedures (SOPs) for Responding to Operation Tomodachi Individual Dose Assessments and Responding to VA Radiogenic Disease Compensation Claims (AIPH SM/SOP).

1.2 Purpose and Objectives

Cassata et al. (2012) reported doses for 13 shore locations where DOD-affiliated persons are known to have lived, worked, or been deployed. In that assessment, the estimated doses were intended to be high-sided through the use of conservative assumptions to ensure that the range of dose are credible estimates for all or nearly all shore-based individuals. For this report, probabilistic analyses were performed to estimate dose distributions using model input parameters with corresponding uncertainty distributions that represent the current state of knowledge. The results of the probabilistic analyses were compared with the doses estimated by deterministic methods reported in Cassata et al. (2012) to assess whether the latter doses are sufficiently conservative (high-sided). For this exercise, the doses estimated by deterministic methods were compared with the 95th percentile of the dose distributions estimated by probabilistic analysis. Additionally, a sensitivity analysis was carried out to evaluate the relative effect of variation in model parameter values on the estimated doses.

For the probabilistic approach, 3 out of the 13 shore locations evaluated in the shore-based assessment and an additional sub-location were selected using the rationale presented in Section 3 to form five PEPs that are evaluated in this report. The first two PEPs consist of adults (17 years of age or greater) who were located at Yokosuka Naval Base and

Yokota Air Base. Because the highest doses to children in Cassata et al. (2012) were found to be for the 1-to-2 year-old age group at Yokota Air Base, another PEP is included in this probabilistic analysis. The last two PEPs consist of adults at Sendai Airport and Camp Sendai. The individuals at Sendai Airport, who lived in tents at a temporarily camp erected in the airport parking lot, provided humanitarian assistance in the field working mostly outdoors. The units deployed at Camp Sendai coordinated relief and recovery efforts with the Japanese Self-Defense Forces, e.g., the Bilateral Crisis Action Team. The Camp Sendai group lived and worked mostly indoors in fixed facilities. All adult populations consisted of males and females.

The specific objectives of the study are to:

- Develop and define dose assessment parameter distributions.
- Estimate external and internal dose distributions by Monte Carlo simulation.
- Compare the probability distributions of doses with the doses estimated by deterministic methods to assess whether the latter are sufficiently conservative.
- Carry out a sensitivity analysis to assess the effects of parameter variations on the estimated dose distributions.

The definitions of dose terms, modeling of uncertainty, Monte Carlo simulations, and basic statistical analysis processes used in this study are introduced in Section 2. The selected assessment locations and relationship with efforts performed in support of Operation Tomodachi are described in Section 3. The dose estimation models and input parameter distributions are described in Section 4. The doses from the probabilistic analyses are reported and compared with the doses estimated by deterministic methods in Section 5 and the results of the sensitivity analyses are reported in Section 6.

Section 2.

Modeling of Uncertainty

2.1 Definitions

This report refers to the calculation of central estimates of doses, doses estimated by deterministic methods, and doses using probabilistic methods. These three dose models are described below.

2.1.1 Central Estimates of Doses

To build model input parameter distributions for the probabilistic analyses performed in this study, central estimates of doses were based on field and laboratory measurements documented in technical reports, databases, and after action reports of the response to the Fukushima nuclear accident. In other cases where data were not available or not well documented, surrogate data are used. Analysts with extensive knowledge and experience in radiation dose assessment methodologies used their collective and subjective judgments within a collaborative process to select estimates of input parameters and related uncertainty distributions. The estimates for central values of model parameters are termed “nominal values.” Nominal values may also be extracted from the numerically generated theoretical distributions assigned to the model input parameter (Weitz et al., 2009). Central dose calculations provide point estimates using a dose reconstruction model with nominal values for all of its input parameters. In other words, the nominal values are considered to produce the best estimate of model predictions (Kirchner, 2008).

Furthermore, in sensitivity analyses, one single input parameter is allowed to vary within its range of values based on its own distribution while all other parameters in the model are held to their nominal values. While this is the method used in this report, other strategies can be used to minimize the importance of the selection of nominal values of model parameters. Sensitivity analyses indicate which input parameter uncertainties have the most influence on dose distributions.

2.1.2 Doses Estimated by Deterministic Methods

The Operation Tomodachi dose assessment for shore-based individuals, performed in Cassata et al. (2012), used dose reconstruction models with conservative “high-sided” input parameter values and conservative assumptions to estimate location-specific doses by deterministic methods. Such doses are not central estimates and should, by design, be much higher. The conservative assumptions used by the DARWG in Cassata et al. (2012) are intended to result in radiation doses that are equal to or greater than the 95th percentile value of the dose distributions resulting from a credible probabilistic analysis. In this report, this assertion will be checked for the scenarios analyzed.

2.1.3 Doses Estimated Using Probabilistic Analysis

The probabilistic models use either assumed nominal values as central estimates or existing measurement or statistical data to define the distributions for each input parameter. The central estimate can be represented by the mean, geometric mean, median or mode depending on the type of distribution used. A full probabilistic analysis, where all uncertain input parameters are assigned distributions, results in a dose distribution that reflects the uncertainty in the calculated dose. The upper-bound dose for a probabilistic analysis is defined for the purpose of this report as the 95th percentile value of the dose distribution. The uncertainty factor is defined as the ratio of the 95th percentile value and the central value of the dose distribution. Note that “uncertainty analysis” is sometimes used in place of “probabilistic analysis.” (Weitz et al., 2009)

2.2 Uncertainty Modeling

Uncertainty modeling refers to the techniques used to statistically model input parameters taking into account the various sources of uncertainty due to lack of specific knowledge of variables such as spatial variability, measurement errors, and variations due to data pre-processing, among others. The probability distribution functions used in this study and their principal properties are described in Appendix A.

As used in this report, a probability density function (pdf) is the probability that the random variable takes on a given value. The integral of a pdf is the cumulative probability distribution (cpd) that gives the probability that the random variable of interest can take any real value that is less than or equal to a given value within a defined continuous range.

2.2.1 Monte Carlo Method

In the Monte Carlo method, all key parameters are regarded as random variables with assigned pdf's. During the many trials or “simulations,” values are randomly selected for those pdf's. The calculated model results from all trials are assembled into distributions which are themselves characterized by their distribution parameters. (Morgan and Henrion, 1990; Hahn and Shapiro, 1967; Vose, 2008)

This method is applicable and appropriate to probabilistic dose reconstruction of the type addressed in this report. Here, a typical dose reconstruction production run consists of 10,000 simulations, each involving the random sampling of all input parameter distributions. Use of a small number of simulations, such as 100, has been tried and often results in distributions that are bumpy with limited sampling of the tails. Also a small number of simulations fail to properly replicate the statistics of input parameter distributions. To accelerate the development of the calculation tools, models are run using 1,000 simulations initially and the final results are generated using 10,000 trials. For correlated parameters, the assigned model input parameter distributions and the cpd values are the same. The result consists of the same parameter distribution repeatedly sampled in the same way within each simulation.

The nominal values and uncertainty distributions used in external and internal dose calculations are discussed in Section 4 and details listed in Appendix B. A description of the dependencies and correlations for the major input parameters used in this assessment are found in Appendix C.

2.2.2 Quantifying Uncertainty

The uncertainty of a model input parameter is explicit in the assignment of its pdf. Specifically, the uncertainty of an input model parameter is quantified by the probability distribution that is assigned to model the parameter to best represent the current state of knowledge. The attributes of the parameter distribution are then estimated using the same rationale for selecting central estimates. This includes relying on results published in the literature or reported in practitioner handbooks and reports. However, often the assignment of the probability distribution and its characterization to a model input parameter are based on expert opinion and judgment. (Morgan and Henrion, 1990; Vose 2008; NCRP 1996; NCRP, 2007)

Uncertainties in the model output parameters (calculated doses) may be specified in terms appropriate to the probability distribution used to describe that parameter, i.e., mean (μ), and standard deviation (σ) or geometric mean (GM) and geometric standard deviation (GSD). Also, uncertainty may be quantified in terms of variability about the representative parameter value “ x ,” e.g., μ or GM . Examples of how uncertainty is characterized in this study are confidence intervals about the central value, the central value multiplied by a “factor of x ,” or as an error band “ $x \pm error$ ” (Morgan and Henrion, 1990; Vose 2008; NCRP 1996; NCRP, 2007).

Section 3.

Selected Locations and Populations of Concern

3.1 General Approach to Selection of Populations of Concern

The radiation dose assessment reported in Cassata et al. (2012) covered 13 shore locations where DOD-affiliated persons are known to have lived, worked, or deployed. In this study, 3 of the 13 shore locations and an additional sub-location were selected using the rationale shown in Table 1. The four selected locations are Yokosuka Naval Base, Yokota Air Base, Sendai Airport and Camp Sendai. These locations are shown in Figure 1 with more detailed information given below this section.

The populations of concern studied in this report consist of adults (age > 17 years) for Yokosuka Naval Base, Yokota Air Base, and Camp Sendai. For Sendai Airport, the population of concern is adults who carried out humanitarian assistance in the field, mostly working outdoors. For all four locations, adults include both males and females.

The support personnel who were located at Yokosuka Naval Base, Yokota Air Base, and Camp Sendai are considered the generic PEPs who performed work and off-work activities with mostly low to moderate exertion levels. The service members who provided humanitarian assistance in the field while living at the temporary camp located on Sendai Airport constitute the humanitarian field workers PEP.

Furthermore, because the highest doses to children in Cassata et al. (2012) were found to be for the 1-to-2 year-old age group at Yokota Air Base, this PEP is included in this probabilistic analysis. For other age groups shown in Table 2 for whom doses were assessed in Cassata et al. (2012), parameter distributions are defined for all dose input variables. Probabilistic dose assessments for age groups not included in this study may be the subject of future studies if deemed necessary.

Table 1. Locations selected for probabilistic analysis with selection rationale

Location	Estimated PEP Size	Distance from FDNPS km (mi)	Rationale for Selection
Yokosuka Naval Base	16,500	260 (165)	Large population potentially exposed
Yokota Air Base	7,900	240 (150)	Large population potentially exposed
Camp Sendai	50 – 100*	95 (60)	Closest location to FDNPS with deployed DOD-affiliated individuals conducting forward humanitarian assistance mostly outdoors
Sendai Airport	200	80 (50)	

*The number of personnel varied from 50-100 for most of the time. Many people passed through there, so the 50–100 is the number that were actually sleeping in the barracks at any one time. (Allen, 2012)



Figure 1. Locations of DoD-Affiliated Populations of Concern on the Islands of Honshu and Kyushu, Japan

(U.S. military bases are shown with red stars. FDNPS is shown as a yellow trefoil.)

Table 2. Age groups and locations of potentially exposed populations addressed by probabilistic and deterministic methods

Age Group	Age Range	Deterministic Methods (Cassata et al. (2012))	Probabilistic Methods (This Study)
3 months	$0 < \text{age} \leq 1$	All locations	
1 year	$1 < \text{age} \leq 2$	All locations	Yokota Air Base
5 years	$2 < \text{age} \leq 7$	All locations	
10 years	$7 < \text{age} \leq 12$	All locations	
15 years	$12 < \text{age} \leq 17$	All locations	
Adults (> 17 years)	$17 < \text{age} \leq 65$	All locations	Yokosuka Naval Base Yokota Air Base Camp Sendai
Humanitarian field workers	$17 < \text{age} \leq 65$	All locations	Sendai Airport

3.2 Description of Selected Locations

3.2.1 Yokosuka Naval Base

Yokosuka Naval Base is located on the island of Honshu, Japan, on the Kanto Plain, 65 km (40 mi) south of Tokyo on the Miura Peninsula. Figure 2 shows general views of the housing and harbor at Yokosuka Naval Base. Every one of the 11 ships assigned to Yokosuka Naval Base supported Operation Tomodachi. During the operation, U.S. Navy ships replenished supplies at Yokosuka Naval Base. Barges from Yokosuka were loaded with relief supplies for towing to the Sendai area (USA Today, 2011; National Bureau of Asian Research, 2011).

3.2.2 Yokota Air Base

Yokota Air Base is located on the island of Honshu, Japan, on the Kanto Plain, 40 km (25 mi) west-northwest of Tokyo at the foothills of the Okutama Mountains. Yokota Air Base is the home base for Headquarters, U.S. Forces, Japan. During Operation Tomodachi, Yokota Air Base served as the air hub for units deployed to support relief efforts, such as the 353rd Special Operations Group and the 374th Airlift Wing. Yokota Air Base provided a base of operations and transportation to other relief efforts such as those carried out by the U.S. Department of Energy (DOE), the Royal Australian Air Force, and the Japanese Ground Self-Defense Forces (JGDSF). Yokota Air Base served as maintenance and operations center for aircraft diverted there after the initial disaster and for aircraft from other organizations involved in humanitarian assistance in Japan. During March of 2011, Yokota Air Base supported a voluntary departure program where the families of U.S. service members could depart Japan. Figure 3 shows the loading of relief supplies onto a C-17 Globemaster III aircraft at Yokota Air Base to be transported to Sendai Airport. (U.S. Air Force, 2011a-c)



Figure 2. Yokosuka Naval Base

(left: on-base housing, right: base shoreline and USS George Washington)



Figure 3. Loading of a C-17 Globemaster III with relief supplies at Yokota Air Base

3.2.3 Sendai Airport and Camp Sendai

For the Sendai location, the population of concern consists of two PEPs of adult service members. One PEP comprised individuals deployed at Sendai Airport, a commercial airport 15 km (9 mi) south-southwest from the center of Sendai City in Miyagi Prefecture. The other PEP was deployed to Camp Sendai, a JGSDF base located 4 km (2.5 mi) east of Sendai City center. Those service members at Sendai Airport lived in tents, worked mostly outdoors at a temporary camp, and provided humanitarian assistance in the field. Those service members at Camp Sendai lived and worked mostly indoors in fixed facilities while manning and operating a command and control center.

According to the April 8 issue of the Okinawa Marine newspaper (Stroad, 2011), Marines, Sailors, and Soldiers with Logistics Combat Element (LCE), 3rd Marine Expeditionary Brigade worked with JGSDF personnel at completing a variety of missions to aid the Japanese communities from March 18 to April 6. The LCE, operating from Sendai Airport, provided logistical support for Joint Support Force-Japan that oversaw the humanitarian assistance and disaster relief missions of Operation Tomodachi in coordination with the GOJ. In an April 4, 2011 Stars and Stripes article (Robson, 2011), a Marine Master Sergeant relayed that “the first Marines to hit the ground didn’t have tents, so they slept on cots in a freezing cold terminal in between missions.”

A contingent of 200 Marines and Soldiers from Okinawa, Camp Fuji, and Camp Zama, as well as a few Airmen out of Hawaii, set up a tent camp in a parking lot outside the terminal of Sendai Airport, shown in Figure 4. They were in charge of coordinating with the JGSDF to provide humanitarian assistance and disaster relief following the earthquake, tsunami, and nuclear accident at the FDNPS. This group was involved in planning, command and control, and field missions delivering relief supplies and helping clean up the areas damaged by the earthquake and tsunami. (Robson, 2011)

An unknown number of U.S. service members were deployed to Camp Sendai to help coordinate relief and recovery efforts with the JGSDF at a joint command center. An aerial view

of Camp Sendai is provided in Figure 5. The U.S. service members at Camp Sendai lived in temporary barracks that used existing buildings for living quarters as shown in Figure 6. In a personal communication, a major from the 3rd Marine Expeditionary Brigade stated that he and others in his unit moved to Sendai as early as March 13, 2011, and remained there until April 10, 2011 (Allen, 2012). It is believed that these individuals moved to and remained at Camp Sendai.



Figure 4. A tent camp set up for about 200 service members at Sendai Airport
(Photo by Nathan A. Bailey. © Stars and Stripes)

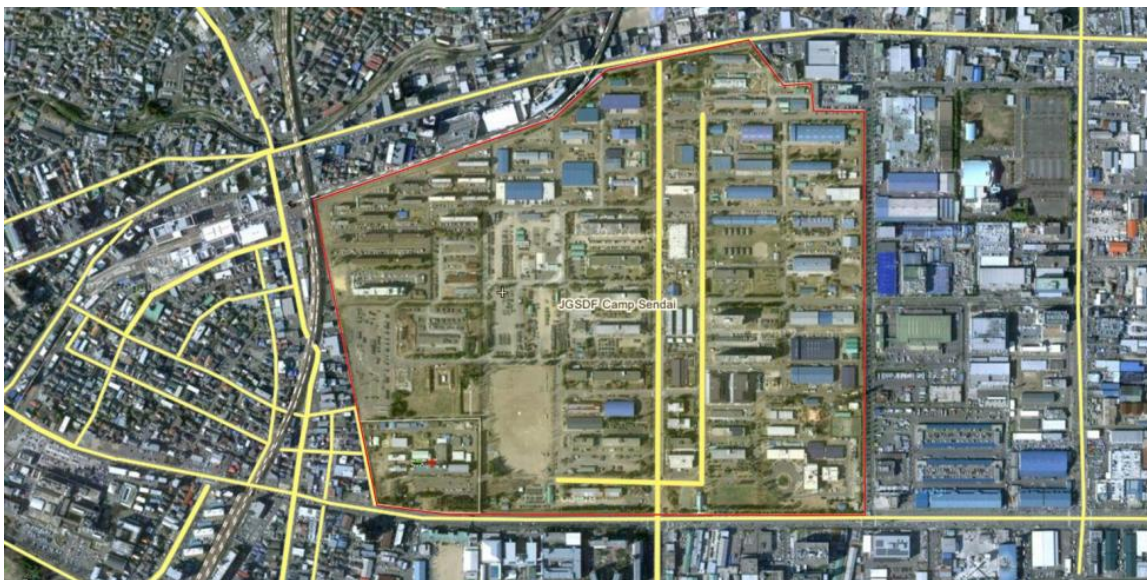


Figure 5. Aerial view of Camp Sendai, Miyagi Prefecture



Figure 6. Temporary barracks at Camp Sendai
(Photo by Nathan A. Bailey. © Stars and Stripes)

Section 4.

Radiation Dose Estimation and Parameter Distributions

Damage to the facilities at FDNPS resulted in the environmental release and off-site dispersion of radioactive materials as described in Cassata et al. (2012). The releases resulted in the potential exposure to radiation of members of the populations of concern described in Section 3. This section provides details of the methods, assumptions, and parameters used to calculate the radiation doses using probabilistic analysis techniques. The rationale for specific assumptions and parameter uncertainty distributions are included. The information is provided for each PEP and for all relevant pathways for external and internal radiation exposures.

The dose from exposure to external radiation sources, or external dose, that is calculated in this report is assumed to be the portion of the effective dose prescribed in ICRP Publication 103 (ICRP, 2007). The total dose from all sources of exposures is the sum of the external dose and the committed effective dose or committed equivalent dose to an organ from internally-deposited radioactive materials.

A listing of all parameters and their uncertainty distributions is given in Appendix B. A description of the dependencies and correlations among the dose input parameters used in this assessment are found in Appendix C. Measurement or modeled data that were used to calculate internal doses and not shown in this section can be found in the Data Compendium. All reported times and dates are Japan Standard Time (JST).

4.1 Exposure to External Radiation

In this report, the external dose for an individual is equal to the sum of the external doses accrued at each location that the person occupied during the period from March 12, 2011, to May 11, 2011. This period starts immediately following the accident at the FDNPS and was selected based on dose limiting criteria developed in Cassata et al. (2012) for persons exposed to radiation during Operation Tomodachi. The external dose for each location is calculated using Equation 1 as follows:

$$E_{\gamma} = IDRF \int_{t_{start}}^{t_{end}} I(t) dt \quad (1)$$

where:

E_{γ}	=	Net dose from external radiation while outdoors (Sv)
$I(t)$	=	Net dose rate outdoors at time t due to releases from FDNPS (Sv h ⁻¹)
$IDRF$	=	Indoor dose reduction factor due to presence indoors and shielding (unitless)

t_{start}	=	Beginning time of an individual's exposure
t_{end}	=	End time of an individual's exposure

Consistent with the shored-based dose calculations reported in Cassata et al. (2012) and information provided by the Japanese Ministry of Education, Culture, Sports, Science and Technology (MEXT), the reported external dose rates are assumed to be the absorbed dose rates in tissues. The equivalent dose is assumed to be equal to the absorbed dose ($1 \text{ Sv} = 1 \text{ Gy}$) with no uncertainty incorporated with this assumption. The outdoors net dose rate from gamma radiation, which is the measured or modeled dose rate minus the measured background in the days preceding the first release from the FDNPS, and the indoor dose reduction factor (IDRF), which includes building protection factors and time spent indoors, are discussed in the following subsections.

4.1.1 Net Dose Rate from Gamma Radiation for Presence Outdoors

The external dose (E_{γ}) in the probabilistic analysis is calculated using the net external dose rates, ($I(t)$), using measurements collected by MEXT and supplemented by other data sources. MEXT in partnership with each of Japan's 47 prefectures collected exposure rate data and made them available on its website (MEXT, 2013). These exposure rates are referred to as MEXT data in this report (MEXT, 2013). Additional dose rate measurements were made by the monitoring network that supports the System for Predictions of Environmental Emergency Dose Information (SPEEDI) overseen by Japan's Nuclear Regulatory Authority (Misawa and Nagamori, 2008), which resulted in what is referred to in this report as "SPEEDI data" available from the Nuclear Safety Technology Center website (NSTC, 2013). Other measurements were made by other organizations, but they were rather sparse and in many cases the data collection did not include the times of the first or more initial waves of contaminant passage and deposition as described in Cassata et al. (2012). Furthermore, MEXT data were highly consistent, providing hourly measurements with a few gaps, and SPEEDI data were collected at 10-minute intervals. Although SPEEDI data have a higher resolution and are taken with detectors that are located much closer to some DARWG locations than MEXT monitoring stations, geographical coverage is not available in all the areas studied in this report as shown in Table 3. The external doses reported in Cassata et al. (2012) also used MEXT data for the prefectures of interest. However, an adjustment factor was applied to increase the external doses to bring the external dose results reported by MEXT to the same level as those reported by various DOD and DOE response organizations that were in Japan after the Fukushima accident. The adjustment of the external dose rates collected by MEXT is one of the conservative assumptions used in Cassata et al. (2012).

To obtain net dose rates attributable to the FDNPS releases, background radiation levels based on dose rates measured at the same monitoring station prior to the March 11, 2011, accident were subtracted from all later measurements for the same locations when calculating external doses. For the probabilistic assessment, the source of dose rate data used and the characteristics for each assessed location are shown in Table 3 and discussed in the sections below.

Table 3. Dose rate data sources and characteristics

Location	Data Source	Monitoring Stations (City (Prefecture))	Distance, Bearing from Station to Location
Yokosuka Naval Base	SPEEDI	Nishihami (Kanagawa) Hinode Town (Kanagawa)	0.8 km (0.5 mi), SW, 209° 2.4 km (1.5 mi), ESE, 110°
	MEXT	Chigasaki (Kanagawa)	24 km (15 mi), WNW, 281°
Yokota Air Base	MEXT	Shinjuku (Tokyo)	34 km (21 mi), ESE, 102°
		Saitama (Saitama)	30 km (19 mi), ENE, 66°
Sendai Airport	MEXT	Sendai City (Miyagi)	15 km (9 mi), NNW, 340°
		Yamagata City (Yamagata)	54 km (33 mi), WNW, 284°
Camp Sendai (JGSDF)	MEXT	Sendai City (Miyagi)	4 km (2.5 mi), W, 265°
		Yamagata City (Yamagata)	51 km (32 mi), W, 269°

4.1.1.1 Yokosuka Naval Base

For Yokosuka Naval Base, dose rate data from 13 SPEEDI monitoring stations and one MEXT prefecture station were available and their locations are shown in Figure 7. Figure 8 shows the dose rates from all available stations as well as the mean of the SPEEDI station data. Dose rates from the two closest SPEEDI stations, Nishihami and Hinode Town, are corrected for background, averaged and plotted in Figure 9 along with MEXT prefecture dose rate data at Chigasaki. The two time-series are similar and would result in doses summed over the 60-day assessment period that agree to within 10 percent. Therefore, for this assessment, the average of the net dose rates from the monitoring stations at Nishihami and Hinode Town are used as central estimates for the calculation of the external dose of the Yokosuka Naval Base PEP.

The sources of uncertainty in the net dose rates for Yokosuka Naval Base are those due to spatial variability and those resulting from measurement and data processing errors (Weitz et al., 2009). The uncertainty from spatial variability due to differences in the actual dose rates experienced by an individual and the mean rates based on measurements are accounted for in the external dose assessment at Yokosuka Naval Base through the analysis of variations in dose rates at the 13 SPEEDI stations shown in Figure 8. The overall shape of the time-series plots of the external radiation levels shown in Figure 8 has been attributed to xenon-133 (Xe-133), gaseous iodine-131 (I-131) and iodine-132 (I-132) for March 15-16, 2011, and to radioactive isotopes of iodine, cesium, tellurium along with other radioactive materials attached to aerosols (tiny particles or droplets suspended in air) on March 21, 2011, as shown in Nagaoka et al. (2012).

To estimate the spatial variability of dose rates in the areas surrounding Yokosuka Naval Base, the maximum range of dose rate values among all 13 SPEEDI monitoring stations over the 60-day assessment period was determined for each measurement time (10-minute intervals). The average deviations from the mean data values of all 13 stations were found to be about $\pm 30\%$. The variations from the mean data were fitted to various probability distribution functions to evaluate which most closely fit such variations. A uniform distribution was judged adequate to represent the variability of the dose rate at the Yokosuka Naval Base and its surrounding areas about the mean value. A range of $\pm 30\%$ about the mean is selected to reflect a uniform distribution with a minimum value of $0.7 \times \text{mean}$ and a maximum value of $1.3 \times \text{mean}$.



Figure 7. Yokosuka Naval Base - locations of radiation monitoring stations in Kanagawa Prefecture

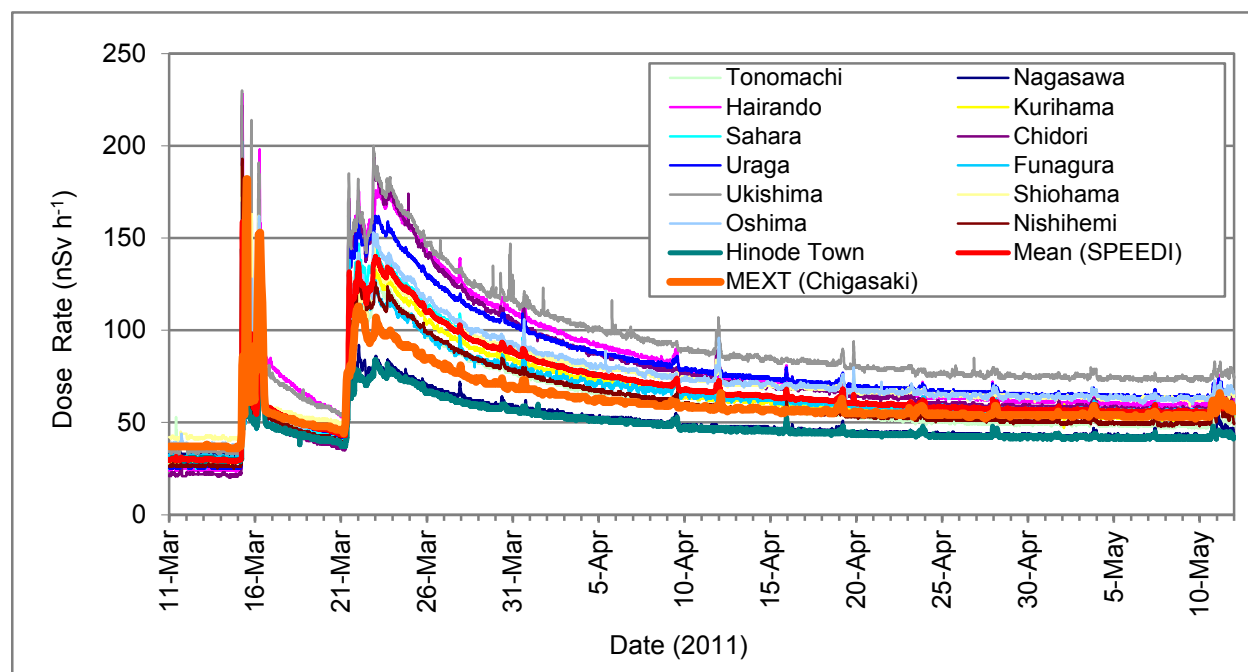


Figure 8. Radiation dose rates in Kanagawa Prefecture near Yokosuka Naval Base

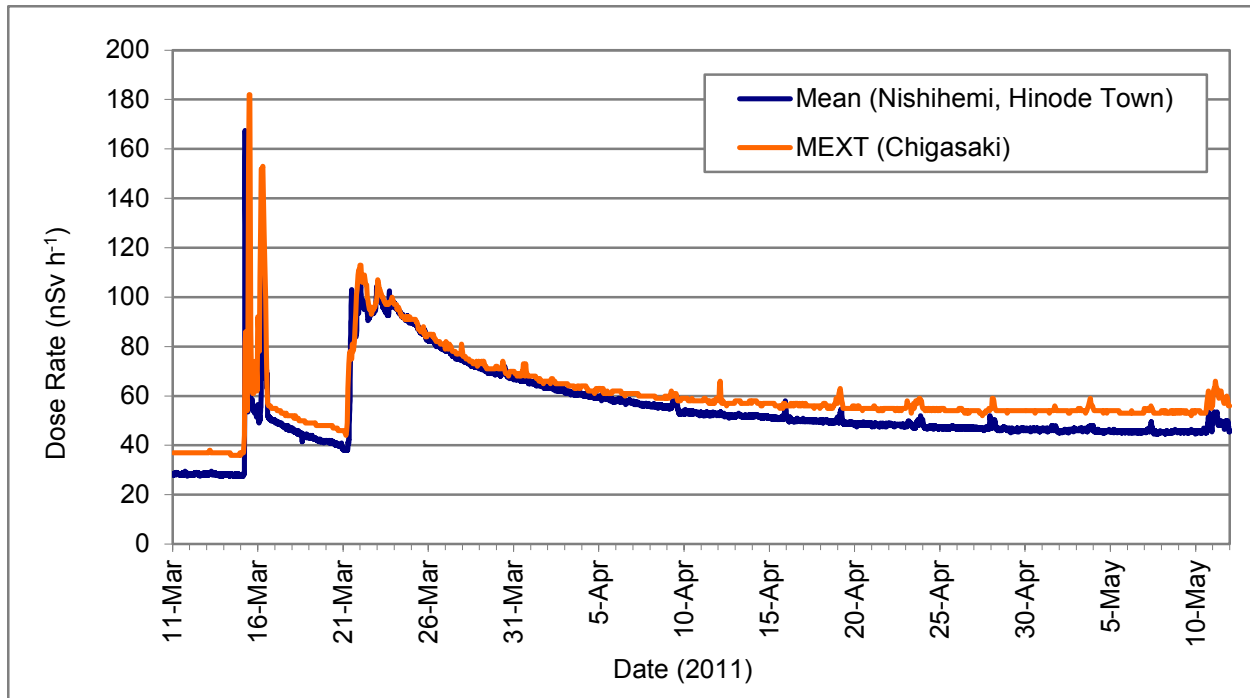


Figure 9. Dose rates for MEXT station and mean of the two SPEEDI stations closest to Yokosuka Naval Base

The uncertainty in dose rates from measurements and data errors is due to instrument precision and calibration, operator manipulation and recording errors, data analysis uncertainties, and reporting mistakes. On the basis of previous probabilistic modeling analyses and practices of other DOD radiation dose assessment programs (Weitz et al., 2009; DTRA, 2010, SM UA01), the uncertainty in dose rate measurements and data errors is modeled as a normal distribution with an uncertainty factor (ratio of 95th percentile to the mean value) of 1.5. The standard deviation for this distribution is $0.3 \times \text{mean}$.

4.1.1.2 Yokota Air Base

The dose rates for Yokota Air Base were derived from the measured dose rates at the two closest MEXT prefecture stations in Tokyo Prefecture (Shinjuku) and Saitama Prefecture (Saitama). The location of each monitoring station is shown in Figure 10 and the distances to Yokota Air Base are given in Table 3. The data from these two closest monitoring stations are plotted in Figure 11. The overall shape of the plots is due to same conditions as explained above for Yokosuka Naval Base. The dose rate time variations for the two monitoring stations are similar except during the initial peaks on March 15–16 and would result in integrated net external doses over the 60-day assessment period that differ by about 20 percent. Therefore, use of the average of the net hourly dose rates from the two monitoring stations is judged to be reasonable. Similar to the data for Yokosuka Naval Base, the sources of uncertainty in the net dose rates at Yokota Air Base are spatial variability and those resulting from measurement and data processing errors (Weitz et al., 2009).

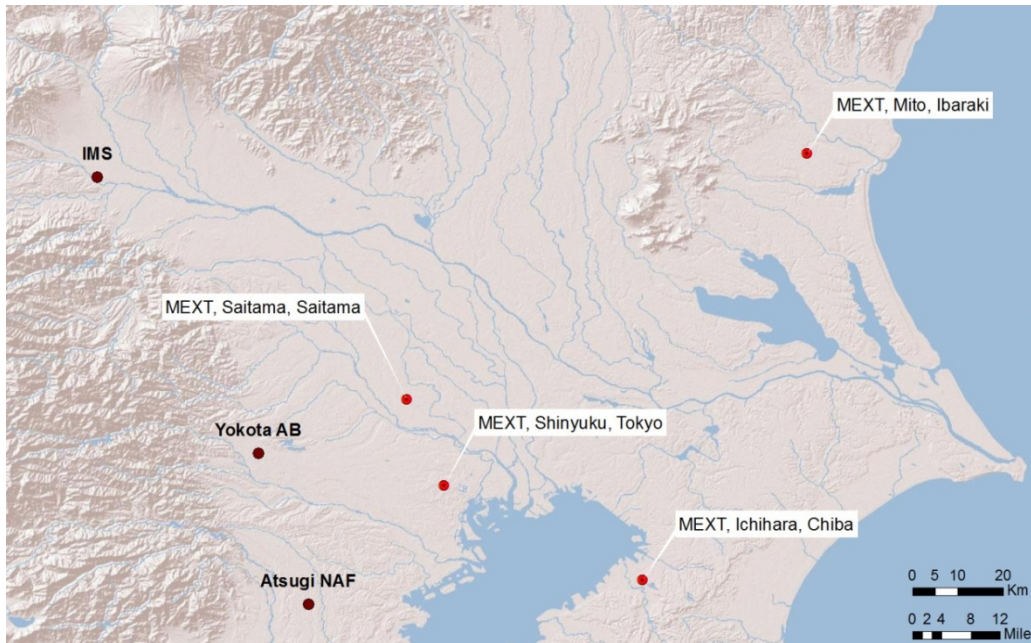


Figure 10. Yokota Air Base—locations of radiation monitoring stations in Tokyo and Saitama Prefectures

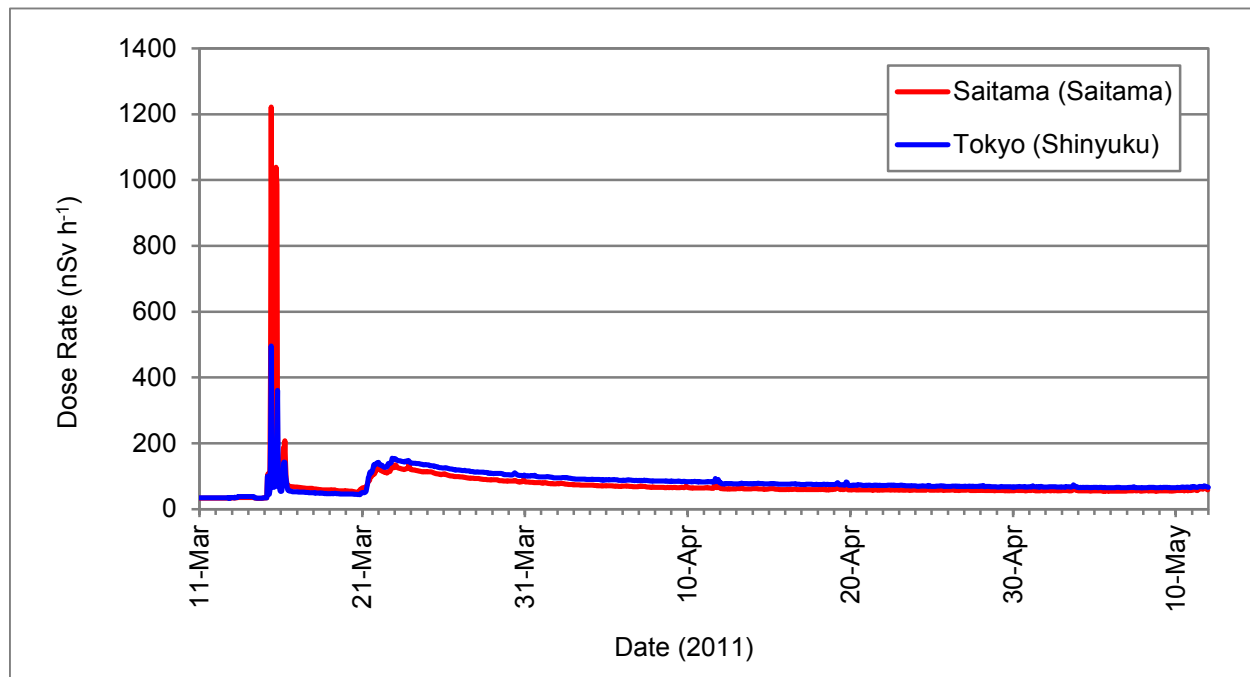


Figure 11. Dose rates from MEXT data at Tokyo and Saitama (stations closest to Yokota Air Base)

Spatial variation in the actual dose rates experienced by an individual and the modeled mean rates based on measurements are accounted for in the external dose estimation for Yokota

Air Base through analysis of the dose rate data at the two MEXT stations shown in Figure 11. To quantify the spatial variability of dose rates in the areas surrounding Yokota Naval Base, the range of dose rate values between the two monitoring stations over the 60-day assessment period was determined for each measurement. The average deviations from the mean data values of the two stations were found to be about $\pm 10\%$. A uniform distribution was selected with a range of $\pm 10\%$ about the mean, i.e., the uniform distribution has a minimum value of $0.9 \times \text{mean}$ and a maximum value of $1.1 \times \text{mean}$. Additional uncertainties could be attributed to the use of surrogate data that are farther from the location of interest. However, the use of the average dose rates from the two closest stations and accounting for their variability are deemed sufficient to implicitly account for such uncertainties. The two monitoring stations and Yokota Air Base are located in the Kanto Plain at an average 225 km (140 mi) from the FDNPS plus or minus 5 percent. At these distances from the source of the release, the three locations would be expected to experience similar radiation fields. Examination of the external dose rate data for these locations in the Kanto Plain supports this expectation. Such radiation fields would be quasi uniform especially since the three locations are not in complex mountainous terrain but rather in a vast, flat plain (Figure 12). Deposition patterns derived from aerial monitoring surveys of external gamma radiation levels conducted by DOE (DOE, 2013) and GOJ show that dose rates and surface activities across the Kanto Plain were nearly uniform as shown in Figure 13 (MEXT, 2011a).

The uncertainty in dose rates from measurements and data errors is modeled in the same manner as for Yokosuka Naval Base above. Thus, it is assumed that the uncertainty in dose rate data follows a normal distribution with an uncertainty factor (ratio of 95th percentile to the mean value) of 1.5. This results in a standard deviation for this normal distribution of $0.3 \times \text{mean}$.



Figure 12. Kanto Plain shown between the mountains and the ocean

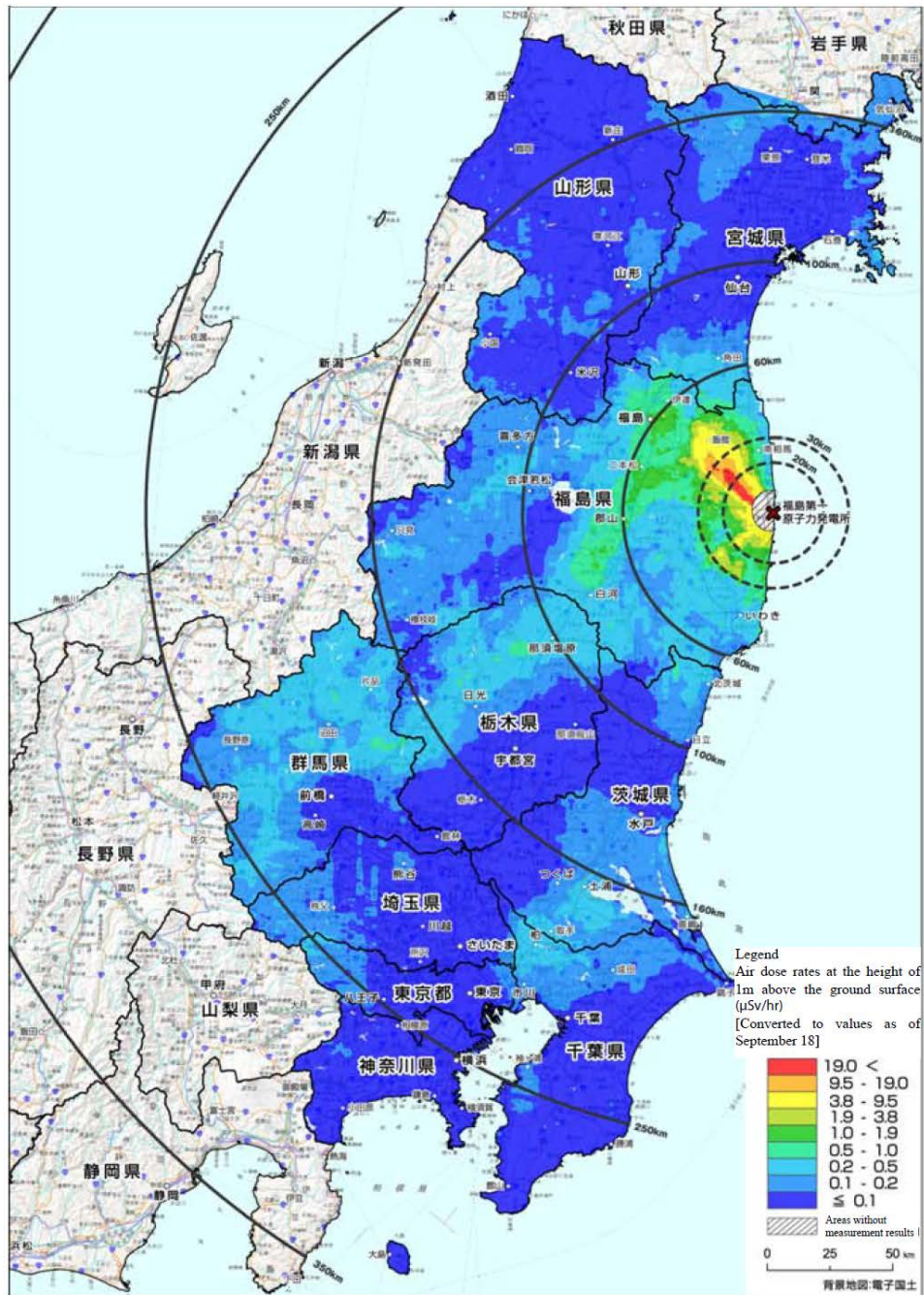


Figure 13. Dose rates at 1 meter above the ground derived from airborne monitoring surveys

4.1.1.3 Sendai Airport and Camp Sendai

The closest radiation monitoring station to Sendai Airport and Camp Sendai with nearly continuous dose rate measurements is the MEXT Miyagi Prefecture station in Sendai City. The

next closest monitoring station is the MEXT Yamagata Prefecture station in Yamagata City. The location of this monitoring station, Camp Sendai, and the Sendai Airport are shown in Figure 14. The data from Miyagi and Yamagata Prefectures are shown in Figure 15. The monitoring station in Sendai City was off line from March 11, 2011, until 1600 local time on March 15, 2011. The monitoring station went offline again at 1600 on March 17, 2011, and did not become operational until 1600 on March 28, 2011.

To account for the missing MEXT data for Miyagi Prefecture, first the ratio of the peak intensities of Miyagi and Yamagata on March 16, 2011, was calculated. Then, the resulting ratio of 1.75 was used as an adjustment factor for the Yamagata Prefecture dose rate data for every hour where Miyagi data were missing. The resulting dose rates from the combination of the Miyagi MEXT data and the data modeled using Yamagata data are shown in Figure 16. The sources of radiation and the profile of the dose rates for Sendai and Yamagata are caused by same conditions as those for Yokosuka Naval Base explained above.

Similar to the data for Yokosuka Naval Base and Yokota Air Base, the sources of uncertainty in the dose rates for Sendai locations are those due to spatial variability and those resulting from measurement and data processing errors (Weitz et al., 2009).

The spatial variability is due to differences in the actual dose rates experienced by an individual and the modeled mean rates that are based on measurements at one or more monitoring stations. This source of variation in dose rates can be accounted for in the external dose assessment through analysis of dose rate data at monitoring locations at or nearby Sendai. Unfortunately, data from only one nearby MEXT station were available for the dose calculations for the two Sendai PEPs. To estimate spatial variability of dose rates in the areas where members of these PEPs may have operated and accounting for movement in a large area, dose rate variability from two sources of data were used. First, the measured dose rates at the MEXT station at Yamagata, located about 54 km (33 mi) roughly west-northwest of Sendai Airport, were analyzed. The dose rates at Yamagata were about a factor of 2 lower than those at Sendai City for periods of time where measurements at both stations are available. It was concluded that this difference is likely due to the presence of mountains east of Yamagata that might have diverted the movement of the plume. For the second source, the map that resulted from the airborne monitoring survey of Miyagi Prefecture made from June 22 to June 30, 2011, was analyzed (MEXT, 2011b). The map showed that the external dose rates in the area of Sendai Airport and Camp Sendai ranged from 0.05 to 0.15 $\mu\text{Sv h}^{-1}$ with a mean of 0.1 $\mu\text{Sv h}^{-1}$. Combining the range of measurements shows that the external dose rates vary by $\pm 50\%$ across the areas near Sendai. Therefore, to model the uncertainty due to spatial variability for Camp Sendai and Sendai Airport PEPs, a uniform distribution was selected with a range of $\pm 50\%$ about the mean, i.e., the uniform distribution has a minimum value of $0.5 \times \text{mean}$ and a maximum value of $1.5 \times \text{mean}$.

The uncertainty in dose rates from measurements and data errors is estimated in a similar manner as for Yokosuka Naval Base shown above. Therefore, the uncertainty in dose rate data were modeled as a normal distribution with an uncertainty factor (ratio of 95th percentile to the mean value) of 1.5, which results in a standard deviation of $0.3 \times \text{mean}$.

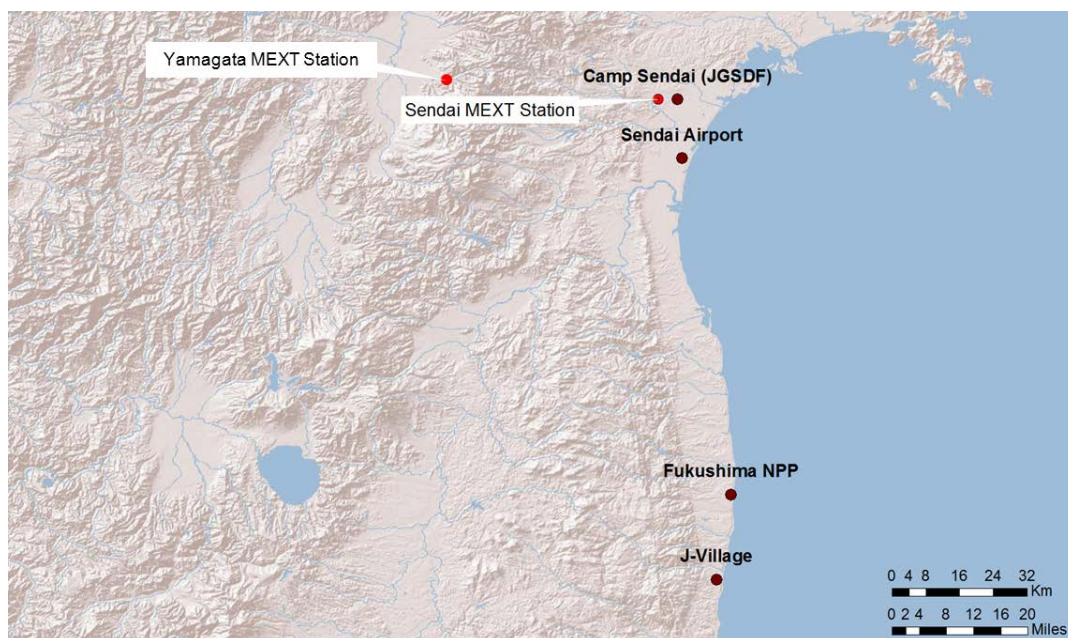


Figure 14. Location of the radiation monitoring stations in Sendai City and Yamagata City

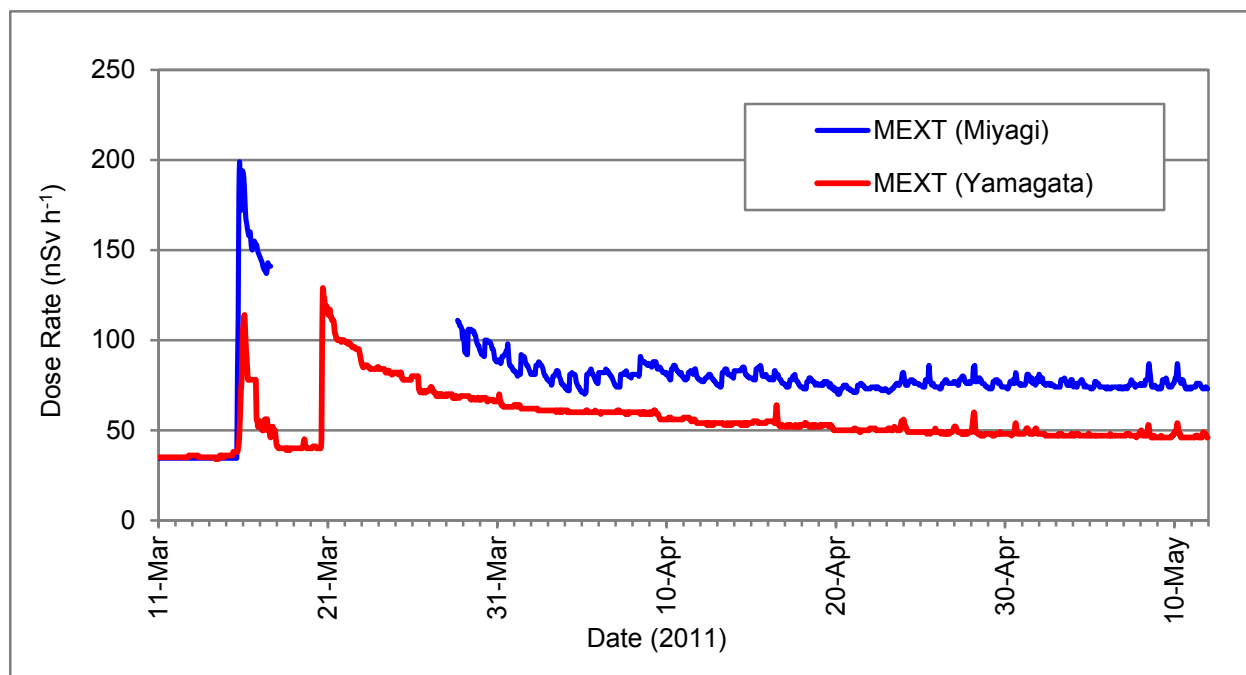


Figure 15. Dose rates from MEXT monitoring stations at Sendai City and Yamagata City

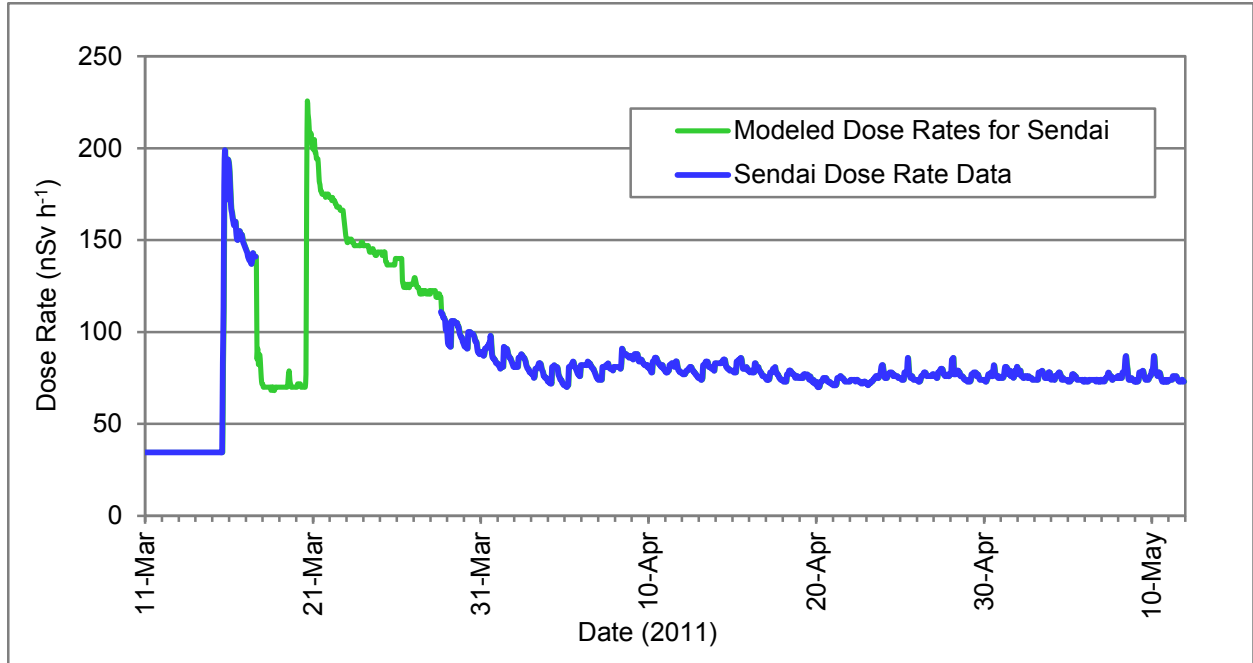


Figure 16. Combined measured and modeled dose rates for Sendai locations

4.1.2 Indoor Dose Reduction Factor

Buildings and other structures provide partial shielding from the effects of gamma radiation emitted by radioactive materials present outside the structure. The amount of time that an individual spends outdoors and indoors affects the external dose received and is accounted for through the use of the *IDRF*. The *IDRF* is calculated based on NTPR standard method SM ED02 (DTRA, 2010) and is defined in Equation 2 as follows:

$$IDRF = F_{OD} + \left[(1 - F_{OD}) \times \left(\frac{F_{Res}}{PF_{Res}} + \frac{F_{NR}}{PF_{NR}} \right) \right] \quad (2)$$

where:

F_{OD}	=	Fraction of each day spent outdoors (unitless)
F_{Res}	=	Fraction of indoor time spent in a residence (unitless)
PF_{Res}	=	Protection factor for a residence (unitless)
F_{NR}	=	Fraction of indoor time spent in a non-residence (unitless)
PF_{NR}	=	Protection factor for non-residence structures (unitless)

4.1.3 Time Spent Outdoors

The time spent outdoors is used for calculating the doses due to exposure to external radiation and the inhalation of radioactive materials. Estimates of the amount of time spent outdoors for the various age groups considered by the DARWG, except for the humanitarian field workers at Sendai, were obtained from the statistical results reported in the USEPA Exposure Factors Handbook (USEPA, 2011). The statistical results, based on the Consolidated Human Activity Database (CHAD) for 14 age groups, consisted primarily of values for the minimum, median, maximum, mean, and standard deviation. The values reported in Exposure Factors Handbook were given as time spent outdoors in minutes per day. The use of distributions based on Exposure Factors Handbook/CHAD data are the best available information and is deemed adequate for DOD-affiliated individuals living and working at U.S. and other installations in Japan.

The median and maximum values reported in USEPA (2011) were used as the basis for the mode and maximum values for defining triangular distributions for each age group. Because the age groups in the Operation Tomodachi assessments do not coincide with the age groups studied in USEPA (2011), averages among multiple age groups were estimated and rounded to the nearest half-hour. The minimum values of the triangular distributions were based on subjective judgment to be 0 or 15 minutes. The mean values and standard deviations, for ages greater than 17 years, were calculated using the assumed triangular distributions and compared to the averaged values from the corresponding age groups reported in USEPA (2011). This comparison revealed that the values from the assumed triangular distribution were significantly larger than the values reported in the USEPA (2011). To tighten and further skew the modeled distributions to better match the reported statistical results, the triangular distributions were replaced with log-triangular distributions that used the same properties as the triangular distributions, except where the minimum was 0, which was changed to 6 min (0.1 h) to avoid calculations using the logarithm of 0. The mean and standard deviation of the log-triangular distribution showed a close match to the published values in the Exposure Factors Handbook (USEPA, 2011). Therefore, for the purpose of this study, log-triangular distributions were retained to represent the time spent outdoors for the various age groups, except for the humanitarian field workers at Sendai. The attributes of these distributions are given in Table 4. The values selected for age groups other than adults and humanitarian field workers are included for completeness and possible future application. The basis for the time spent outdoors for all age groups is the Exposure Factors Handbook (USEPA, 2011) except for humanitarian field workers.

The humanitarian field workers are assumed to have spent most of their shift hours outdoors. Although exact PEP information was not available, many interviews and anecdotal information can be found in various articles published on military and non-military websites (Stroad, 2011; Bonson, 2011). In addition, the authors based their assumptions on the military practice for troops working up to 12-hour shifts in the field during humanitarian response missions assuming 24 hour a day and seven days a week operations. It was assumed that humanitarian field workers at Sendai Airport spent no less than 6 h outdoors on days performing assistance duties when conditions inhibited a full 12-hour shift presence outside. It was also assumed that the most time in a day these workers could have been present outdoors was 14 h, which includes a full 12-hour shift and an additional allowance of 2 h for shift handover, exercising, and resting outdoors. A median of 10 h was selected as a reasonable value for the assumed outdoor time. A triangular distribution was deemed reasonable (Table 4) based on

information that humanitarian field workers operated mostly outside of their tents and more likely spent about 10 h outdoors, on average. The likelihood that these individuals spent more than 14 h or less than 6 h outdoors is judged to be less than 5 percent.

Table 4. Distributions of the amount of time spent outdoors

Age Group	Distribution	Minimum* (h d ⁻¹)	Mode* (h d ⁻¹)	Maximum* (h d ⁻¹)
3 months	Log-triangular	0.1	1	10
1 year	Log-triangular	0.1	1.5	13.5
5 years	Log-triangular	0.25	2	16
10 years	Log-triangular	0.25	2	16
15 years	Log-triangular	0.25	2	16
Adults (> 17 years)	Log-triangular	0.25	1	17
Humanitarian field workers	Triangular	6	10	14

*For log-triangular distributions, entries are the time values in hours per day that correspond to the exponentials of the min/mode/max of the distribution; these values are easier to relate to actual time durations. The actual parameters that are used for the minimum, mode and maximum for the log-triangular distributions are the logarithms of the numbers shown in this table.

The time spent indoors, i.e., 24 h minus hours spent outdoors, was assumed to consist either of time spent in a residence, typically a house or an apartment, or a non-residential structure such as office building, hangar, repair shop, etc. Based on subjective judgment, for the adult PEPs stationed at Yokosuka Naval Base, Yokota Air Base and Camp Sendai, a reasonable distribution of the fraction of indoor time spent in a residence is uniform and ranged between a minimum of 0.4 and 1.0. The low end of the range is a reasonable assumption based on the time needed for sleep and minimal personal care. The top end of the range reflects non-work days where an individual spent all time indoors in a residence. For the 1-to-2 year-old PEP at Yokota Air Base, the fraction of indoor time spent in a residence was assumed to have varied uniformly between a minimum of 0.8 and a maximum of 1.0, which reflects that small children do not have jobs and would spend fewer hours away from home than adults while indoors. The fraction of non-residential time spent indoors by any group was then obtained as the difference (1 minus the fraction of time in a residence).

The humanitarian field workers who camped in tents at Sendai Airport spent a small amount of time inside buildings. For these individuals, the fraction of indoor time spent in tents for work, sleep and personal care was modeled with a uniform distribution between 0.8 and 1.0. The fraction of non-residential time spent indoors, such as the airport terminal, Camp Sendai or in other administrative buildings, was then obtained as the difference (1 minus the fraction of time in a residence). The parameter values of the uncertainty distributions for the time fractions spent for residential and non-residential locations are found in Appendix B.

4.1.4 Protection Factor

The types of structures an individual occupied while indoors affect the dose from exposure to external radiation. Structures of different types and sizes provide varying degrees of

protection from radiation emitted by radioactive materials in the environment. A protection factor, defined as the ratio of the outdoor to indoor dose rates, quantifies the degree of radiological protection afforded by various structures.

In this study, the distributions of protection factors for buildings and tents are estimated using the models reported in Weitz et al. (2009). In these models, the point-kernel method (Stevens and Trubey, 1972) is applied. The propagation of gamma radiation through air is estimated by a point kernel that accounts for all the propagation effects (i.e., attenuation, scattering and build-up, air-ground interface) except dispersion. The point-kernel function is derived with the two-dimensional transport code CYLTRAN (Halbleib et al., 1992) for propagation of gamma radiation through air over soil. Spectra provided in Finn et al. (1979) for fast neutron fission of U-235 were used to characterize the gamma radiation emitted by a field of deposited radioactive materials. It is assumed that structures are situated in a field of uniformly deposited radioactive materials that extends infinitely in all directions.

Numerical distributions of protection factors are calculated for locations inside an assumed rectangular structure with user-specified dimensions, and wall and roof thicknesses. The walls and roof of a building may be composed of wood, aluminum, iron/steel, or concrete; glass windows may be substituted for a portion of the wall space. The model is also capable of calculating protection factor distributions for tents made of canvas for which the wall and roof thicknesses are set to zero.

4.1.4.1 Protection Factors for Yokosuka Naval Base, Yokota Air Base and Camp Sendai

Based on published information on housing and billeting quarters at Yokosuka Naval Base and Yokota Air Base (CNIC, 2013; Air Force Housing, 2013), the residence building is assumed to be a two-story concrete structure of the town-house type with a sample shown in Figure 17. Furthermore, published floor plans allowed selecting typical dimensions of a three-bedroom town-house as 10 m by 7 m (33 ft by 23 ft) with a total height of 7 m (23 ft). A total of 4 m (13 ft) of the front and back walls assumed to include glass windows. The concrete walls, roof and intermediate floor-ceiling are specified to be 10 cm (4 in) in thickness. Using the method described above, the protection factor distribution for a residence building is estimated. The resulting probability density, shown as a histogram, and the cumulative probability function are presented in Figure 18. The mean protection factor for the selected residence building is 4.7 and the corresponding 95th percentile is 6.2.

For the non-residential buildings, a three-story concrete structure is selected with dimensions of 50 m by 15 m (160 ft by 50 ft) and a total height of 15 m (50 ft) (Figure 19). About half of the perimeter wall is assumed to include glass windows. The thickness of the concrete walls is specified as 15 cm (6 in), while the roof and intermediate floor ceilings are 10 cm (4 in) each. Using the method described above, the protection factor distribution for a non-residential building is estimated with the probability density, shown as a histogram, and the cumulative probability function are presented in Figure 20. The mean protection factor for the selected non-residential building is 11 and the corresponding 95th percentile is 22.

Many office and housing facilities at Yokosuka Naval Base and Yokota Air Base are hi-rise buildings, which afford higher protection levels than those selected for this study. For such buildings, protection factors can vary from about 10 for the lower or top floors, to 50 for interior rooms in upper floors, to over 100 for rooms centrally located in the middle of the

building or below grade levels as shown in Figure 21 (Glasstone and Dolan, 1977; OSTP, 2010; Buddemeier and Dillon, 2009). However, the building type chosen to represent non-residential buildings in this study is representative of a large majority of the buildings at Yokosuka Naval Base and Yokota Air Base.



Figure 17. Example of a two-story townhouse at Yokosuka Naval Base

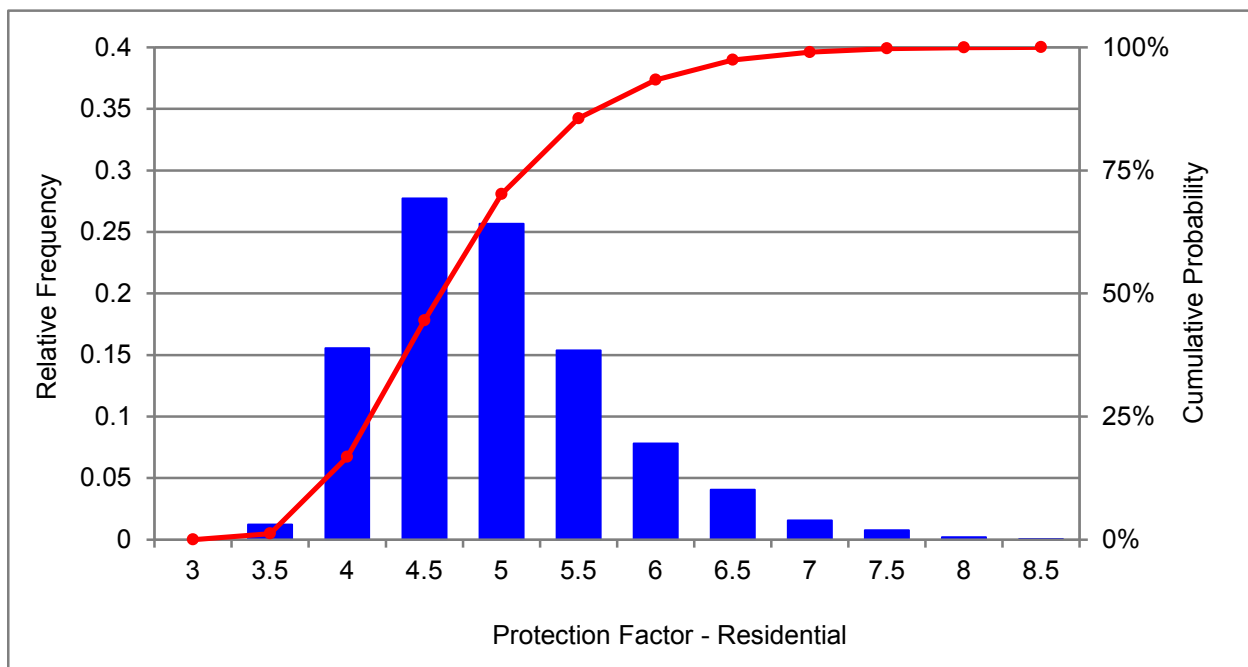


Figure 18. Probability density and cumulative distribution functions of the protection factor for a residential structure



Figure 19. Example of non-residential building at Yokosuka Naval Base

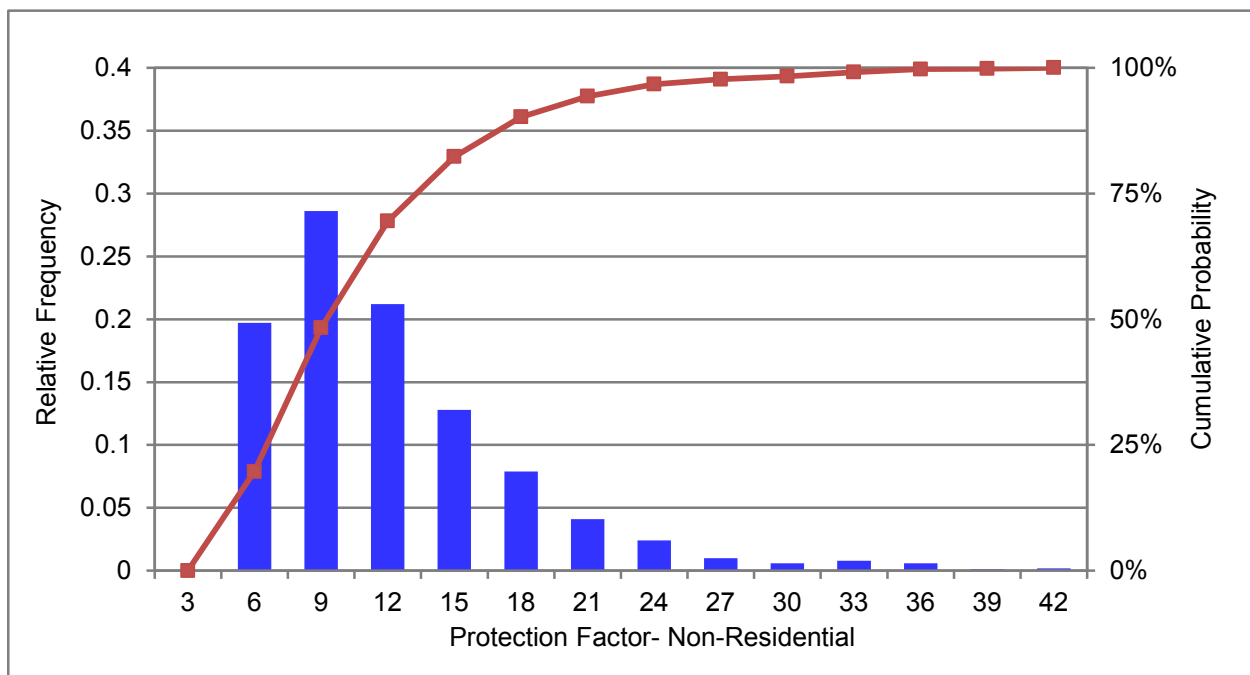


Figure 20. Probability density and cumulative distribution functions of the protection factor for a non-residential structure

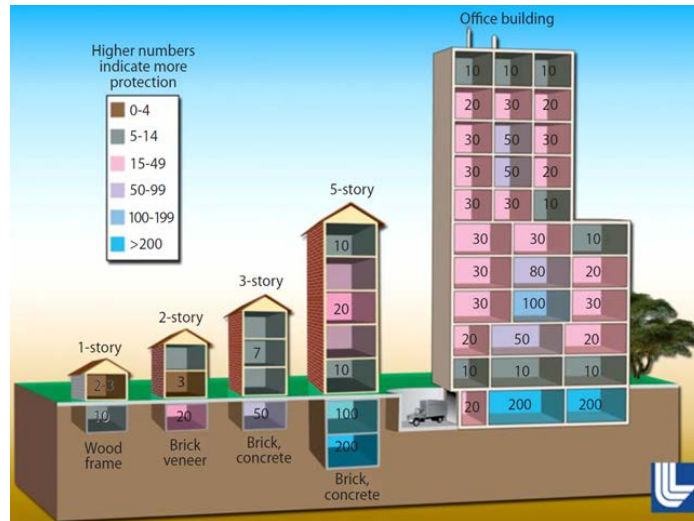


Figure 21. Protection factors for a variety of building types and locations (from Buddemeier and Dillon, 2009)

4.1.4.2 Protection Factors for Tents at Sendai Airport

The 200 service members who set up camp at the Sendai Airport lived and worked in about 20 tents in addition to carrying out humanitarian missions in the field. The tents were of the type shown in Figure 22 and Figure 23 with dimensions of 5 m by 11 m (18 ft by 35 ft) with a height at the crest of 4 m (12 ft) (3 m (10 ft) average roof height). Using these characteristics and assuming a negligible canvas thickness, the protection factor distribution for this type of tent was numerically calculated resulting in a mean of about 1.5 and a 95th percentile of about 2.0. The probability density, shown as a histogram, and the cumulative probability distribution are presented in Figure 24.



Figure 22. Military personnel spending time inside a tent at the camp erected at Sendai Airport

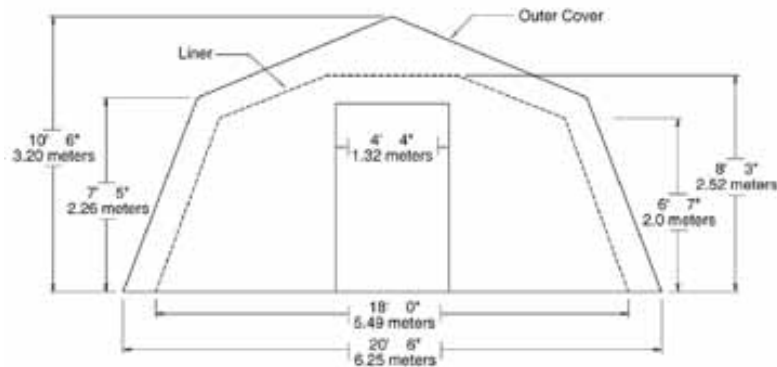


Figure 23. Tents used by service members in the camp erected at Sendai Airport

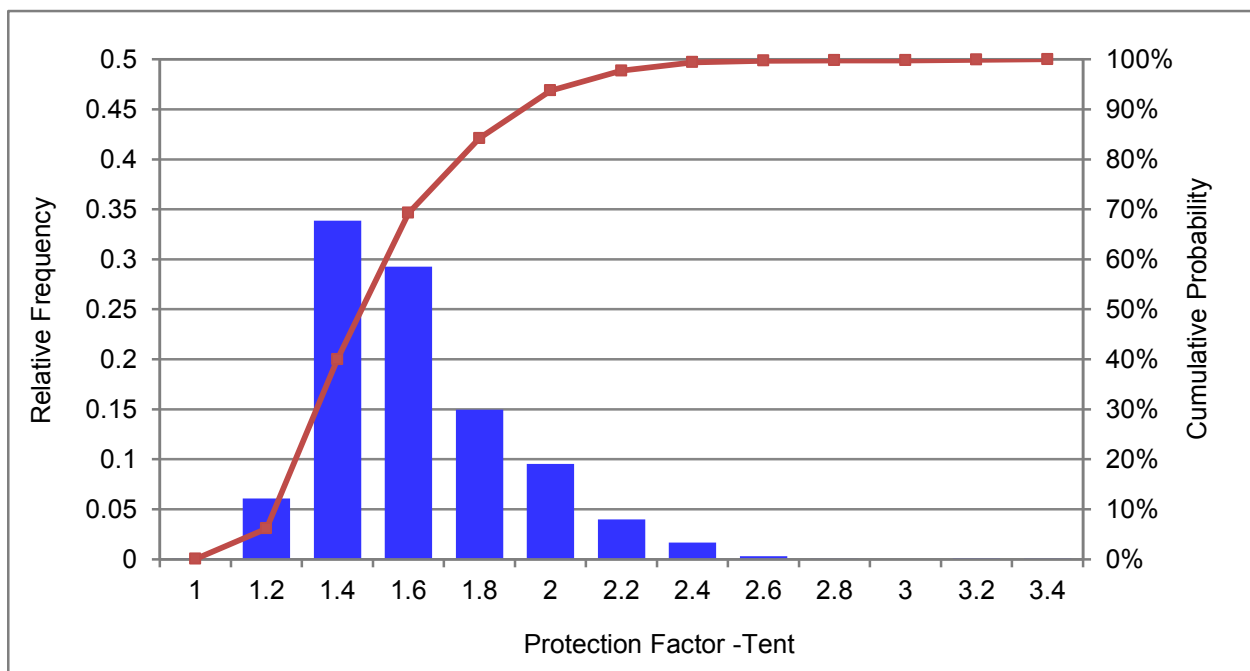


Figure 24. Probability density and cumulative distribution functions of the protection factor for a tent

4.2 Exposure to Internally-Deposited Radioactive Materials

Following the FDNPS accident, environmental releases of radioactive materials to the air occurred with subsequent deposition in and contamination of water and soil. The sources of exposure to internally-deposited radioactive materials are:

- Inhalation of air contaminated with radioactive gases or aerosols due to either the releases from the FDNPS or the resuspension of radioactive materials deposited on the ground and other surfaces.
- Ingestion of drinking water (tap water) derived from surface sources that are contaminated with deposited radioactive materials.
- Incidental ingestion of soil and dust from handling contaminated surfaces and potentially contaminants that deposit on food or in beverages containers.

In this report, internal doses are assessed for both males and females using the male-specific intake rates and dose coefficients because gender-specific parameter values produce nearly the same results (ICRP, 1995a, Paragraph 24). This assumption is based on the fact that, on average, the total body mass of a female is approximately 20 percent less than that of a male and that a female's intake rates are also less than the male's by the same amount.

For food consumption, based on the discussion in Cassata et al. (2012), it is presumed that DOD-affiliated individuals consumed food that was monitored and tested in accordance with DOD and FDA procedures and regulations, and found unaffected by FDNPS releases of radioactive materials. Radiation doses due to food consumption have been estimated for DOD-affiliated individuals who may have eaten some local produce, meat, fish, or dairy products in Cassata et al. (2012) and the estimated doses were considered low.

4.2.1 Inhalation Intakes

The internal exposure to radioactive materials could have occurred from inhaling radioactive materials in a passing plume or from resuspended particles that were previously deposited on the ground or other surfaces. The committed effective dose or committed equivalent dose to the thyroid from inhalation of airborne radionuclides is calculated using Equation 3 as follows:

$$E_{Inh} = V_{Air} \sum_j \left(DC_{Inh j} \int_{t_{start}}^{t_{end}} C_{Air j}(t) dt \right) \quad (3)$$

where:

E_{Inh} = Either the committed effective dose or the committed equivalent dose to the thyroid (Sv) due to inhalation of radioactive materials

V_{Air}	=	Effective volume of contaminated air inhaled per day for each activity level ($\text{m}^3 \text{d}^{-1}$) (details of this parameter are discussed below)
$DC_{Inh j}$	=	Inhalation dose coefficient for radionuclide j (Sv Bq^{-1})
t_{start}	=	Beginning time of an individual's exposure
t_{end}	=	End time of an individual's exposure
$C_{Air j}(t)$	=	Measured or modeled air activity concentration of radionuclide j at time t (Bq m^{-3})

4.2.1.1 Airborne Activity Concentration

The values for the measured or modeled air activity concentration ($C_{Air j}(t)$) were based on laboratory analyses of filter media and activated charcoal cartridges, and were for the isotopes normally associated with releases due to accidents at nuclear power plants. Isotopes associated with naturally occurring gamma emitters such as in the uranium decay chain were excluded. During the DOD response to the accident, various military organizations made air sampling measurements in an attempt to determine the airborne activity concentrations of radioactive materials to which DOD-affiliated persons were being exposed. All isotopes measured using air sampling were assumed to exist in aerosol form. Isotopes of iodine were also assumed to exist in gaseous form because air sampling of iodine gases was limited. Furthermore, gaseous iodine was assumed to exist in both elemental and organic forms even though no samples were analyzed to determine composition of iodine gases. The radionuclides included in the modeled air activity and their chemical/physical forms are shown in Table 5. The radionuclides relevant to inhalation doses are described in detail in Cassata et al. (2012).

The values for most aerosol air activity concentrations for Yokosuka Naval Base and Yokota Air Base were obtained directly from the air concentration measurement data made at Yokota and reported in Cassata et al. (2012). The values for Sendai Airport and Camp Sendai were modeled using air concentration measurements made at those locations augmented with modeled values as described below and in Appendix D. Because of limitations of the air sampling measurements, most air samples were not analyzed for Sr-89 and Sr-90. The air activity concentrations for the isotopes of strontium and the gaseous forms of iodine were estimated using ratios to concentration of radionuclides that were measured in a limited number of air samples. Also, several low-volume air samples were taken using in-line glass fiber/charcoal canisters that were capable of collecting both aerosol and gaseous forms of iodine as described in Cassata et al. (2012). These measurements were used to estimate the distribution of gas-to-aerosol ratio of radioiodines.

**Table 5. Radionuclides and chemical forms considered
for air activity and inhalation pathway**

Aerosols		Gaseous (Elemental)	Gaseous (Organic)
Sr-89	I-131	I-131 I-132 I-133	I-131
Sr-90	I-132		
Mo-99	I-133		I-132
Tc-99m	Cs-134		I-133
Te-129	Cs-136		
Te-129m	Cs-137		
Te-131m	La-140		
Te-132			

The air activity concentration results for Yokota Air Base are from sample measurements and are provided in Figure 25 (Cassata et al., 2012). The air activity concentration at Yokota Air Base is from 24-h continuous sampling using very high flow rate samplers with filters that were subsequently analyzed for isotopic activity concentrations. These measurements are used as the central estimates in the calculation of air inhalation doses for Yokota Air Base PEPs in this study.

Most of the air activity concentration samples taken at Yokosuka Naval Base used low-volume portable samplers that were not capable of collecting sufficient activity for reliable analysis. In addition, many of the air concentration measurements were made for short durations that would not adequately record the variation over the course of a day, which is the time duration used in calculating inhalation doses. This resulted in reported air activity concentrations that varied by several orders of magnitude for samples made at similar times and in similar areas as described in Cassata et al. (2012). Given the issues of limited sampling and non-representativeness of the results for the purpose of dose assessment in this study, the Yokosuka Naval Base air activity concentration measurements were not used in the probabilistic analysis. Rather, the Yokota Air Base air activity concentrations were used as surrogate data for Yokosuka Naval Base with an appropriate adjustment. The Yokota Air Base air activity concentrations are assumed to be similar to Yokosuka Naval Base because of similar external radiation levels, comparable distance and direction from FDNPS, and analogous time variation of the dose rates associated with the passing of airborne radioactive materials.

To account for possible differences between air activity concentrations at Yokosuka Naval Base and Yokota Air Base, the Yokota Air Base data were adjusted using a ratio of the external dose rates for the two locations. The ratio of the external dose rates at Yokosuka Naval Base to Yokota Air Base were calculated for each hour. The calculated hourly ratios have a 5th percentile of 0.45, a 95th percentile of 0.9 and a median of about 0.5. These values were used to create a triangular distribution that was used to represent the uncertainty of the adjusting ratio, which accounts for differences between air activity concentrations at Yokota Air Base and Yokosuka Naval Base.

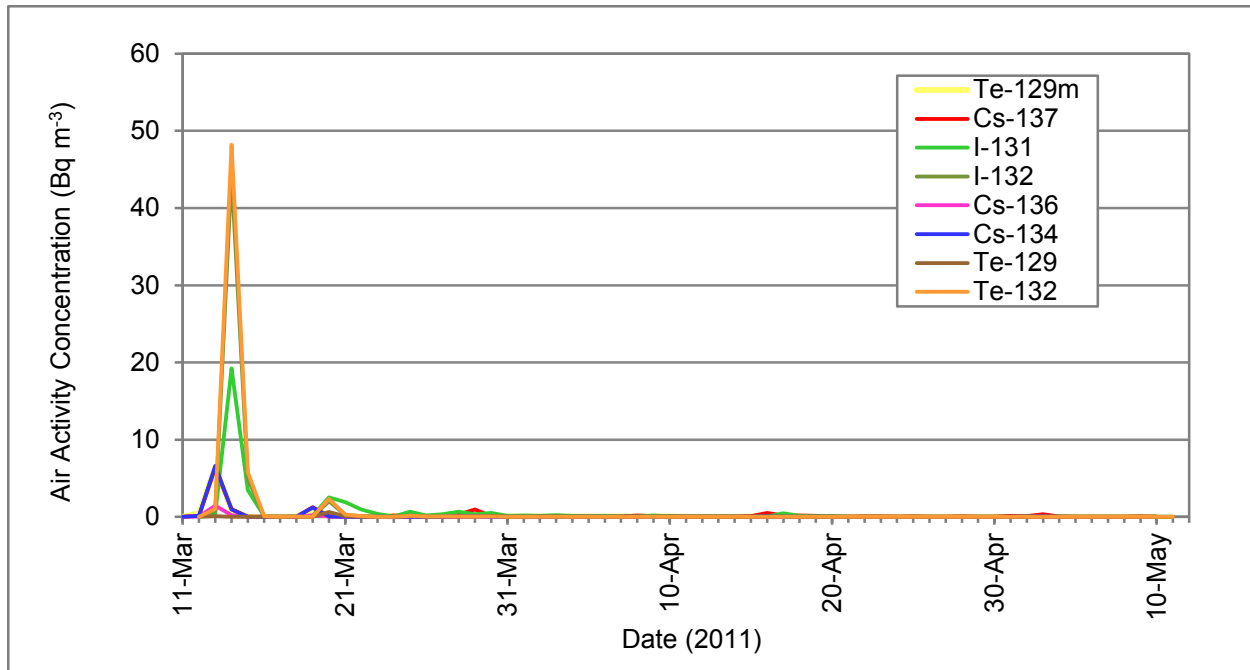


Figure 25. Air activity concentrations measured at Yokota Air Base for selected radionuclide

For Sendai Airport and Camp Sendai, air concentration data from limited measurements by DOD teams were available. Air samples were collected on six separate days between March 21 and April 11, 2011 and are included in Table 6. This means that no samples were collected on the days where air concentrations peaked between March 15 and March 21, 2011. In addition, all samples were low volume and were collected over durations of a few hours. Given the lack of representativeness and limited amount of this data, only the mean assigned to the mid-point date of March 31, 2011, is used to develop air activity concentration models for I-131, Cs-137 and Cs-134.

In addition to using the mean value of the available air activity concentration data at Sendai Airport for each of the three radionuclides mentioned above, the model relies on the 24-h continuous daily measurements at Yokota Air Base and the patterns of change in daily doses compiled from dose rate data collected at Sendai and Yamagata MEXT monitoring stations. The details of the model are presented in Appendix D and the results for I-131 are shown in Figure 26. All other isotopes were modeled using the methods from Cassata et al. (2012).

Table 6. Measured air activity concentrations at Sendai locations

Sample Number	Sampling End Date as Reported	Cs-134 (Bq m ⁻³)	Cs-137 (Bq m ⁻³)	I-131 (Bq m ⁻³)
SEN21MAR110915	21-Mar-11	0.14	0.18	0.42
SAP28MAR111422	28-Mar-11	0.20	0.23	0.98
SAP28MAR112130	28-Mar-11	0.16	0.16	0.37
20241B	28-Mar-11	0.52	0.52	1.85
SAP31MAR110625	31-Mar-11	1.35	1.45	1.03
SAP31MAR111726	31-Mar-11	0.02	0.02	<MDA *
21198A	7-Apr-11	0.48	0.47	0.64
21199A	8-Apr-11	1.04	0.07	0.14
21200A	8-Apr-11	1.01	1.00	1.00
21208A	11-Apr-11	0.05	<MDA	<MDA
Average		0.50	0.46	0.80

* Minimum detectable activity

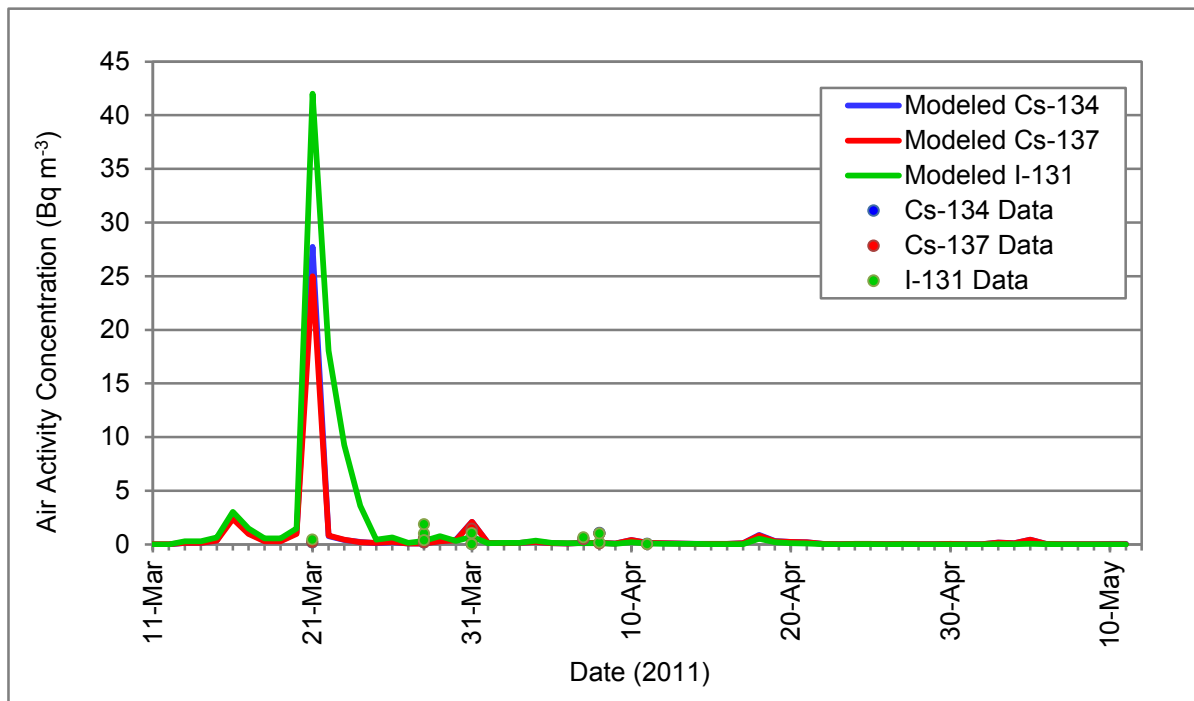


Figure 26. Sendai air activity concentration model based on daily dose rates and activity measurements at Yokota Air Base

Air activity concentrations for gaseous forms of three isotopes of iodine (I-131, I-132, and I-133) were estimated using the ratio of activities from measured gaseous to aerosol iodine. In addition, an elemental or organic fraction was used to partition the four isotopes of gaseous iodine into elemental or organic forms (Cassata et al., 2012). The air activity concentrations of gaseous elemental or organic iodine are calculated using Equation 4a-b as follows:

$$C_{I-GEj}(t) = C_{I-MAj}(t) R_{GA} F_{Elem} \quad (4a)$$

$$C_{I-GOj}(t) = C_{I-MAj}(t) R_{GA} (1 - F_{Elem}) \quad (4b)$$

where:

$C_{I-GEj}(t)$	=	Modeled air activity concentration of gaseous elemental iodine for radioiodine j (Bq m ⁻³)
$C_{I-GOj}(t)$	=	Modeled air activity concentration of organic gas for radioiodine j (Bq m ⁻³)
$C_{I-MAj}(t)$	=	Measured air activity concentration of aerosol iodine for radioiodine j (Bq m ⁻³)
R_{GA}	=	Gas-to-aerosol concentration ratio (unitless)
F_{Elem}	=	Elemental fraction of gaseous iodine (unitless)

The main sources of uncertainty in air activity concentration are comprised of the following:

- Spatial variability.
- Measurement and data errors.
- Uncertainty in the ratio of gaseous to aerosol air concentrations of radioiodines.
- Uncertainty in the fraction of elemental or organic iodine in gaseous radioiodines.
- Uncertainty in the ratio of strontium radionuclides-to-cesium.
- Uncertainties from using surrogate or modeled data at Yokosuka Naval Base and Sendai.

Spatial variability in the air activity concentrations of radioactive materials inhaled by an individual is accounted for by assuming that the uncertainties are similar to those of the external dose rates for Yokosuka Naval Base and Sendai. A uniform distribution was selected with a range of variability of $\pm 30\%$ for Yokosuka Naval Base and $\pm 50\%$ for Sendai of the total air activity concentration for each included isotope.

The spatial variability for Yokota Air Base was based on a comparison of the daily average air activity measured at Yokota Air Base and the International Monitoring Station (IMS) in Takasaki, Japan. The range of total air activity between the two air monitoring stations was determined for each day of the 60-day assessment period. The average deviation of air activity concentrations between the two monitoring stations was ± 30 . A uniform distribution was selected for the spatial variability of air activity concentration at Yokota Air Base with a minimum value of $0.7 \times \text{mean}$ and a maximum value of $1.3 \times \text{mean}$.

The uncertainty from measurements and data errors in air activity concentration is due to the uncertainties inherent to sampling and measurement instrument precision, calibration error, data processing tools, and data recording errors. The measurement uncertainty is considered the same for all four sites since measurements (air filter samples) were made using similar instruments (high volume air samplers) and were made by personnel with comparable levels of training and experience (Air Force and Army health physicists and radiation protection technologists). The measurement uncertainty used in this study is derived from the methods for estimating measurement and data error used for the NTPR program (Weitz et al., 2009; DTRA, 2010, SM UA01). The selected distribution is the normal distribution with an uncertainty factor of 1.5 and a standard deviation of 0.304 times the mean.

The uncertainty in the ratio of gaseous to aerosol iodine was determined using the results of in-line air samples collected with both glass-fiber filters and activated charcoal canisters by DOD organizations at Yokota Air Base and at the U.S. Embassy in Tokyo (Cassata et al., 2012). Air activity concentration measurements were analyzed for both aerosol and gaseous I-131 for 102 samples and the ratio of concentrations were calculated. The relative frequency distribution of the ratio of gaseous to aerosol iodine is shown in Figure 27. The 102 results were rank ordered and fitted to a log-normal distribution, a normal distribution, a uniform distribution, a log-triangular distribution, and a triangular distribution. The results of the fitted distributions were then plotted against population percentiles from the collected data to determine which distribution best fit the dataset. A plot of the fitted distributions and the percentile values are shown in Figure 28. A log-normal distribution with a geometric mean of 2.4 and a geometric standard deviation of 1.9 was selected as the best fit to the statistical data from the measured activity concentration ratios. This distribution of gas-to-aerosol ratio was used for all four locations.

No measurements were made to determine the fractions of the gaseous iodine in elemental or organic forms. Consequently, the uncertainty in these fractions was based on published data for iodine concentrations in the environment after release from a nuclear power station (Nair et al., 2000). The partition depends on environmental conditions such as temperature, humidity, time after release, distance from the source, and ozone concentration in the air. The published data indicates that the fraction of organic or elemental form in gaseous iodine can range from 0 to 1. To account for this parameter uncertainty, a triangular distribution was selected with a minimum of 0, a mode of 0.5, and a maximum of 1 for the elemental iodine. The fraction of organic iodine is then calculated as (1 minus the fraction of elemental iodine).

The uncertainty of strontium radionuclides-to-cesium ratio was determined using the results of 15 soil samples taken in Fukushima Prefecture that were analyzed for Cs-137 and Sr-90. Three of the soil samples were taken in March 2011, six in April 2011, and six in May 2011. The calculated ratios ranged from a minimum of 0.0002 to a maximum of 0.00143 and a mean of 0.00053 (Cassata et al., 2012). For the probabilistic analysis, a triangular distribution

was selected to represent the strontium radionuclides-to-cesium ratio with a minimum of 0.0002, a mode of 0.00053, and a maximum of 0.0015. This distribution was then applied to both Sr-89 and Sr-90 (Cassata et al., 2012).

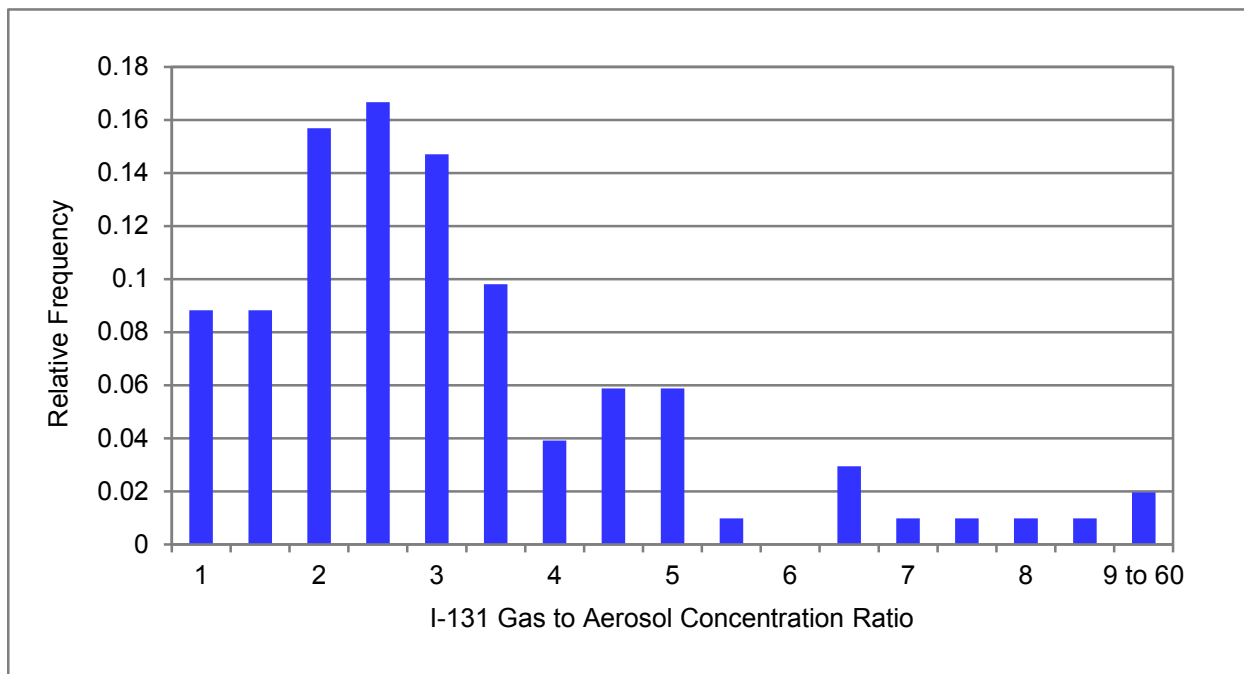


Figure 27. Relative frequency distribution of I-131 gas-to-aerosol air activity concentration ratios at U.S. Embassy (Tokyo) and Yokota Air Base

Additional uncertainties are due to the use of surrogate or modeled air activity concentration data for Yokosuka Naval Base and Sendai locations. For Yokosuka Naval Base, it is assumed that the uncertainty introduced through the use of adjusted measurement data from Yokota Air Base has an uncertainty factor of 2 that then follows a normal distribution with a standard deviation of 0.56. The basis for this assumption is provided in the analysis of uncertainties introduced through the use of surrogate environmental data that corresponds to an additional uncertainty factor of 2 (Weitz et al., 2009). For Sendai, it is assumed that the additional uncertainty introduced by using modeled and surrogate air activity concentration measurement data from Yokota Air Base corresponds to a log-normal distribution with an uncertainty factor of 3 corresponding to a geometric standard deviation of 1.95. This assumed distribution is based on an analysis of additional uncertainties from using surrogate extrapolated data (Weitz et al., 2009).

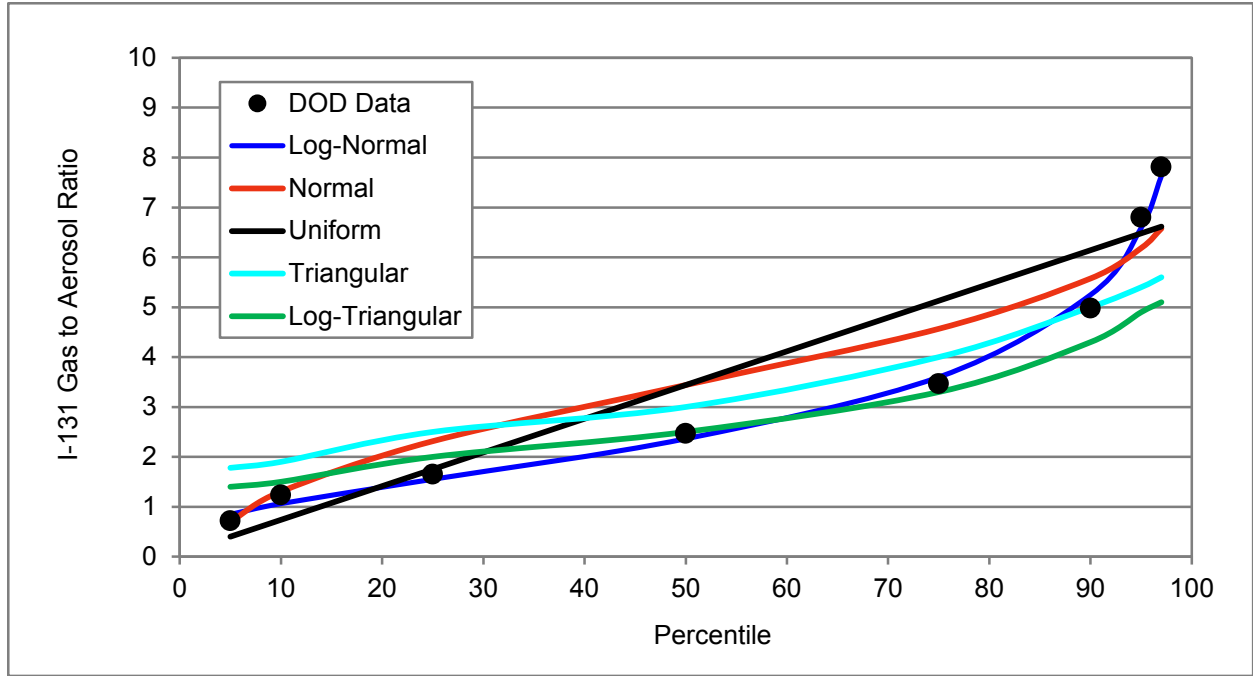


Figure 28. Fitted distributions and statistical data of the ratios of I-131 gas-to-aerosol air activity concentration collected at U.S. Embassy (Tokyo) and Yokota Air Base

4.2.1.2 Inhalation Rate

The total volume of air a person inhales per day is referred to as the daily inhalation rate (USEPA, 2009). The volume of contaminated air inhaled per day is the “effective” volume of air that is used as the basis for calculating intakes by inhalation. The volume of contaminated air inhaled each day is calculated using four primary factors: the fractions of time spent indoors and outdoors, the fractions of time spent in four activity (exertion) levels, the inhalation rates for these activity levels, and the degree of infiltration of contaminants from outdoors to indoors that is represented by a ratio of air concentration indoors versus outdoors. The model used to calculate the effective volume of inhaled contaminated air is given by Equation 5 as follows:

$$V_{Eff} = F_{OD} \sum_k F_{ALout\ k} IR_{AL\ k} + (1 - F_{OD}) SIF \sum_k F_{ALin\ k} IR_{AL\ k} \quad (5)$$

where:

V_{Eff}	=	Daily effective volume inhaled ($m^3 d^{-1}$)
F_{OD}	=	Fraction of time spent outdoors (unitless)
$F_{ALout\ k}$	=	Fraction of outdoor time spent in activity level k (unitless)
$IR_{AL\ k}$	=	Inhalation rate for activity level k ($m^3 d^{-1}$)

SIF	=	Structure infiltration factor (unitless)
$F_{ALin\ k}$	=	Fraction of indoor time spent in activity level k (unitless)

For the inhalation dose calculations, all sources of airborne radioactive materials are assumed to be outdoors and buildings and other structures are assumed to act as filters and barriers to reduce the air concentration of radioactive materials indoors. The structure infiltration factor (SIF) (IDRFI in Cassata et al., 2012) is used to quantify the indoor contaminant air concentration as a function of the outdoor concentration and is discussed later in this section.

According to Equation 5, the total volume of inhaled contaminated air is calculated as an average daily volume weighted by the fractions of the day spent at the four levels of physical activity and the corresponding activity level inhalation rates for the duration of time while indoors and outdoors. In this approach, estimates of the amounts of time spent in various activity levels and corresponding activity-specific inhalation rates are required. For this, the time in a day was partitioned between times spent outdoors and indoors as described earlier. The time spent outdoors and indoors is further subdivided in fractions corresponding to one of four activity levels defined as sedentary, light, moderate and high. Using this framework, 20 categories of individuals with different occupations and life styles were generated, ten for indoor workers and ten for outdoor workers. The time fractions at the various activity levels assigned for each of the 18 categories of workers are found in Appendix E and are based on the American Time Use Survey 2003-2010 (DOL, 2011) and subjective judgment. The 18 combinations of time fractions spent at the sedentary, light, moderate and high activity levels allow for selecting the most appropriate worker category for the PEPs studied.

Similar categories were generated for the five age groups of children using time activity data from USEPA (2011), metabolic equivalent of task (MET) values from USEPA (2009), and subjective judgment. The time fractions at the various activity levels assigned for each of the five age groups are found in Appendix E.

For this analysis, an indoor worker at Yokosuka Naval Base, Yokota Air Base, and Camp Sendai (generic PEPs for the locations) was assumed to have performed activities at light to moderate levels while outdoors and at light to moderate level while indoors; this is an L/M-L/M indoor worker category (see Appendix E). The 1-to-2 year-old at Yokota Air Base was assumed to have performed activity at the normal levels for a 1 year-old child (See Appendix E).

The humanitarian field workers at Sendai Airport were assumed to have performed activities at moderate to high levels while outdoors working or exercising, and light to moderate levels while indoors inside a tent, hanger or building for meetings, personal care and sleeping; this is an M/H-L/M outdoor worker category (See Appendix E).

Activity-specific inhalation rates were estimated using statistical data found in USEPA (2009). Table C-4 of that report contains detailed gender-specific percentile data for seven age categories and four activity levels. For each activity level and age group, the statistical results include the arithmetic mean; the 5th, 10th, 25th, 50th, 75th, 90th, and 95th percentiles; and the maximum value. Log-normal probability distribution fits to the percentile data were made. Results of the log-normal (LN) probability distribution fits of the USEPA (2009) inhalation rate for adult males (age > 17 years) for the four activity levels are shown in Figure 29. The

geometric mean and geometric standard deviation of the fitted log-normal distributions for the six age groups and the humanitarian field workers category are shown in Table 7.

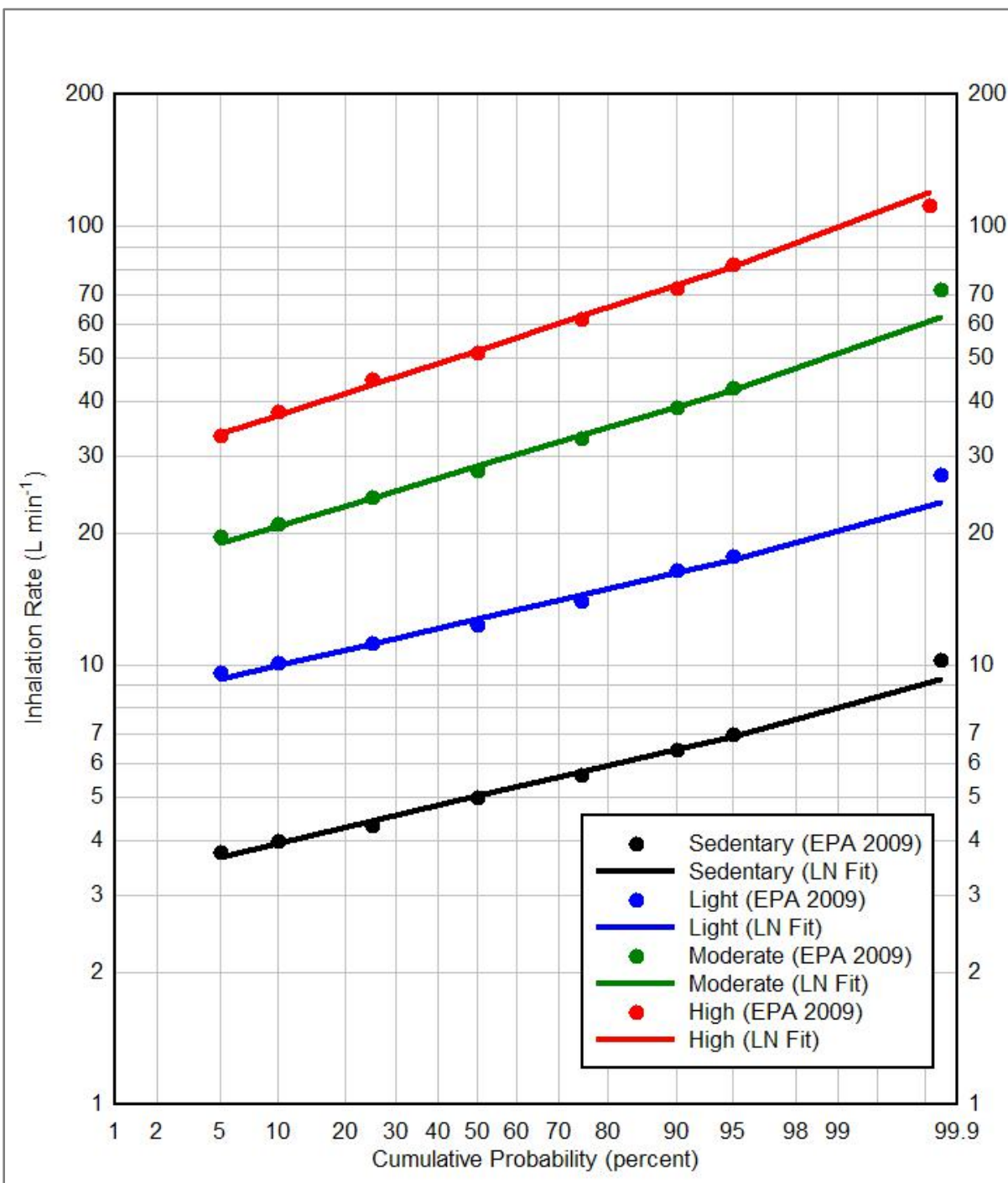


Figure 29. Log-normal (LN) cumulative probability functions of inhalation rates for adults (age > 17 years)

The relative frequency of the probability distribution of the composite daily inhalation rate for adult males (age > 17 years) is shown in Figure 30 and for a one year-old child in Figure 31. The composite daily inhalation rate accounts for the fractions of time an individual inhales at the four activity levels indoors and outdoors, regardless of contaminant concentrations. The fractions of the time indoors and outdoors are given in Table E-1 for adults and Table E-2 for children (Appendix E). The composite daily inhalation rate, also referred to as daily inhalation rate, is calculated using Equation 5 with the value of SIF set to 1.

Table 7. Inhalation rate log-normal distributions for four activity levels

Age Group	Inhalation Rates (L min^{-1}) for Physical Activity Levels							
	Sedentary		Light		Moderate		High	
	GM	GSD	GM	GSD	GM	GSD	GM	GSD
3 months	3.0	1.4	7.5	1.3	14	1.4	26	1.4
1 year	4.5	1.2	11	1.2	21	1.2	40	1.2
5 years	4.5	1.2	11	1.2	21	1.2	39	1.2
10 years	4.8	1.2	12	1.2	22	1.2	43	1.3
15 years	5.5	1.2	13	1.2	26	1.2	49	1.3
Adults (> 17 years)	5.0	1.2	13	1.2	28	1.3	52	1.3
Humanitarian Field Workers	5.0	1.2	13	1.2	28	1.3	56	1.3

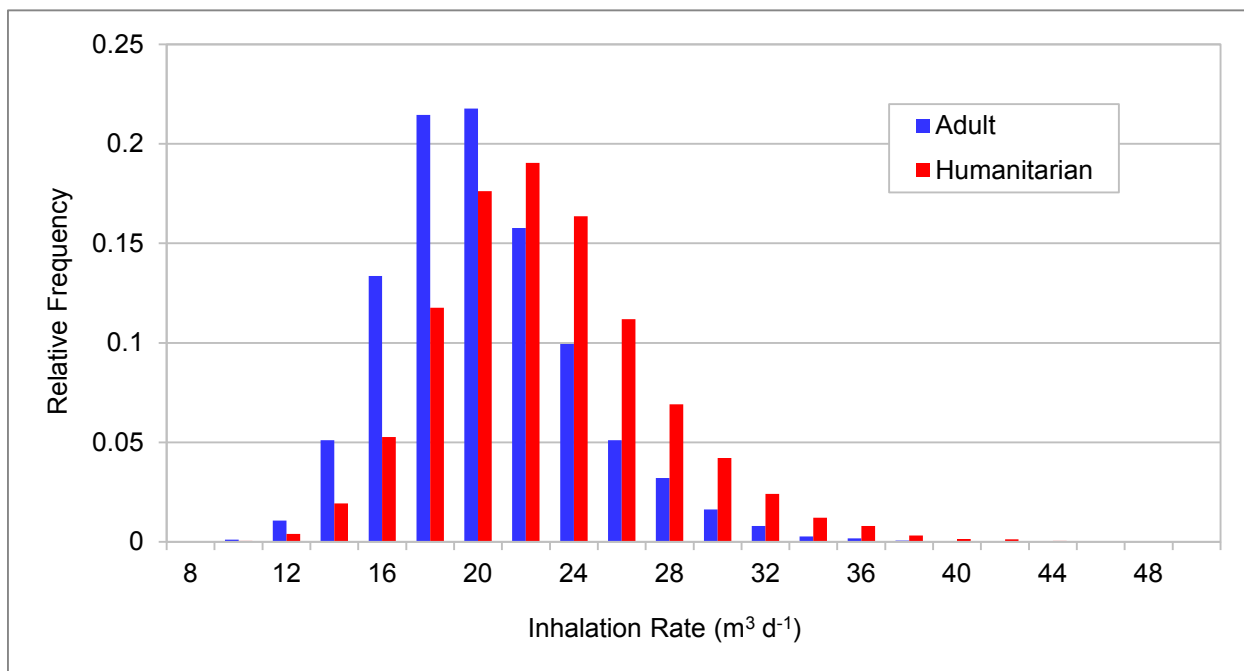


Figure 30. Relative frequency distribution of the composite daily inhalation rate for adults (age > 17 years) and humanitarian field workers

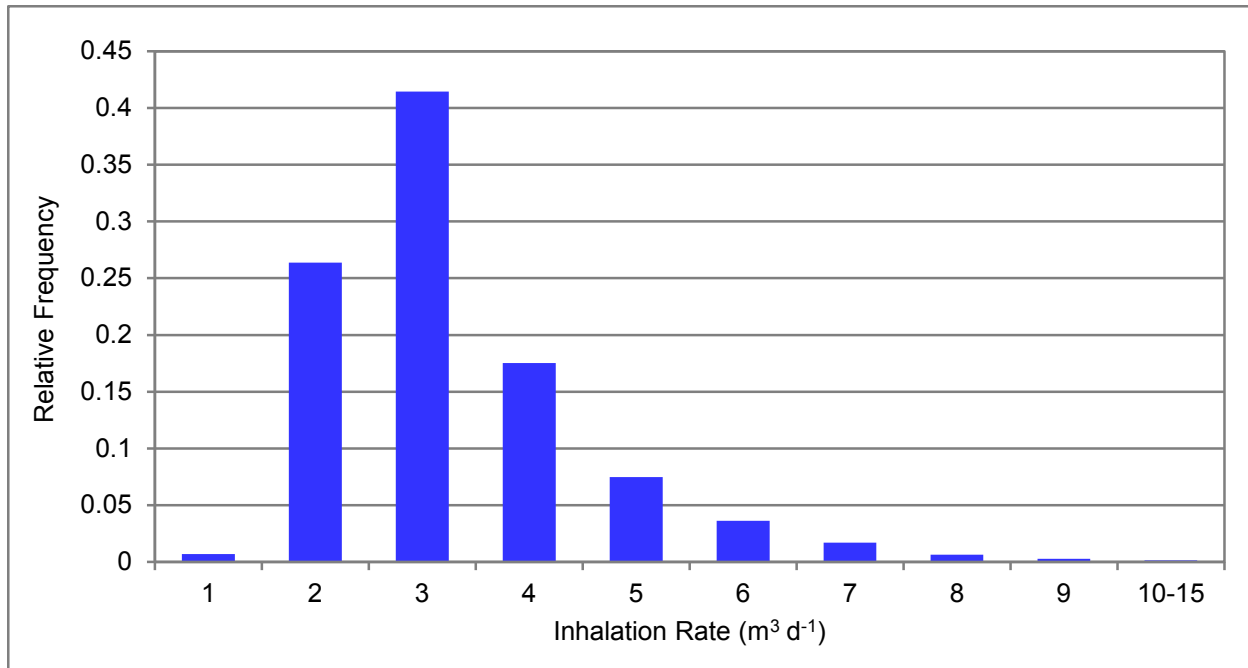


Figure 31. Relative frequency distribution of the daily inhalation rate for 1-to-2 year-old children

4.2.1.3 Structure Infiltration Factor

Outdoor airborne contaminants in either gaseous or aerosol form can infiltrate into residences and other buildings. Buildings reduce the airborne concentrations of infiltrating materials through the filtering effect of the building shell (Thatcher and Layton, 1995). If there is no indoor source of contaminants, the amount of the reduction of infiltrating materials can be modeled by a structure infiltration factor, *SIF*, which is the ratio of the indoor to outdoor air activity concentrations. The *SIF* is used in Equation 5 to modify the volume of air inhaled by a person while indoors to account for any reducing effects of the building or other enclosures.

Although the indoor concentrations of contaminants can temporarily exceed outdoor concentrations depending on particle characteristics, building characteristics, and the degree of resuspension involved (Thatcher and Layton, 1995), the range of *SIF* is typically 0 to 1.0. For the probabilistic analysis in this study, the uncertainty in *SIF* for aerosols of radioactive materials was based on the indoor to outdoor ratios of aerosols containing metals such as iron, lead, and zinc that ranged from a low of 0.1 to a high of 0.5 (Yocom, 1982). A triangular distribution was selected with a minimum of 0.1, a mode of 0.3, and a maximum of 0.5. The uncertainty for the *SIF* for gases was based on the indoor to outdoor ratios for sulfur oxides that ranged from a low of 0.2 to a high of 0.8 (Yocom, 1982). A triangular distribution was selected with a minimum of 0.2, a mode of 0.5, and a maximum of 0.8.

4.2.1.4 Dose Coefficients for Inhalation

Dose coefficients for calculating committed effective dose or committed equivalent dose to the thyroid due to the inhalation of radioactive materials were obtained from the ICRP

Database of Dose Coefficients Version 3.0 (ICRP, 2011). The dose coefficients in this database were compiled from ICRP Publications 68, 71 and 72 (ICRP, 1994; ICRP 1995a; ICRP, 1996). The inhalation dose coefficients for committed effective dose and committed equivalent dose to the thyroid from the ICRP database for members of the public were used. For all radionuclides, the dose coefficients selected correspond to a particle size distribution of 1 micrometer activity median aerodynamic diameter (AMAD) and absorption Type F, which are assumed to be readily absorbed into the bodily fluids of the respiratory tract. The inhalation dose coefficients for adults for all radionuclides used in this assessment are shown in Appendix F. On the basis of previous probabilistic analysis studies and practices of other DOD dose assessment programs on uncertainties associated with ICRP inhalation dose coefficients (NCRP, 1998; DTRA, 2010, UA01), the uncertainty in inhalation dose coefficients was modeled as a log-normal distribution. For this distribution, an uncertainty factor of 3 (95th percentile divided by the geometric mean) and a geometric standard deviation of 1.95 were used.

4.2.2 Ingestion of Drinking Water

Following the accident at the FDNPS in March 2011, radioactive contaminants were detected in tap water and several water purification plants in Tokyo and other prefectures. Therefore, drinking water was intensely monitored at the tap and at water treatment plants to measure the activity concentrations from radionuclides that could have made its way to the potable water system.

Contamination of drinking water would have been the result of the deposition of contaminants onto or their transport by surface runoff into surface water bodies, such as rivers, lakes and reservoirs, which was subsequently pumped via intakes to water treatment plants. It is highly unlikely that water supplied from groundwater wells would have been affected by contamination due to the long time it takes for contaminants to move underground from recharge zones to supply wells, and the high potential for contaminants to be absorbed into the porous medium matrix while transported underground.

In this study, individuals are assumed to have ingested water that was contaminated with radioactive materials if they consumed water from municipal supplies. The committed effective dose or the committed equivalent dose to the thyroid from the ingestion of contaminated water is calculated using Equation 6 as follows:

$$E_{IngW} = IR_{Water} \sum_j \left(DC_{Ingj} \int_{t_{start}}^{t_{end}} C_{Waterj}(t) dt \right) \quad (6)$$

where:

E_{IngW}	=	Committed effective dose or committed equivalent dose to the thyroid (Sv)
IR_{Water}	=	Ingestion rate of contaminated water (L d ⁻¹)
DC_{Ingj}	=	Ingestion dose coefficient for radionuclide j (Sv Bq ⁻¹)

t_{start}	=	Beginning time of an individual's exposure
t_{end}	=	Ending time of an individual's exposure
$C_{Waterj}(t)$	=	Water activity concentration of radionuclide j at time t (Bq L ⁻¹)

4.2.2.1 Water Activity Concentration

Data for water activity concentration were extracted from data published by MEXT (2012b) for the prefectures where the populations of concern were located. These are shown in Figure 32 and Figure 33 for Yokosuka Naval Base and Yokota Air Base, respectively. Water activity levels for other radionuclides at Yokosuka Naval Base were below detection limits. Individuals at both Camp Sendai and Sendai Airport were assumed to have consumed bottled water since the municipal waterworks were not operational during the time that U.S. service members were in Sendai.

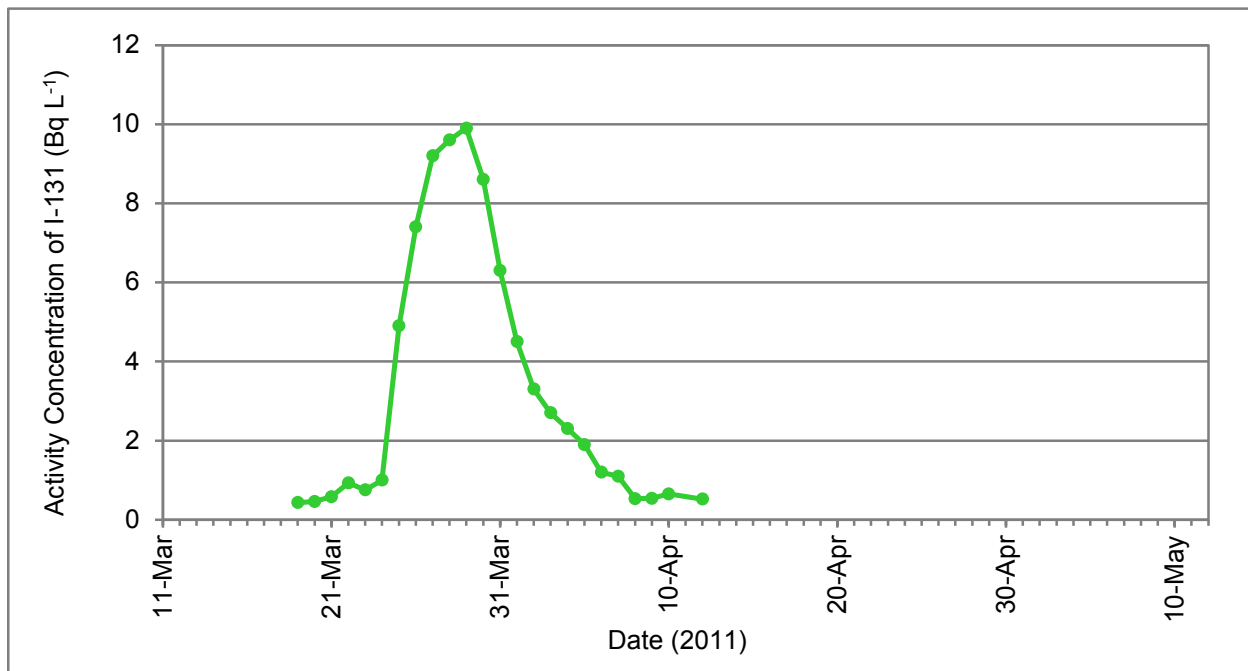


Figure 32. Water activity concentration of I-131 for Yokosuka Naval Base

No uncertainty from spatial variability in the water activity concentration was assumed since drinking water samples were made of municipal tap drinking water that would not be based on specific geographic locations. Although there could be small differences in drinking water properties based on location, the sensitivity of the calculated dose to this uncertainty is extremely low due to activity concentration levels mostly below detection limits or very low (see the sensitivity analysis in Section 6).

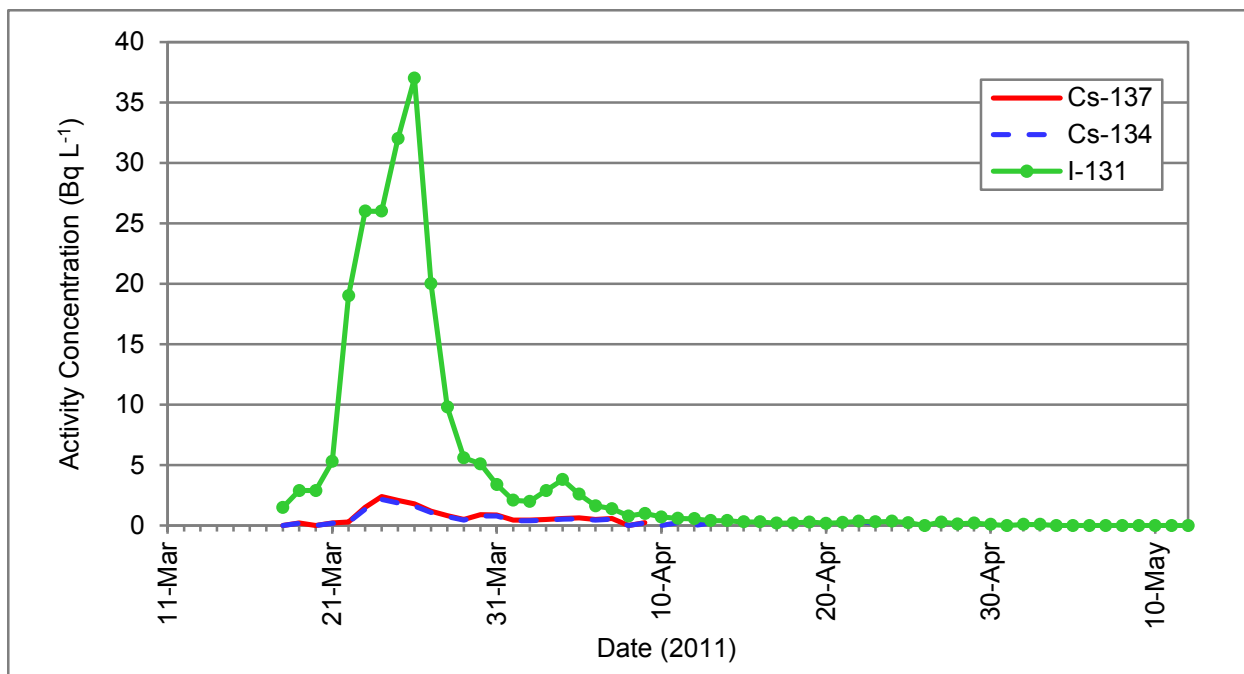


Figure 33. Water activity concentrations for Yokota Air Base

The measurement and data related uncertainties in water activity concentration are due to the uncertainties inherent to sampling and laboratory procedures, instrument precision, calibration errors, data processing tools, and data recording errors. These uncertainties are considered to be similar for both locations where municipal supplied water was consumed. The measurement and data related uncertainties in water activity concentration are assumed to be the same as those used for other measurements data discussed earlier in this section. The normal distribution was selected with an uncertainty factor of 1.5 and a standard deviation of $0.304 \times \text{mean}$.

4.2.2.2 Water Ingestion Rate

The water ingestion rates are based on data published in the USEPA Exposure Factors Handbook (USEPA, 2011). Cumulative probability density functions were calculated for five different types of distributions to fit the statistical percentiles given in the Exposure Factors Handbook for each of the age groups shown in Table 8. The results were then compared to the statistical percentiles to determine which distribution type constitutes a best fit. Based on the results shown in Figure 34, the log-normal distribution with an uncertainty factor (ratio of the 95th percentile to the geometric mean) of 2.8 is selected for use in the probabilistic analysis for adults. Based on the results shown in Figure 35, the log-normal distribution with an uncertainty factor of 3.1 was selected for use in the probabilistic analysis for children in the 1-to-2 year-old age group. The parameters of the log-normal distributions for all age groups and the humanitarian field workers are given in Table 8.

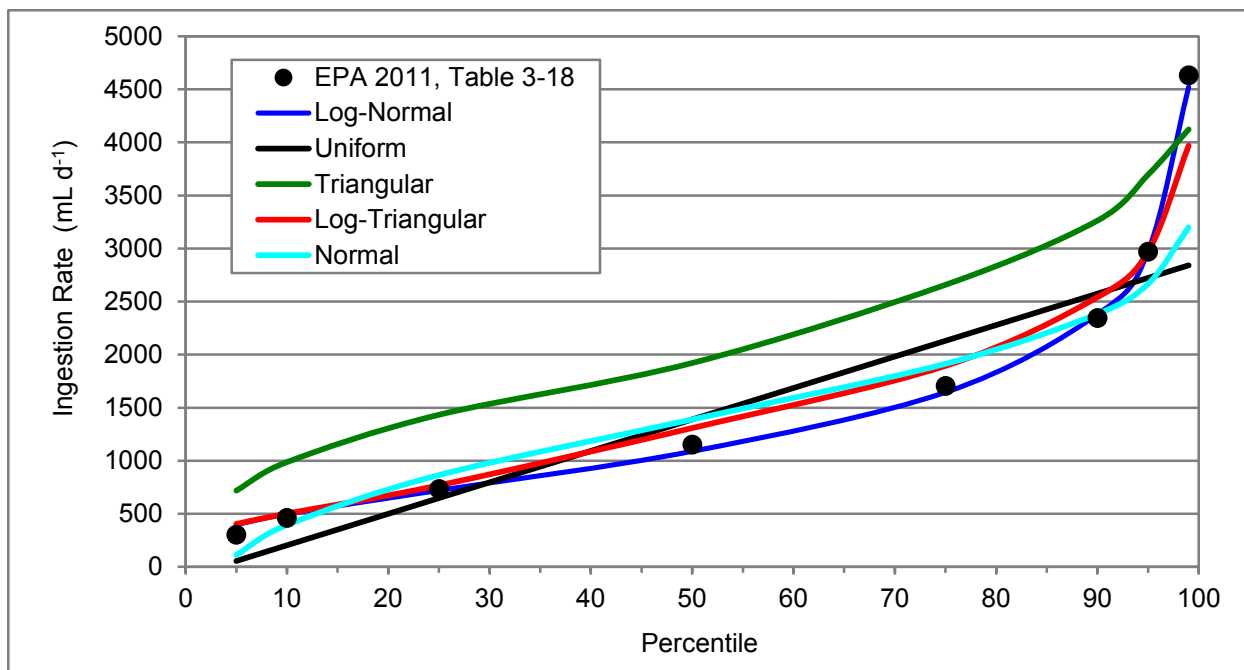


Figure 34. Cumulative probability distribution functions fitted to the published statistical data for water ingestion rate of adults

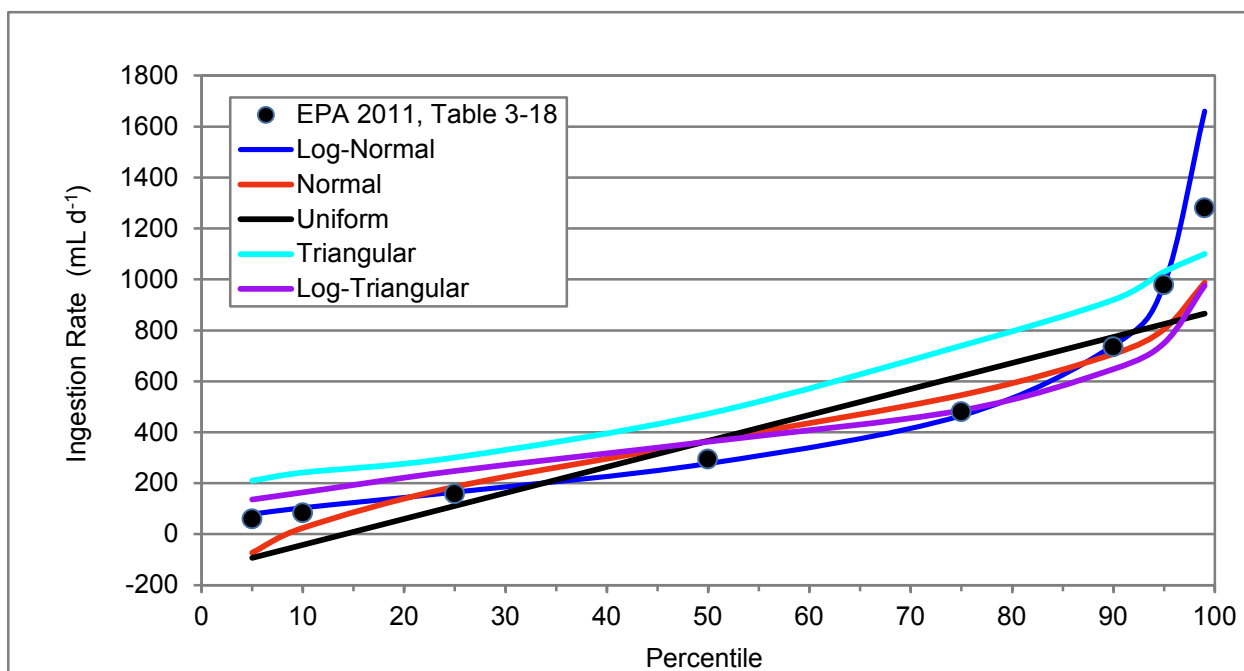


Figure 35. Cumulative probability distribution functions fitted to the published statistical data for water ingestion rate of 1-to-2 year-old children

Table 8. Log-normal distributions selected for the water ingestion rate

Age Group	Ingestion Rate (L d ⁻¹)	
	Geometric Mean	Geometric Standard Deviation
3 months	0.4	1.8
1 year	0.3	2.0
5 years	0.4	1.9
10 years	0.5	1.9
15 years	0.7	2.0
Adults (> 17 years)	1.1	1.8
Humanitarian Field Workers	1.1	1.8

4.2.2.3 Dose Coefficients for Water Ingestion

Dose coefficients for ingestion of water were obtained from the ICRP Database of Dose Coefficients Version 3.0 (ICRP, 2011). The dose coefficients in this database are compiled from ICRP Publications 68, 71 and 72 (ICRP, 1994; ICRP 1995b; ICRP, 1996). Ingestion dose coefficients for committed effective dose and committed equivalent dose to the thyroid from the ICRP database for members of the public were used. Tabulations of the dose coefficients for all radionuclides included in this assessment are shown in Appendix F. On the basis of previous probabilistic analysis studies and practices of other DOD dose assessment programs on uncertainties associated with ICRP inhalation dose coefficients (NCRP, 1998; DTRA, 2010, UA01), the uncertainty in ingestion dose coefficients was modeled as a log-normal distribution. For this distribution, an uncertainty factor of 3 (95th percentile divided by the geometric mean) and a geometric standard deviation of 1.95 were used.

4.2.3 Incidental Ingestion of Soil and Dust

Individuals are assumed to have incidentally ingested soil and dust that was contaminated with radioactive materials. Incidental ingestion of soil and dust could have resulted from various behaviors, such as transfers through food and beverage, smoking, mouthing/licking, etc. (USEPA, 2011).

The committed effective dose or the committed equivalent dose to the thyroid from the incidental ingestion of soil and dust contaminated with radioactive materials are calculated using Equation 7 as follows:

$$E_{IngS} = IR_{Soil} \sum_j \left(DC_{Ingj} \int_{t_{start}}^{t_{end}} C_{Soilj}(t) dt \right) \quad (7)$$

where:

E_{IngS}	=	Committed effective dose or committed equivalent dose to the thyroid (Sv)
IR_{Soil}	=	Ingestion rate of contaminated soil and dust (g d^{-1})
DC_{Ingj}	=	Ingestion dose coefficient for radionuclide j (Sv Bq^{-1})
t_{start}	=	Beginning day of an individual's exposure
t_{end}	=	End day of an individual's exposure
$C_{Soilj}(t)$	=	Soil and dust activity concentration of radionuclide j (Bq g^{-1})

4.2.3.1 Soil Activity Concentration

As described in Cassata et al. (2012), soil activity concentration measurements were made at Yokosuka Naval Base, Yokota Air Base, and Sendai. Soil concentrations for five radionuclides (I-131, Cs-134, Cs-136, Cs-137, and Te-132) were available and were used in the probabilistic analysis. Doses from other radionuclides are much less than 1 percent of the soil ingestion dose and were not included. The soil activity concentration data were limited for all the assessed locations. The available soil activity concentration data were used to develop modeled soil activity concentrations for the probabilistic analysis conducted in this study. Details of the development of the modeled soil activity concentrations are given below.

The soil activity concentration model for Yokosuka Naval Base was developed using the data in Table 9, the assumption that no significant ground deposition of radionuclides occurred before March 19, 2011, and that peak activity concentrations were observed on March 21, 2011. To create the modeled average daily soil activity concentrations, first, a reference point was calculated using the available data for each selected radionuclide except Te-132. For this, the results of all soil activity concentration measurements for each radionuclide except Te-132 were averaged and assigned to April 4, 2011, which is the midpoint day of all samples. Second, soil activity values for the days prior to the midpoint were calculated using back decay to March 21, 2011. For days following the midpoint day through May 11, 2011, daily soil activity concentrations were estimated using radiological decay. Third, for all radionuclides, no activity was assigned to days prior to and including March 19, 2011, and half of the calculated peak values on March 21 were assigned to March 20, 2011. No effects other than radiological decay were included in the modeled soil activity concentrations. The modeled and measured soil activity concentrations are shown in Figure 36.

For Te-132, the average for Te-132 was assigned to March 25, 2011, the first day of any sample measurement results due to the relatively short half-life of 3.3 d and due to the average activity being within a factor of two of the measured activity on March 25 and 26, 2011. The Te-132 activity was then back-decayed from March 24, 2011, to March 21, 2011, and decayed from March 26 to May 11 assuming only radiological decay. The modeled and measured soil activity concentrations for Te-132 are shown in Figure 36.

Table 9. Measured soil activity concentrations at Yokosuka Naval Base

Sample Number	Date	Cs-134 (pCi g ⁻¹)	Cs-136 (pCi g ⁻¹)	Cs-137 (pCi g ⁻¹)	I-131 (pCi g ⁻¹)	Te-132 (pCi g ⁻¹)
DOD-RAW00037	3/25/2011	4.04	0.54	4.56	27.10	2.75
DOD-RAW00040	3/26/2011	6.00	0.68	6.94	27.20	2.70
DOD-RAW00062	3/28/2011	4.70	0.50	5.36	24.65	2.28
DOD-RAW00056	3/28/2011	3.20	0.34	3.69	19.20	1.55
DOD-RAW00061	3/28/2011	7.02	0.80	7.60	64.88	2.99
DOD-RAW00057	3/28/2011	8.06	0.91	9.13	85.89	4.06
20590	4/2/2011	1.40	0.13	1.61	5.51	0.30
20929	4/6/2011	8.32	0.10	9.29	17.23	0.35
21076	4/8/2011	0.26	–	0.47	0.78	–
21076*	4/8/2011	0.35	–	0.87	2.38	–
21080	4/8/2011	0.06	–	0.12	0.35	–
DOD-RAW00123	4/10/2011	12.49	0.68	14.16	19.23	0.22
DOD-RAX00033	4/10/2011	10.17	0.50	11.43	15.13	0.22
DOD-RAX00034	4/10/2011	11.02	0.55	12.76	36.87	0.23
21362	4/13/2011	0.47	–	0.74	2.22	–
21364	4/13/2011	0.65	–	0.70	1.04	–
Average		4.89	0.52	5.59	21.85	1.60

*Repeat analysis of sample

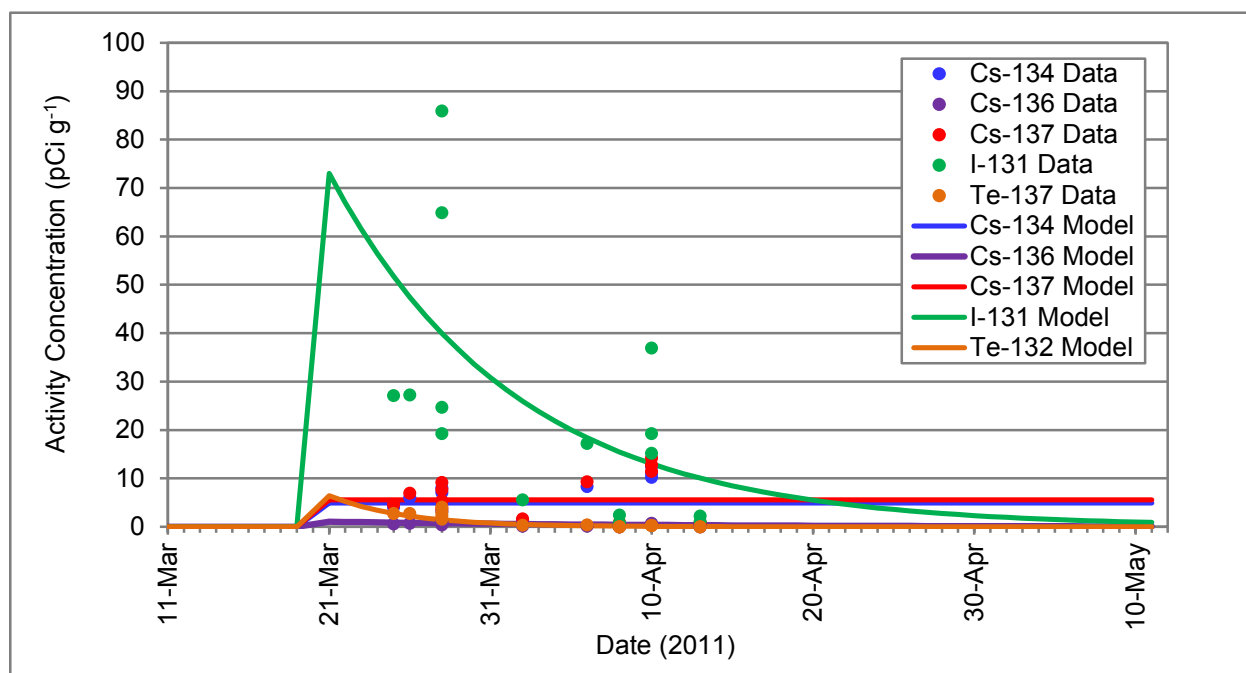


Figure 36. Modeled and measured soil activity concentrations at Yokosuka Naval Base

The soil activity concentration model for Yokota Air Base were developed using the data in Table 10, the assumption that no significant ground deposition of radionuclides occurred before March 19, 2011, and that peak activity concentrations was observed on March 21, 2011. To create the modeled average daily soil activity concentrations, first, a reference point was calculated using the available data for each selected radionuclide except Te-132. For this, the results of all soil activity concentration measurements for each radionuclide except for Te-132 were averaged and assigned to April 7, 2011, which is the midpoint day of all samples. Second, soil activity values for the days prior to the midpoint were calculated using back decay to March 21, 2011. For days following the midpoint day through May 11, 2011, daily soil activity concentrations were estimated using radiological decay. Third, for all radionuclides, no activity was assigned to days prior to and including March 19, 2011, and half of the calculated peak values on March 21, 2011, were assigned to March 20, 2011. No effects other than radiological decay were included in the modeled soil activity concentrations. The modeled and measured soil activity concentrations are shown in Figure 37.

For Te-132, the highest sample measurement for Te-132 was assigned to March 24, 2011, the first day of any sample measurement results due to the relatively short radiological half-life of 3.3 d and due to the highest measurement being similar in magnitude to measurements from March 24 to March 31, 2011. Te-132 activity was back-decayed from March 23 to March 21, 2011, and decayed from March 25 to May 11, 2011, assuming only radiological decay. The modeled and measured soil activity concentrations for Te-132 are shown in Figure 37.

Table 10. Measured soil activity concentrations at Yokota Air Base

Sample Number	Date	Cs-134 (pCi g⁻¹)	Cs-136 (pCi g⁻¹)	Cs-137 (pCi g⁻¹)	I-131 (pCi g⁻¹)	Te-132 (pCi g⁻¹)
20007	3/24/2011	0.95	0.11	1.12	16.10	4.28
DOD-RAW00079	3/31/2011	3.88	0.30	4.39	23.38	1.86
DOD-RAW00080	3/31/2011	6.31	0.61	7.09	34.03	4.09
DOD-RAW00081	3/31/2011	3.53	0.36	4.00	19.84	2.24
DOD-RAW00082	3/31/2011	8.85	0.82	10.09	42.64	5.89
20373	4/8/2011	0.36	–	0.40	0.83	0.03
21386	4/14/2011	1.22	–	1.29	1.95	0.03
21385	4/14/2011	0.81	–	0.86	1.21	0.04
21650	4/21/2011	6.18	0.18	7.32	4.98	–
21650*	4/21/2011	5.08	0.15	6.14	4.64	–
21651	4/21/2011	1.28	–	1.89	1.11	–
21651*	4/21/2011	1.44	–	1.99	1.35	–
Average		3.32	0.36	3.88	12.67	2.31

*Repeat analysis of sample

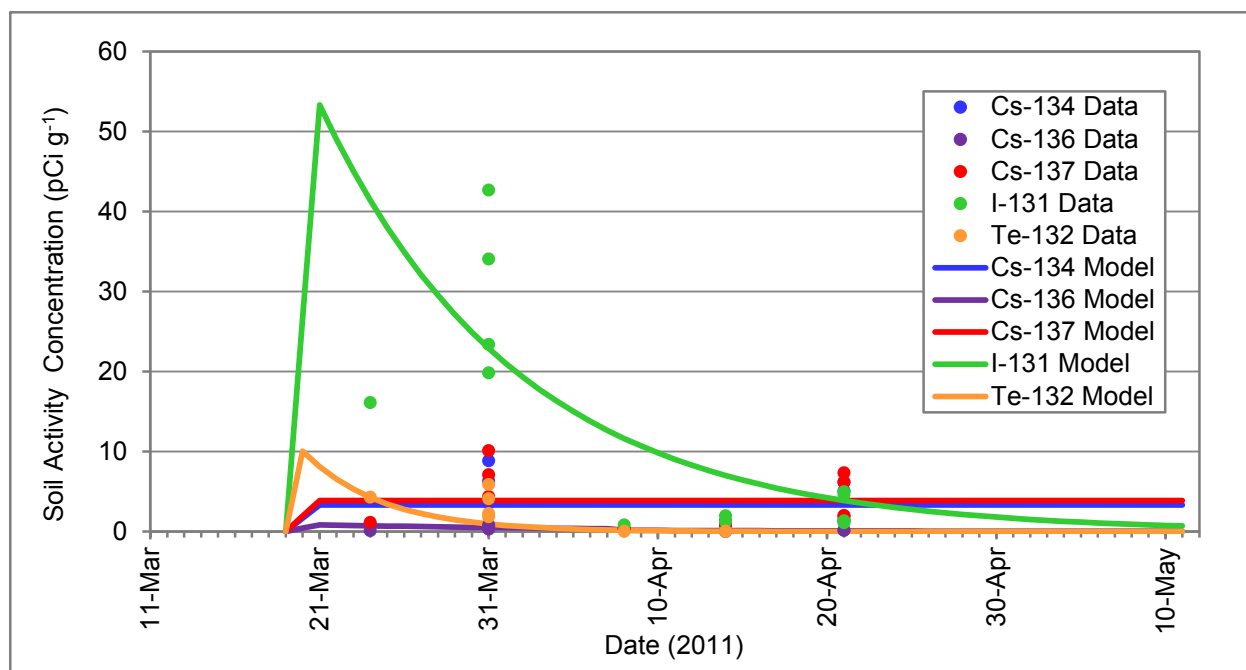


Figure 37. Modeled and measured soil activity concentrations at Yokota Air Base

The soil activity concentration model for Sendai was developed using the same methodology used for Yokosuka Naval Base and Yokota Air Base. Soil sample activity measurements are provided in Table 11. The midpoint day for all measurements for Sendai, which was used for a reference average concentration, was April 2, 2011. No effects other than radiological decay were included in the modeled soil activity concentrations. The modeled and measured soil activity concentrations are shown in Figure 38.

The spatial variability in the soil activity concentration is assumed to be similar to that of the external dose rates for each assessed location. This is based on the fact that dose rates were due to deposited materials on the ground after the period where dose rates were mostly dominated by immersion in passing clouds of radioactive materials. Therefore, uniform distributions were selected with ranges of $\pm 30\%$ for Yokosuka Naval Base, $\pm 10\%$ for Yokota Air Base, and $\pm 50\%$ for Sendai.

The measurement and data related uncertainties of soil activity concentration are due to the uncertainties inherent to sampling procedures, instrument precision, calibration errors, data processing tools, and data recording errors. These uncertainties are considered the same for all assessed locations since similar measurements were made using similar instruments and were made by personnel with similar levels of training and experience. The measurement and data related uncertainties in soil activity concentration are assumed to be the same as those used for other measurements data discussed earlier in this section. Therefore, the normal distribution was selected with an uncertainty factor of 1.5 and a standard deviation of $0.304 \times \text{mean}$.

Table 11. Measured soil activity concentrations at Sendai

Sample Number	Date	Cs-134 (pCi g⁻¹)	Cs-136 (pCi g⁻¹)	Cs-137 (pCi g⁻¹)	I-131 (pCi g⁻¹)	Te-132 (pCi g⁻¹)
20033	3/25/2011	4.24	0.47	4.77	2.68	3.7
20059	3/26/2011	–	0.07	0.6	7.18	0.39
23020003	3/28/2011	0.03		0.05	3.7	–
23020001	3/28/2011	11.0	13.0	–	38.0	–
23020002	3/28/2011	4.90	–	5.6	20.0	–
22910006	3/30/2011	0.46	–	0.58	2.60	–
22910005	3/30/2011	0.73	–	0.87	13.0	–
22910004	3/30/2011	0.33	–	0.38	1.5	–
22910003	3/30/2011	0.19	–	0.23	3.7	–
22910002	3/30/2011	1.7	–	1.4	5.4	–
22910001	3/30/2011	1.7	–	1.9	6.7	–
23040001	3/31/2011	2.1	–	2.7	16.0	–
23180001	3/31/2011	16.0	–	18.0	44.0	–
23180002	3/31/2011	17.0	–	20.0	51.0	–
20862	4/5/2011	1.91	0.14	1.92	6.18	0.21
21192	4/8/2011	9.07	0.51	10.3	19.6	0.48
21193	4/9/2011	1.1	0.03	1.22	2.30	0.03
21194	4/10/2011	1.88	0.1	2.12	4.12	0.05
21191	4/11/2011	0.78	–	0.85	2.32	0.02
21192	4/11/2011	9.07	0.51	10.3	19.60	0.48
Average		4.43	1.85	4.41	13.48	0.67

4.2.3.2 Soil and Dust Ingestion Rate

The ingestion rates of soil and dust are based on data published by the USEPA Exposure Factors Handbook (USEPA, 2011). Triangular distributions for soil and dust ingestion rates were selected for all identified age groups and humanitarian field workers. The attributes characterizing these distributions are shown in Table 12.

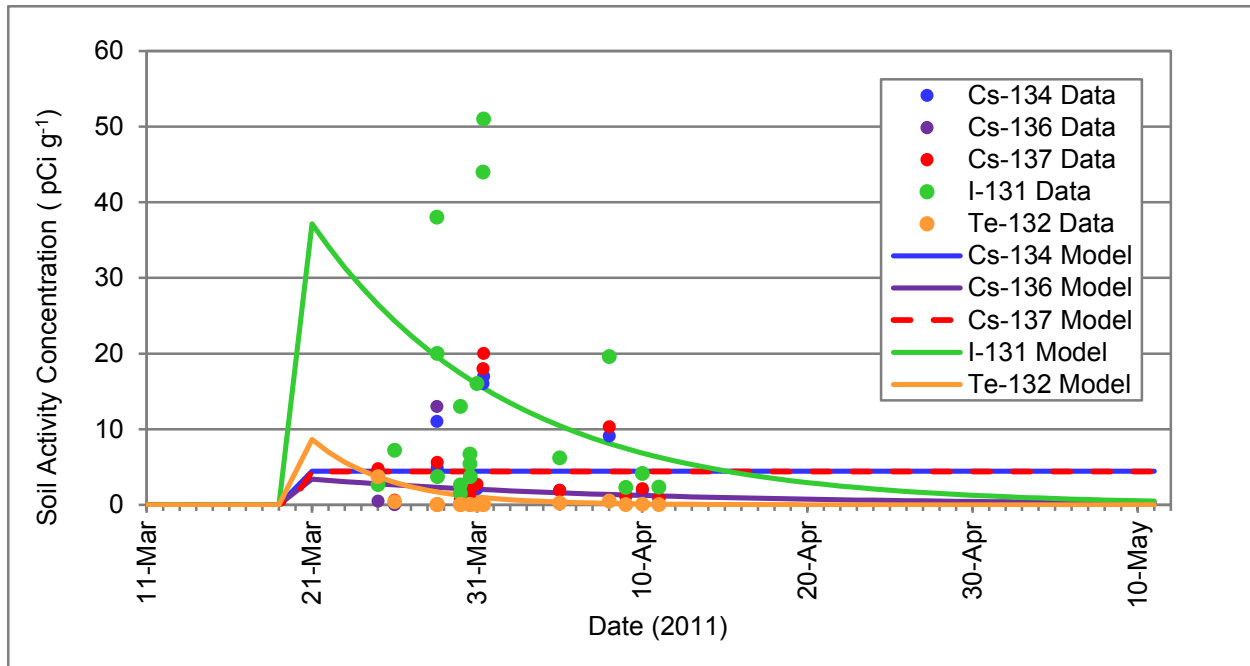


Figure 38. Modeled and measured soil activity concentrations for Sendai locations

Table 12. Triangular distributions selected for soil and dust ingestion rates

Age Group	Ingestion Rates (g d^{-1})		
	Minimum	Mode	Maximum
3 months	0.01	0.06	0.2
1 year	0.01	0.1	1.0
5 years	0.01	0.1	1.0
10 years	0.01	0.1	1.0
15 years	0.01	0.1	0.2
Adults (> 17 years)	0.01	0.05	0.2
Humanitarian Field Workers	0.05	0.2	0.5

4.2.3.3 Dose Coefficients for Ingestion of Soil and Dust

Dose coefficients for ingestion of soil and dust are the same as the dose coefficients for ingestion of water discussed earlier in this section. Therefore, the same uncertainty distributions were assumed.

Section 5.

Results of Probabilistic Analyses and Comparison with Doses Estimated by Deterministic Methods

5.1 Results of Probabilistic Analyses

For each location and PEP considered in this study, the external dose, the committed effective dose and the committed equivalent dose to the thyroid from intakes for each internal dose pathway were calculated. The committed doses are for 50 years for adults and to age 70 for children. Dose components were then summed up to estimate the total effective dose and the total equivalent dose to the thyroid. All doses were calculated by means of a probabilistic analysis model using Monte Carlo simulation with 10,000 histories. All analyses were made using Mathcad[®] software and purely random Monte Carlo sampling. The geometric mean, arithmetic mean, 95th percentile, and the uncertainty factor were determined for all dose pathways. In this study, the geometric mean is used as the central estimate because the geometric mean is considered to be a more representative measure of central tendency for highly-skewed distributions such as those for the calculated doses. The statistical results of the probabilistic analyses of the four locations and five PEPs for each exposure pathway and the total dose are given in Table 13 through Table 17. The frequency distributions for the total effective dose and total equivalent dose to the thyroid are presented in Figure 39 to Figure 48.

Table 13. Dose results for adults at Yokosuka Naval Base using probabilistic analysis

Exposure Pathway	Geometric Mean Dose (mSv)	Arithmetic Mean Dose (mSv)	95th Percentile Dose (mSv)	Uncertainty Factor
External	0.009	0.011	0.021	2.2
Committed Effective Dose				
Inhalation	0.008	0.018	0.058	8.2
Water ingestion	0.002	0.003	0.009	4.8
Soil ingestion	<0.001	<0.001	<0.001	4.6
Total*	0.024	0.031	0.077	3.2
Committed Equivalent Dose to the Thyroid				
Inhalation	0.14	0.33	1.2	8.6
Water ingestion	0.04	0.06	0.17	4.8
Soil ingestion	0.001	0.002	0.005	4.6
Total*	0.24	0.40	1.3	5.3

*The total dose includes the external dose and the committed internal dose from all internal exposure pathways.

Table 14. Dose results for adults at Yokota Air Base using probabilistic analysis

Exposure Pathway	Geometric Mean Dose (mSv)	Arithmetic Mean Dose (mSv)	95th Percentile Dose (mSv)	Uncertainty Factor
External	0.015	0.017	0.031	2.1
Committed Effective Dose				
Inhalation	0.022	0.035	0.11	5.0
Water ingestion	0.006	0.009	0.027	4.8
Soil ingestion	<0.001	<0.001	<0.001	4.4
Total*	0.048	0.060	0.15	3.0
Committed Equivalent Dose to the Thyroid				
Inhalation	0.32	0.52	1.6	5.1
Water ingestion	0.098	0.15	0.47	4.7
Soil ingestion	0.001	0.002	0.004	4.4
Total*	0.48	0.69	2.0	4.1

*The total dose includes the external dose and the committed internal dose from all internal exposure pathways.

Table 15. Dose results for 1-to-2 year-old children at Yokota Air Base using probabilistic analysis

Exposure Pathway	Geometric Mean Dose (mSv)	Arithmetic Mean Dose (mSv)	95th Percentile Dose (mSv)	Uncertainty Factor
External	0.016	0.018	0.031	1.9
Committed Effective Dose				
Inhalation	0.052	0.082	0.25	4.8
Water ingestion	0.012	0.020	0.060	5.2
Soil ingestion	0.002	0.003	0.007	5.3
Total*	0.093	0.12	0.31	3.4
Committed Equivalent Dose to the Thyroid				
Inhalation	0.92	1.5	4.5	4.9
Water ingestion	0.23	0.38	1.2	5.2
Soil ingestion	0.025	0.042	0.13	5.2
Total*	1.4	1.9	5.4	4.2

*The total dose includes the external dose and the committed internal dose from all internal exposure pathways.

Table 16. Dose results for support personnel at Camp Sendai using probabilistic analysis

Exposure Pathway	Geometric Mean Dose (mSv)	Arithmetic Mean Dose (mSv)	95th Percentile Dose (mSv)	Uncertainty Factor
External	0.019	0.021	0.044	2.4
Committed Effective Dose				
Inhalation	0.046	0.095	0.33	7.2
Soil ingestion	<0.001	<0.001	<0.001	4.9
Total*	0.074	0.12	0.36	4.8
Committed Equivalent Dose to the Thyroid				
Inhalation	0.83	1.8	6.2	7.5
Soil ingestion	<0.001	0.001	0.003	4.9
Total*	0.87	1.8	6.3	7.2

*The total dose includes the external dose and the committed internal dose from all internal exposure pathways.

Table 17. Dose results for the humanitarian field workers at Sendai Airport using probabilistic analysis

Exposure Pathway	Geometric Mean Dose (mSv)	Arithmetic Mean Dose (mSv)	95th Percentile Dose (mSv)	Uncertainty Factor
External	0.06	0.06	0.11	2.0
Committed Effective Dose				
Inhalation	0.09	0.17	0.60	7.2
Soil ingestion	<0.001	<0.001	0.001	4.3
Total*	0.17	0.23	0.67	4.2
Committed Equivalent Dose to the Thyroid				
Inhalation	1.5	3.2	11	7.2
Soil ingestion	0.002	0.003	0.008	4.4
Total*	1.7	3.2	12	6.7

*The total dose includes the external dose and the committed internal dose from all internal exposure pathways.

5.2 Comparison of the Doses Using Probabilistic Analysis with Doses Estimated by Deterministic Methods

The results of the probabilistic analyses given in the previous section were compared to the doses estimated by deterministic methods from Cassata et al. (2012) to assess whether the latter are sufficiently conservative (high-sided). For this, the doses estimated by deterministic methods were compared to the 95th percentile of the dose distributions from the probabilistic analysis for the five PEPs assessed in this study. Table 18 identifies and describes the five PEPs in Cassata et al. (2012) that have doses estimated by deterministic methods that were compared to the PEPs assessed using the probabilistic analysis developed in this study. The PEP number is

the number assigned to each specific PEP in Cassata et al. (2012). PEPs are defined for each combination of age range, activity level, and time indoor for the 13 locations.

Table 18. Population exposure factors for PEPs with doses estimated by deterministic methods and the corresponding factors used in the probabilistic analysis

Location/ PEP	Population Exposure Factors for PEPs with Doses Estimated by Deterministic Methods				Population Exposure Factors for Probabilistic Analysis		
	Age Group	PEP No.	Time Indoors [*]	Physical Activity Level [†]	Age Group	Worker Type	Time Activity [‡]
Yokosuka Naval Base	Adult	1106	None	High	Adult	Indoor	W: L/M R: L/M
Yokota Air Base	Adult	806	None	High	Adult	Indoor	W: L/M R: L/M
Yokota Air Base	1-to-2 year-old	802	None	High	1-to-2 year-old	Child	1 year-old
Camp Sendai	Adult	206	None	High	Adult	Indoor	W: L/M R: L/M
Sendai Airport	Humanitarian	207	None	Extreme	Humanitarian	Outdoor	W: M/H R: L/M

^{*} Cassata et al. (2012, Table B-9)

[†] Cassata et al. (2012, Table 29)

[‡] W = work time, R = recreation and leisure time; where Activity levels: L = light, M = moderate, H = high. Children time-activity fractions are the same for each age group. See Appendix E for details.

The total effective doses and total equivalent doses to the thyroid estimated by deterministic methods and probabilistic analysis are listed in Table 19. Also shown is the equivalent percentile rank of the doses estimated by deterministic methods within the probabilistic dose distributions. Finally, the ratio of the doses estimated by deterministic methods to the 95th percentile doses of the probabilistic distribution are calculated and displayed in Table 19. A ratio greater than 1.0 indicates that the dose estimated by deterministic methods is truly conservative by the criteria used in this report.

Figure 39 to Figure 48 show the comparison of the doses estimated by deterministic methods and the doses from the probabilistic analyses. The range of the probabilistic doses is displayed using both a histogram and bars showing the 25th percentile and 95th percentile dose. The range of doses estimated by deterministic methods show all of the doses calculated in Cassata et al. (2012) for the same age group using the various possible time indoors, inhalation rates, and water and soil ingestion rates. The 25th percentile probabilistic dose was chosen as a comparison to the lowest dose estimated by deterministic methods for any PEP since that percentile was considered representative of the lower end of the EPA parameter distributions used in Cassata et al. (2012) to develop parameter values.

**Table 19. Comparison of doses estimated by deterministic methods
with doses from probabilistic analysis**

Dose	Dose Estimated by Deterministic Methods* (mSv)	Probabilistic 95th Percentile Dose (mSv)	Dose Estimated by Deterministic Methods as Percentile of the Probabilistic Distribution	Ratio of Deterministic Analysis to 95th Percentile Dose
Yokosuka Naval Base (Adults)				
Total effective dose	0.32	0.077	99.8	4.1
Total equivalent dose-thyroid	3.6	1.3	99.7	2.9
Yokota Air Base (Adults)				
Total effective dose	0.51	0.15	99.9	3.6
Total equivalent dose-thyroid	4.5	2.0	99.4	2.4
Yokota Air Base (1-to-2 Year-Old Children)				
Total effective dose	0.99	0.31	99.8	3.2
Total equivalent dose-thyroid	14	5.4	99.6	2.6
Camp Sendai Support Personnel (Adults)				
Total effective dose	1.0	0.36	99.6	2.9
Total equivalent dose-thyroid	9.8	6.3	98.6	1.6
Sendai Airport -Humanitarian Field Workers (Adults)				
Total effective dose	1.2	0.67	98.4	1.9
Total equivalent dose-thyroid	13	12	95.8	1.1

*These are the doses estimated by deterministic methods reported in Cassata et al. (2012).

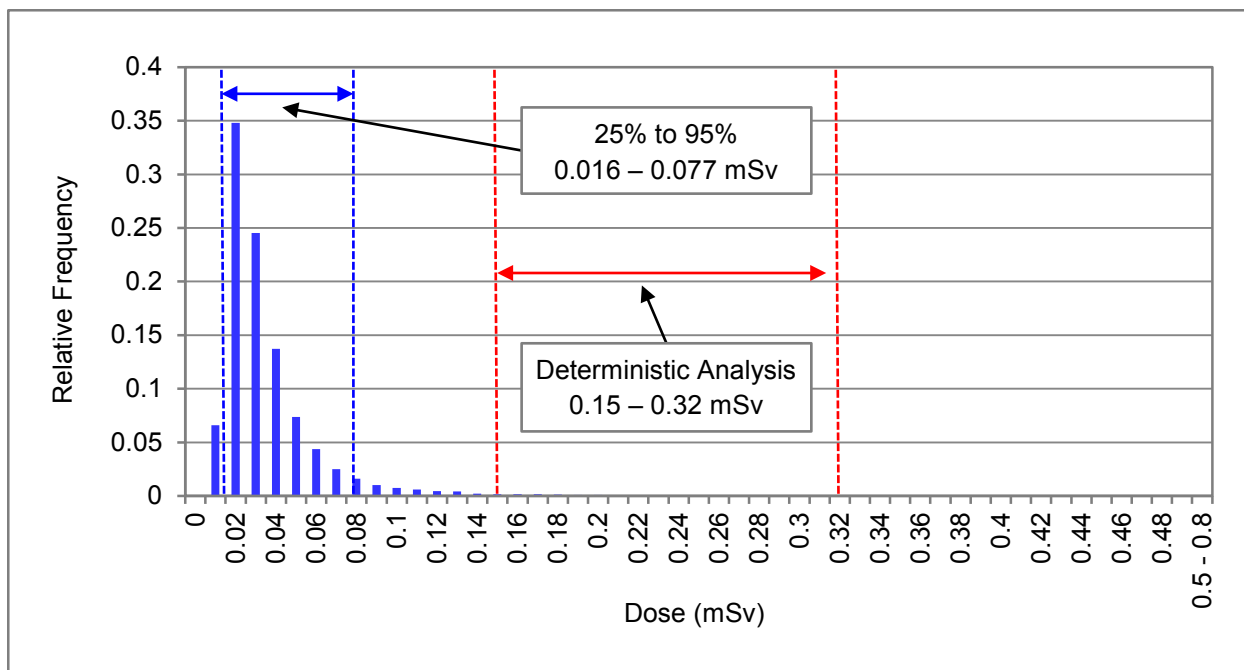


Figure 39. Total effective dose distribution using probabilistic analysis and range of doses estimated by deterministic methods for adults at Yokosuka Naval Base

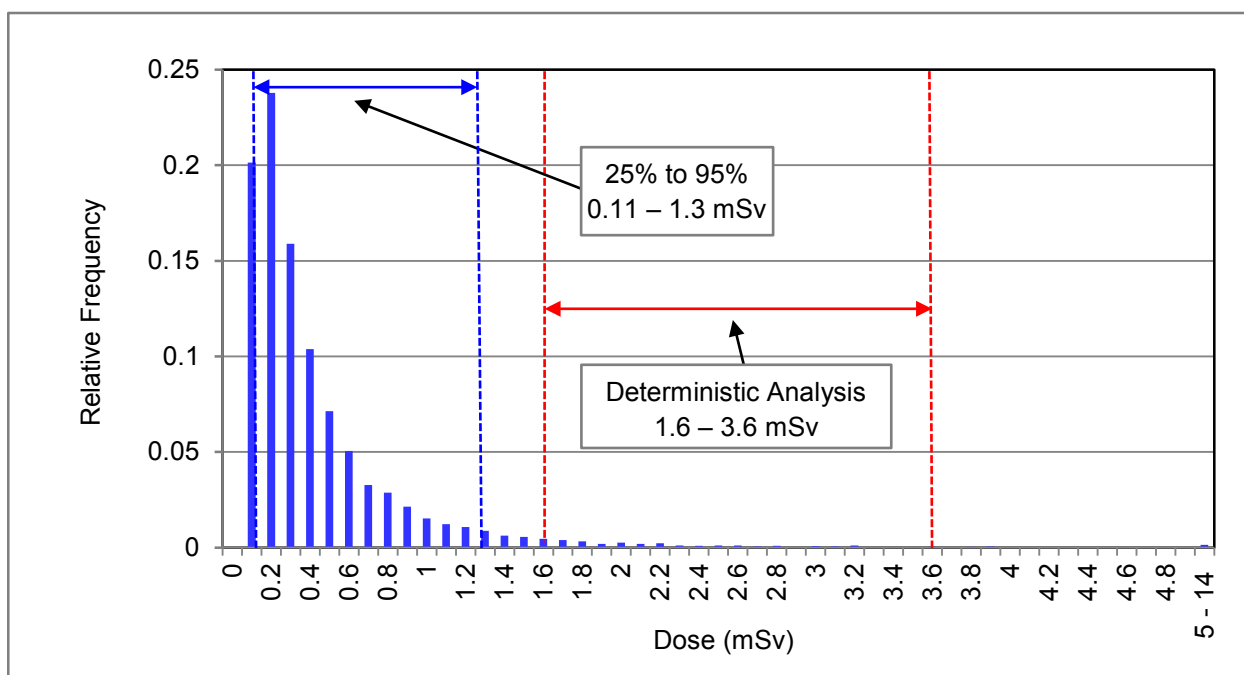


Figure 40. Total equivalent dose to the thyroid distribution using probabilistic analysis and range of doses estimated by deterministic methods for adults at Yokosuka Naval Base

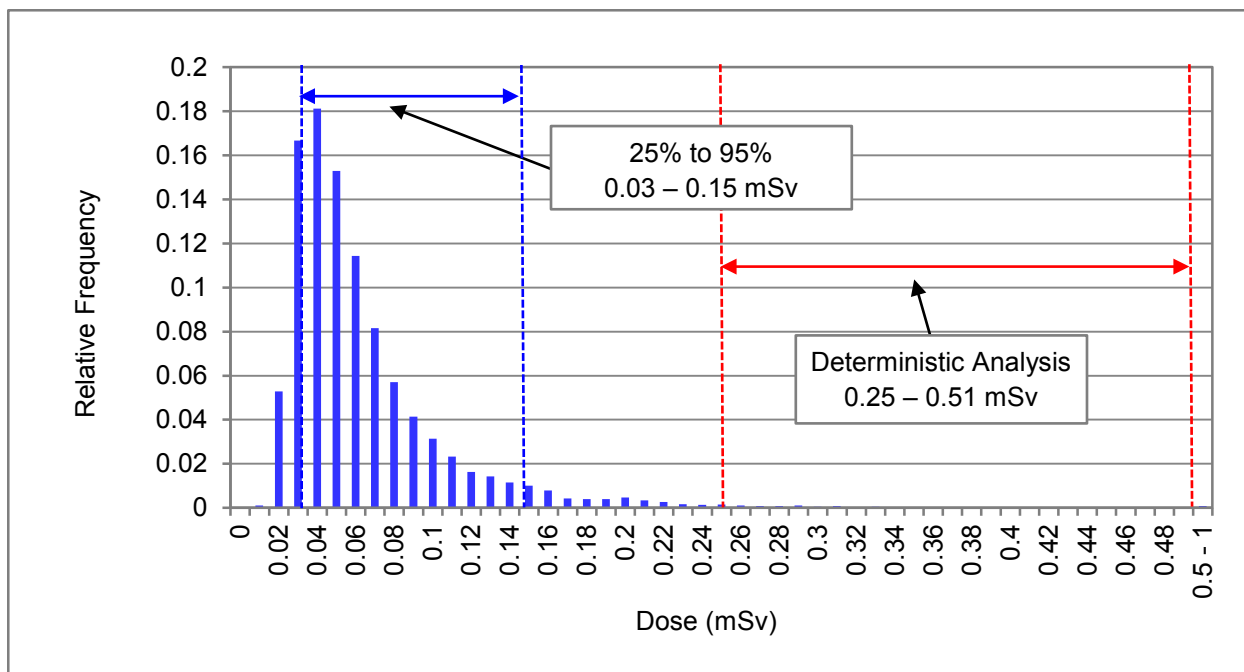


Figure 41. Total effective dose distribution using probabilistic analysis and range of doses estimated by deterministic methods for adults at Yokota Air Base

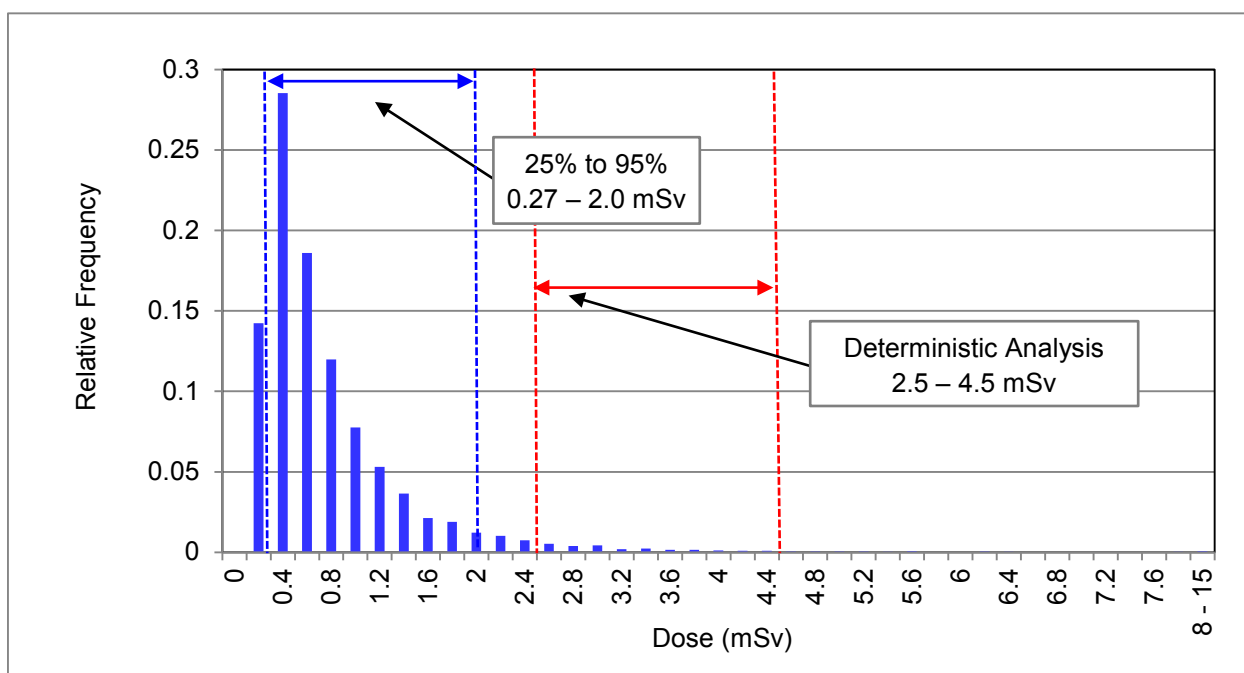


Figure 42. Total equivalent dose to the thyroid distribution using probabilistic analysis and range of doses estimated by deterministic methods for adults at Yokota Air Base

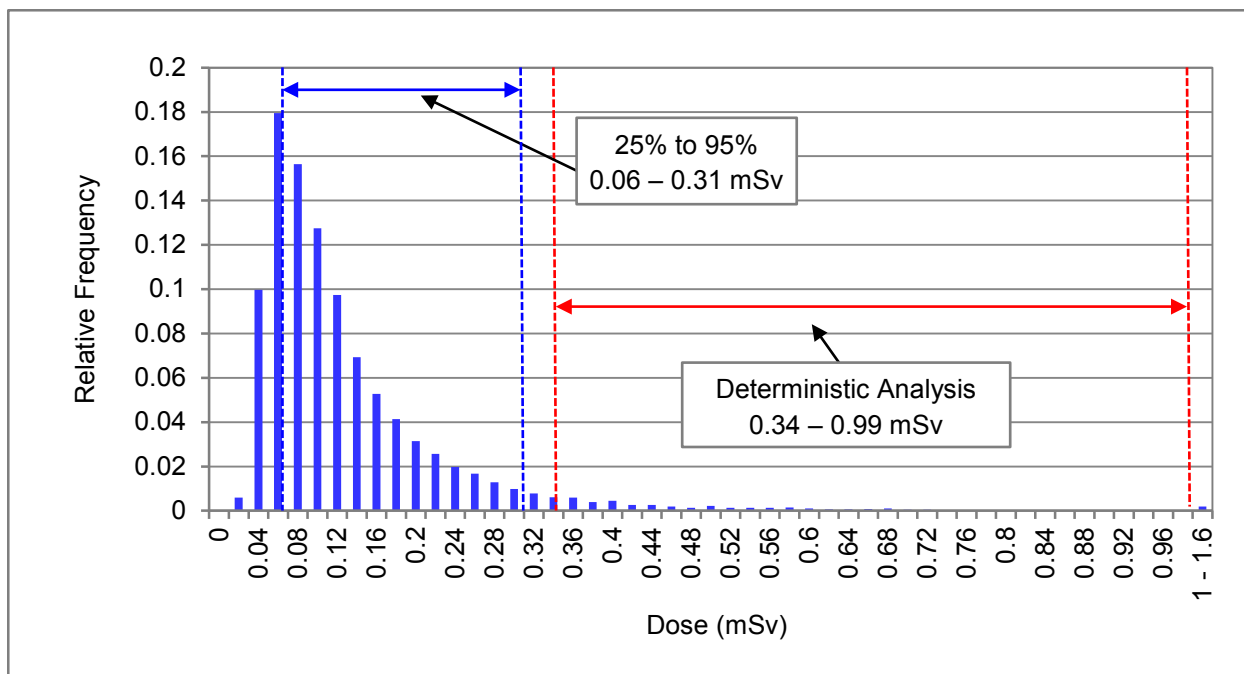


Figure 43. Total effective dose distribution using probabilistic analysis and range of doses estimated by deterministic methods for 1-to-2 year-old children at Yokota Air Base

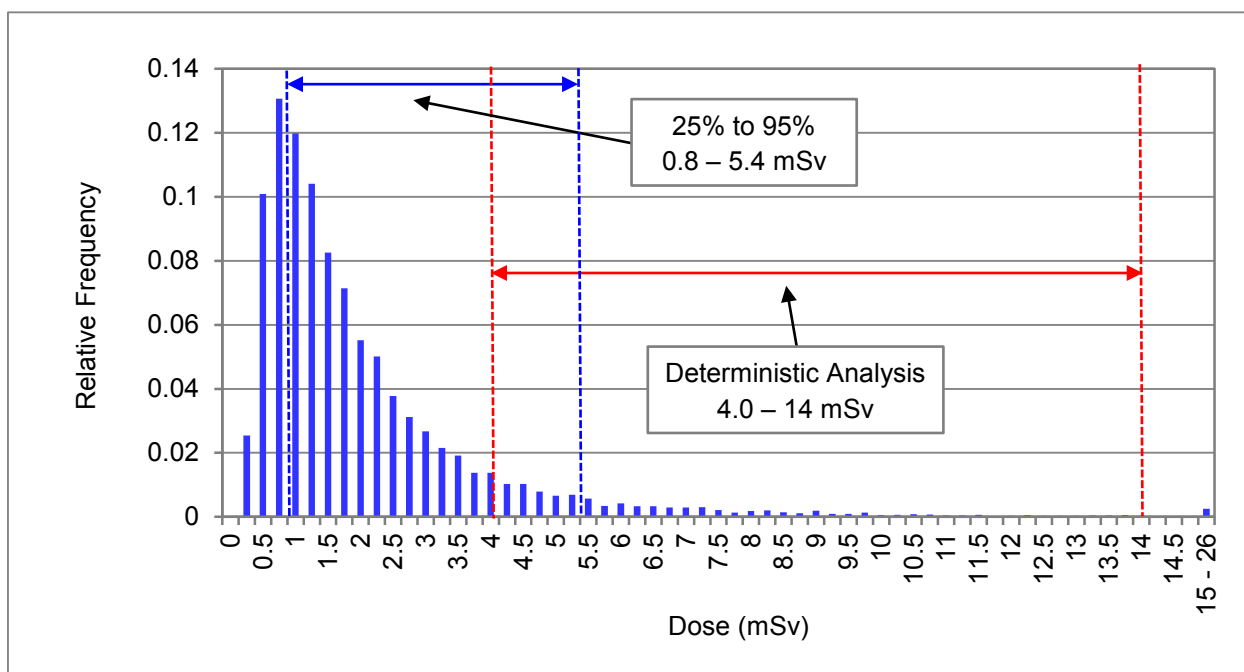


Figure 44. Total equivalent dose to the thyroid distribution using probabilistic analysis and range of doses estimated by deterministic methods for 1-to-2 year-old children at Yokota Air Base

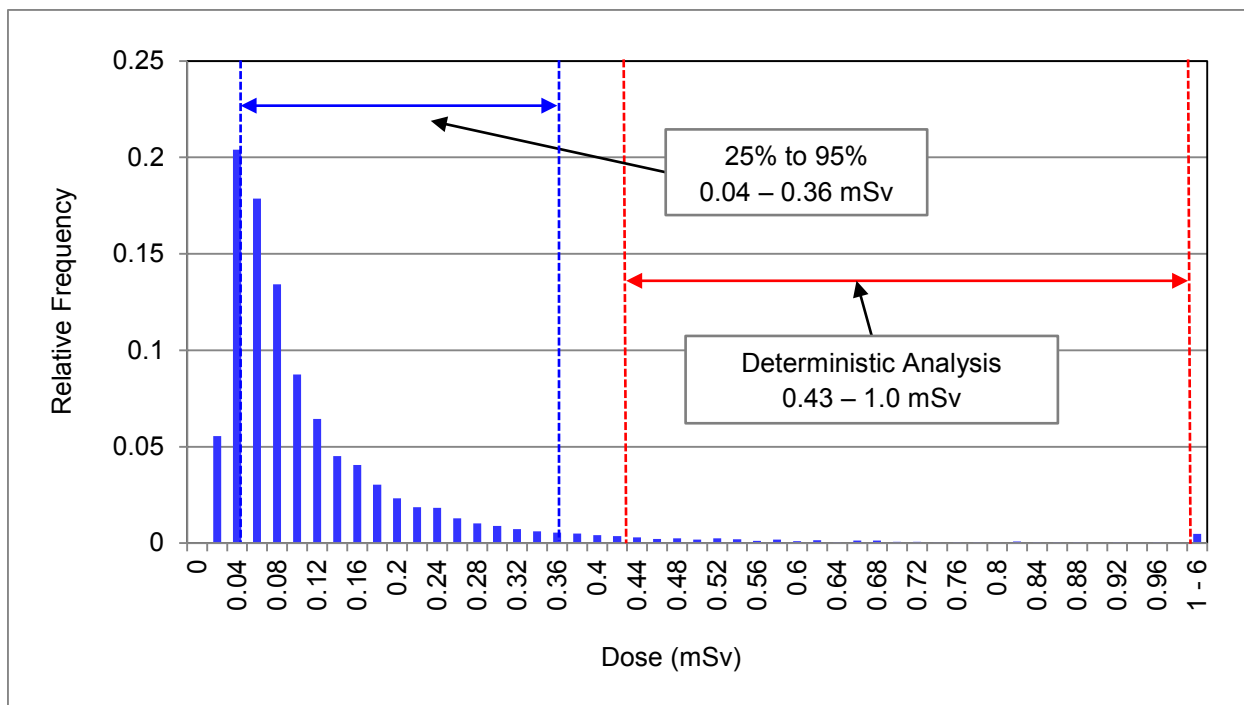


Figure 45. Total effective dose distribution using probabilistic analysis and range of doses estimated by deterministic methods at Camp Sendai

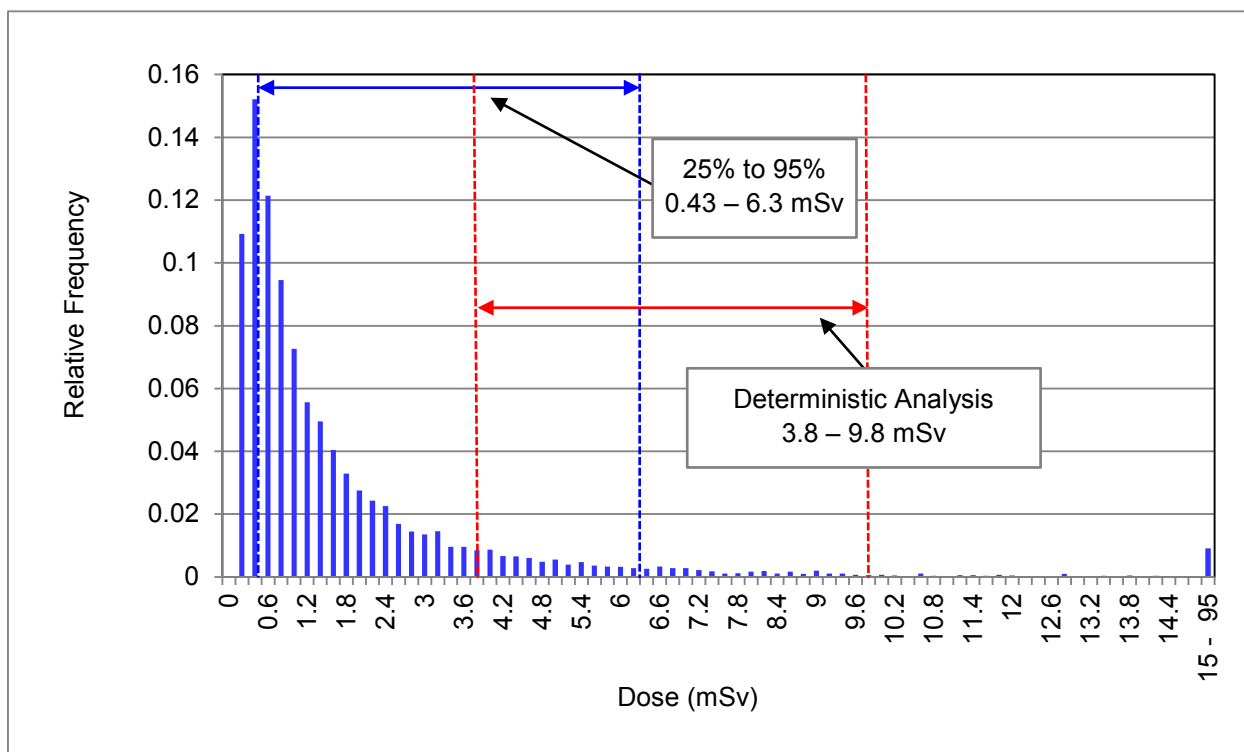


Figure 46. Total equivalent dose to the thyroid distribution using probabilistic analysis and range of doses estimated by deterministic methods at Camp Sendai

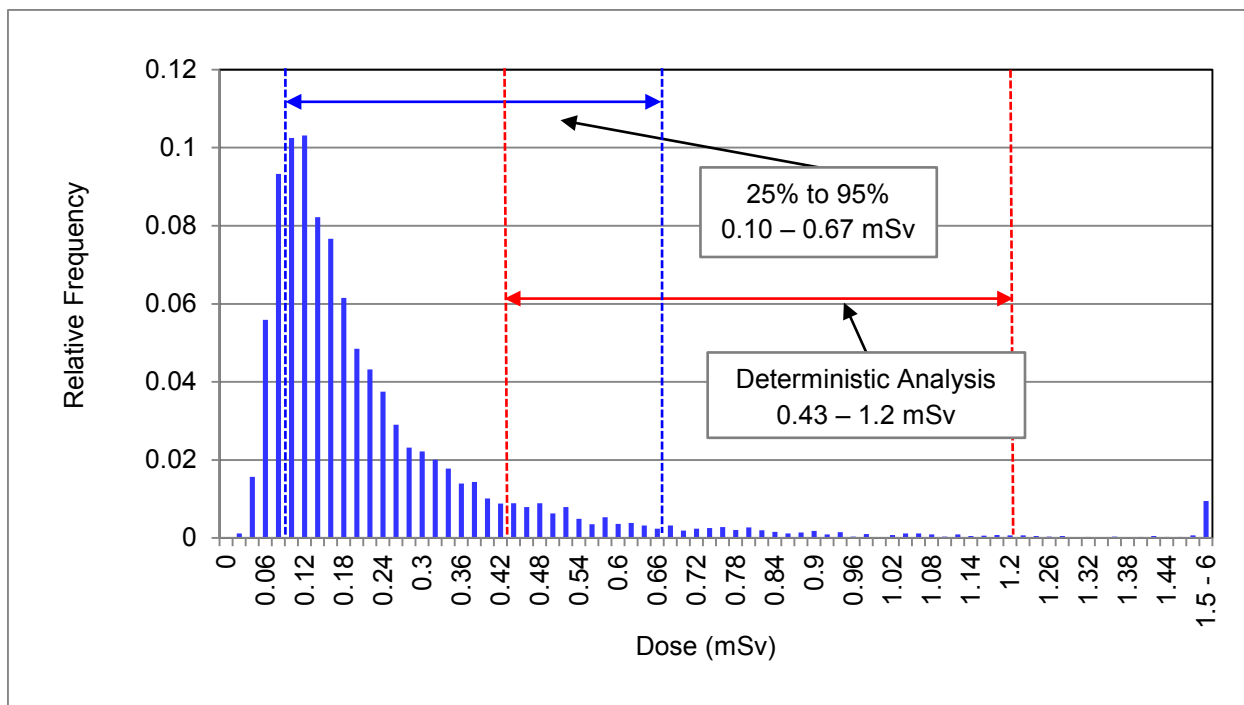


Figure 47. Total effective dose distribution using probabilistic analysis and range of doses estimated by deterministic methods for humanitarian field workers at Sendai Airport

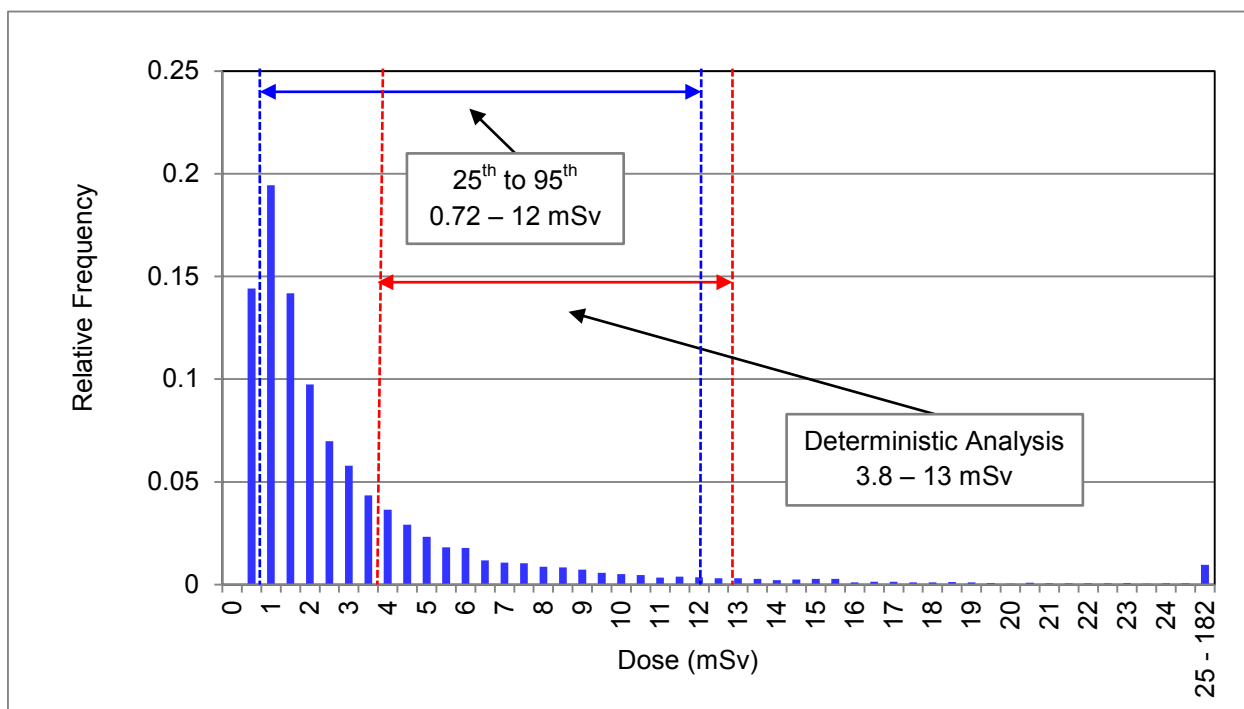


Figure 48. Total equivalent dose to the thyroid distribution using probabilistic analysis and range of doses estimated by deterministic methods for humanitarian field workers at Sendai Airport

5.3 Discussion of Results

The uncertainty factors for the probabilistic analysis of external dose range from 1.9 to 2.4. The uncertainty factors for the internal doses due to the intake of radioactive materials from inhalation, ingestion of water, and incidental ingestion of soil range from 4.3 to 8.6. The uncertainty factors for the probabilistic total effective dose and the total equivalent dose to the thyroid range from 3.0 to 7.2. The magnitude of the uncertainty factors for the total effective doses and total equivalent doses depends on the size of the contributions from the external versus internal doses with the higher uncertainty factors being associated with higher contributions from internal doses. When the 95th percentile external dose comprised 30 percent of the 95th percentile total effective dose, the uncertainty factor ranged from 3.0 to 3.2. However, when the 95th percentile external dose was less than 10 percent of the 95th percentile total equivalent dose for the thyroid, the uncertainty factor ranged from 4.1 to 7.2.

All of the ratios of the doses estimated by deterministic methods to 95th percentile doses from the probabilistic distributions are greater than 1. This ratio ranges from 1.1 to 4.1. The ratio for the total equivalent dose to the thyroid is lower than that of the total effective dose for all five PEPs. The ratios are lower for the total equivalent dose to the thyroid since several of the internal-dose specific parameters have an uncertainty factor of three whereas no external-dose-specific model parameters have an uncertainty larger than two.

All of the doses estimated by deterministic methods are greater than the equivalent 95th percentile dose from the probabilistic distribution for the same PEP indicating that the deterministic analysis (Cassata, et al., 2012) sufficiently captured the total doses for all or nearly all of the population of concern. The lowest percentile rank for a dose estimated by deterministic methods is 95.8 for the total equivalent dose to the thyroid for the humanitarian field workers at Sendai Airport. The highest percentile rank for a dose estimated by deterministic methods was 99.9 for the total effective dose for adults at Yokota Air Base.

Section 6.

Sensitivity Analysis for the Dose Models

Sensitivity analyses were performed for the total effective dose and the total equivalent dose to the thyroid for the PEP at Yokosuka Naval Base. These analyses were performed to determine the sensitivity of the estimated doses to the uncertainty and variability in individual input parameters. Sensitivity analyses are performed to study how the output of probabilistic dose calculations is affected by the magnitude and broadness of uncertainty distributions of input parameters, qualitatively or quantitatively (Saltelli et al., 2008). This section discusses the methodology and the results of the sensitivity analysis.

6.1 Technical Approach and Methodology

The dose distributions estimated by probabilistic analysis were calculated using the Monte Carlo simulation model developed for the exposures to radiation of individuals located at Yokosuka Naval Base, which are described in detail in Section 4. In this study, the dose model parameters were varied one at a time keeping all other parameters at their respective nominal value in separate runs of the Monte Carlo simulation. An additional run was performed where all the parameters were allowed to vary to obtain the distribution of the full probabilistic model. For each dose model parameter varied, the output dose distribution was compared with the distribution that resulted from varying all the parameters. Each distribution was generated using 100 Monte Carlo simulations since past analysis had shown that a larger number of simulations have little effect on the results.

Measures of the sensitivity, or sensitivity scores (SS), of the model to its input parameters and how they are evaluated can be defined in many ways (Hoffman and Gardner, 1983; Kirchner, 2008; Saltelli et al., 2008; Weitz et al., 2009). For this study, three sensitivity scores were adopted to compare ranges of variations in output dose distributions and are given in Equations 8 to 10.

$$SS1_i = \frac{(95_i^{th} - 5_i^{th})}{(95_{All}^{th} - 5_{All}^{th})} \quad (8)$$

$$SS2_i = \frac{\ln(\frac{95_i^{th}}{5_i^{th}})}{\ln(\frac{95_{All}^{th}}{5_{All}^{th}})} \quad (9)$$

$$SS3_i = \frac{(\frac{95_i^{th}}{5_i^{th}})}{(\frac{95_{All}^{th}}{5_{All}^{th}})} \quad (10)$$

where:

5_i^{th}	=	5 th percentile of the dose distribution where parameter i is varied
95_i^{th}	=	95 th percentile of the dose distribution where parameter i is varied
5_{All}^{th}	=	5 th percentile of the dose distribution where all parameters are varied
95_{All}^{th}	=	95 th percentile of the dose distribution where all parameters are varied

The use of the 5th and 95th percentiles eliminates values in the tails of model output distributions that could incorrectly influence the estimated score. The sensitivity scores vary theoretically between 0 and 1 for SS1 and SS2. For SS1 and SS2, a score close to 0 indicates a low sensitivity of the model to the corresponding parameter. The closer a sensitivity score approaches 1, the more sensitive the dose model is to that parameter. For SS3, the lowest value is 1 divided by $\frac{95_{All}^{th}}{5_{All}^{th}}$, which is a finite positive number. This characteristic does not allow for this sensitivity score to approach zero when the model is insensitive to a parameter with a small uncertainty contribution. Therefore, SS3 should be used with caution.

The input parameters to the dose model for Yokosuka Naval Base were varied one at a time. Most parameters were assumed independent of each other because they present at most a weak correlation. A few parameters, such as inhalation rates at various activity levels, were varied as a group because they were assumed partially correlated. A full explanation of the correlations is found in Appendix C. This sensitivity analysis resulted in calculating a total of 22 sensitivity scores for single or grouped input parameter uncertainties, which are listed and defined in Table 20. The “✓” in the columns of Table 20 indicates that the parameter is used in the calculation of that specific exposure pathway.

Table 20. Model parameter and variable names that apply to each exposure pathway

Parameter	Variable	Pathway			
		External	Inhalation	Water Ingestion	Soil Ingestion
Fraction of time outdoors	F_{OD}	✓	✓		
Fraction of time in residence structure	F_{Res}	✓			
Protection factor for residence structure	PF_{Res}	✓			
Protection factor for non-residence structure	PF_{NR}	✓			
Spatial variability of deposited radioactive materials	I_{SV}	✓			
External dose rate measurement	I_{Meas}	✓			
Air activity concentration measurement	$C_{AIR-Meas}$		✓		
Spatial variability of air concentration	C_{AIR-SV}		✓		
Use of surrogate air activity concentration data	$C_{AIR-Sur}$		✓		
Use of external dose ratio to scale the surrogate air activity concentration data	$C_{AIR-Ratio}$		✓		
Gas to aerosol fraction (iodine)	R_{GA}		✓		
Strontium radionuclides to cesium ratio	R_{SrCs}		✓		
Inhalation rate for all activity levels	IR_{AL}		✓		
Structure infiltration factor for aerosols	SIF		✓		
Structure infiltration factor for gas	SIF_{Gas}		✓		
Partition factor for elemental vs. methyl iodide gas	F_{Elem}		✓		
Dose coefficients	$DC_{Inh} \text{ \& } DC_{Ing}$		✓	✓	✓
Water activity concentration measurement	$C_{WATER-Meas}$			✓	
Water ingestion rate	IR_{Water}			✓	
Soil activity concentration measurement	$C_{SOIL-Meas}$				✓
Spatial variability of soil activity concentration for soil measurements	$C_{SOIL-SV}$				✓
Soil ingestion rate	IR_{Soil}				✓

6.2 Sensitivity Analysis for the Total Effective Dose Model

The results of the sensitivity analysis for the model of total effective dose are given in Table 21. Figure 49 through Figure 51 show sensitivity scores for each model parameter using sensitivity scores SS1, SS2, and SS3, respectively. A comparison of the three sensitivity scores for the total effective dose shows that SS1 and SS2 are generally in agreement in terms of the relative importance of parameter sensitivity, and clearly identifies those parameters to which the dose model is insensitive. The score SS3 amplifies the high values for a better differentiation between parameter sensitivity but bottoms at a specific value for those parameters to which the dose model is insensitive as explained above.

The sensitivity analysis results indicate that the model for the total effective dose is most significantly sensitive, based on SS1 or SS2, to the uncertainty in, by decreasing order of importance, inhalation and ingestion dose coefficients, ratio of gaseous to aerosol airborne iodine activity concentrations, fraction of time present outdoors, the use of surrogate air activity concentration data, external dose rate, and measurement of air activity concentration. The remaining model input parameters contribute much less to the overall uncertainty of the total effective dose model, which is therefore of low sensitivity to their variations. As expected, the dose model output is much more sensitive to input parameters that, first, present high uncertainty and, second, are used in the calculation of dose components with the higher contributions to the total effective dose. The total effective doses showed almost zero sensitivity to the ratio of strontium radionuclides to cesium.

6.3 Sensitivity Analysis for the Total Equivalent Dose to the Thyroid Model

The results of the sensitivity analysis for the model of total equivalent dose to the thyroid are listed in Table 22. Figure 52 through Figure 54 show the sensitivity scores for each model parameter using sensitivity scores SS1, SS2, and SS3, respectively. A comparison of the three sensitivity scores for the total equivalent dose to the thyroid shows that the three scores track similarly in terms of the relative importance of parameter sensitivity, except that SS3 bottoms at a non-zero constant value for all low sensitivity parameters, which is not the case for SS1 and SS2.

The results of the sensitivity analysis indicate that the model for the total equivalent dose to the thyroid is most significantly sensitive to the uncertainty in, by decreasing order of importance, inhalation and ingestion dose coefficients, ratio of gaseous to aerosol airborne iodine activity concentrations, the use of surrogate data, measurement of air activity concentration, the scaling ratio for the surrogate air activity concentration data, water ingestion rates, fraction of time present outdoors, inhalation rates, and spatial variability of air concentration. The other model input parameters contribute much less to the overall uncertainty of the total equivalent dose to the thyroid, which is therefore of low sensitivity to variations in those. As expected, the dose model output is much more sensitive to input parameters that, first, present high uncertainty and, second, are used in the calculation of dose components with higher contributions to total dose. The total effective doses showed almost zero sensitivity to the ratio of strontium radionuclides to cesium.

Table 21. Sensitivity scores for input parameters to the total effective dose model

	Input Parameter																						
	All*	F _{OD}	F _{Res}	PF _{Res}	PF _{NR}	I _{SV}	I _{Meas}	C _{AIR-Ratio}	C _{AIR-Meas}	C _{AIR-SV}	C _{AIR-Sur}	R _{GA}	R _{SrCs}	IR _{AL}	SIF	SIF _{Gas}	F _{Elem}	DC _{Inh} & DC _{Ing}	C _{SOIL-Meas}	C _{SOIL-SV}	IR _{Soil}	C _{WATER-Meas}	IR _{Water}
5 th (mrem)	1.15	1.73	1.76	1.74	1.79	1.71	1.6	1.8	1.57	1.73	1.24	1.42	1.87	1.64	1.81	1.71	1.80	1.24	1.87	1.87	1.87	1.78	1.7
Geometric mean (GM) (mrem)	2.88	2.08	1.86	1.89	1.87	1.98	1.9	2.1	1.90	1.97	1.86	1.89	1.87	1.88	1.87	1.88	1.87	1.91	1.87	1.87	1.87	1.86	1.92
Mean (mrem)	3.86	2.13	1.86	1.89	1.87	1.98	1.9	2.1	1.92	1.98	1.90	1.93	1.87	1.89	1.87	1.89	1.87	2.02	1.87	1.87	1.87	1.86	1.94
95 th (mrem)	10.8	3.12	1.99	2.02	1.97	2.27	2.4	2.4	2.3	2.25	2.47	2.84	1.87	2.21	1.94	2.08	1.94	3.69	1.87	1.87	1.88	1.96	2.31
Ratio 95 th /GM	3.76	1.5	1.07	1.07	1.06	1.15	1.27	1.18	1.21	1.14	1.33	1.51	1.00	1.17	1.04	1.11	1.04	1.93	1.00	1.00	1.00	1.05	1.2
Ratio 95 th /5 th	9.42	1.80	1.13	1.16	1.10	1.33	1.56	1.33	1.47	1.30	2.00	2.01	1.00	1.35	1.07	1.22	1.08	2.97	1.00	1.00	1.01	1.11	1.33
SS1	1.00	0.14	0.02	0.03	0.02	0.06	0.09	0.06	0.08	0.05	0.13	0.15	0.00	0.06	0.01	0.04	0.01	0.25	0.00	0.00	0.00	0.02	0.06
SS2	1.00	0.26	0.05	0.07	0.04	0.13	0.20	0.13	0.17	0.12	0.31	0.31	0.00	0.13	0.03	0.09	0.03	0.48	0.00	0.00	0.00	0.04	0.13
SS3	1.00	0.19	0.12	0.12	0.12	0.14	0.17	0.14	0.16	0.14	0.21	0.21	0.11	0.14	0.11	0.13	0.11	0.32	0.11	0.11	0.11	0.12	0.14

*The doses for “All” differ from those reported in Section 5 due to the smaller number of Monte Carlo simulations.

Table 22. Sensitivity scores for input parameters to the committed equivalent dose to the thyroid model

	Input Parameter																						
	All	F _{OD}	F _{Res}	PF _{Res}	PF _{NR}	I _{SV}	I _{Meas}	C _{AIR-Ratio}	C _{AIR-Meas}	C _{AIR-SV}	C _{AIR-Sur}	R _{GA}	R _{Srcs}	IR _{AL}	SIF	SIF _{Gas}	F _{Elem}	DC _{Inh} & DC _{Ing}	C _{SOIL-Meas}	C _{SOIL-SV}	IR _{Soil}	C _{WATER-Meas}	IR _{Water}
5 ⁱ th (mrem)	7	18.7	19.6	19.6	19.7	19.6	19.4	18.9	14.1	17.1	8.0	10.7	19.7	15.5	18.9	16.5	18.7	8.2	19.7	19.7	19.7	17.9	17.3
Geometric mean (GM) (mrem)	31	21.4	19.7	19.8	19.7	19.9	19.8	23.0	20.2	21.5	18.8	19.4	19.7	19.9	19.7	19.9	19.7	20.0	19.8	19.8	19.8	19.6	20.7
Mean (mrem)	65	21.8	19.7	19.8	19.7	19.9	19.8	23.2	20.6	21.7	20.2	21.0	19.7	20.1	19.8	20.1	19.8	23.9	19.8	19.8	19.8	19.6	21.0
95 ⁱ th (mrem)	236	29.6	19.9	19.9	19.9	20.1	20.3	30.0	27.7	26.8	30.9	39.0	19.7	26.1	20.7	24.0	20.8	67.2	19.8	19.8	19.9	21.6	28.4
Ratio 95 ⁱ th /GM	7.61	1.38	1.01	1.01	1.01	1.01	1.03	1.31	1.37	1.25	1.65	2.01	1.00	1.31	1.05	1.20	1.05	3.35	1.00	1.00	1.01	1.10	1.37
Ratio 95 ⁱ th /5 ⁱ th	32.4	1.6	1.0	1.0	1.0	1.0	1.0	1.6	2.0	1.6	3.9	3.6	1.0	1.7	1.1	1.5	1.1	8.2	1.0	1.0	1.0	1.2	1.6
SS1	1.00	0.05	0.00	0.00	0.00	0.00	0.00	0.05	0.06	0.04	0.10	0.12	0.00	0.05	0.01	0.03	0.01	0.26	0.00	0.00	0.00	0.02	0.05
SS2	1.00	0.13	0.00	0.00	0.00	0.01	0.01	0.13	0.19	0.13	0.39	0.37	0.00	0.15	0.03	0.11	0.03	0.60	0.00	0.00	0.00	0.05	0.14
SS3	1.00	0.05	0.03	0.03	0.03	0.03	0.03	0.05	0.06	0.05	0.12	0.11	0.03	0.05	0.03	0.04	0.03	0.25	0.03	0.03	0.03	0.04	0.05

*The doses for “All” differ from those reported in Section 5 due to the smaller number of Monte Carlo simulations.

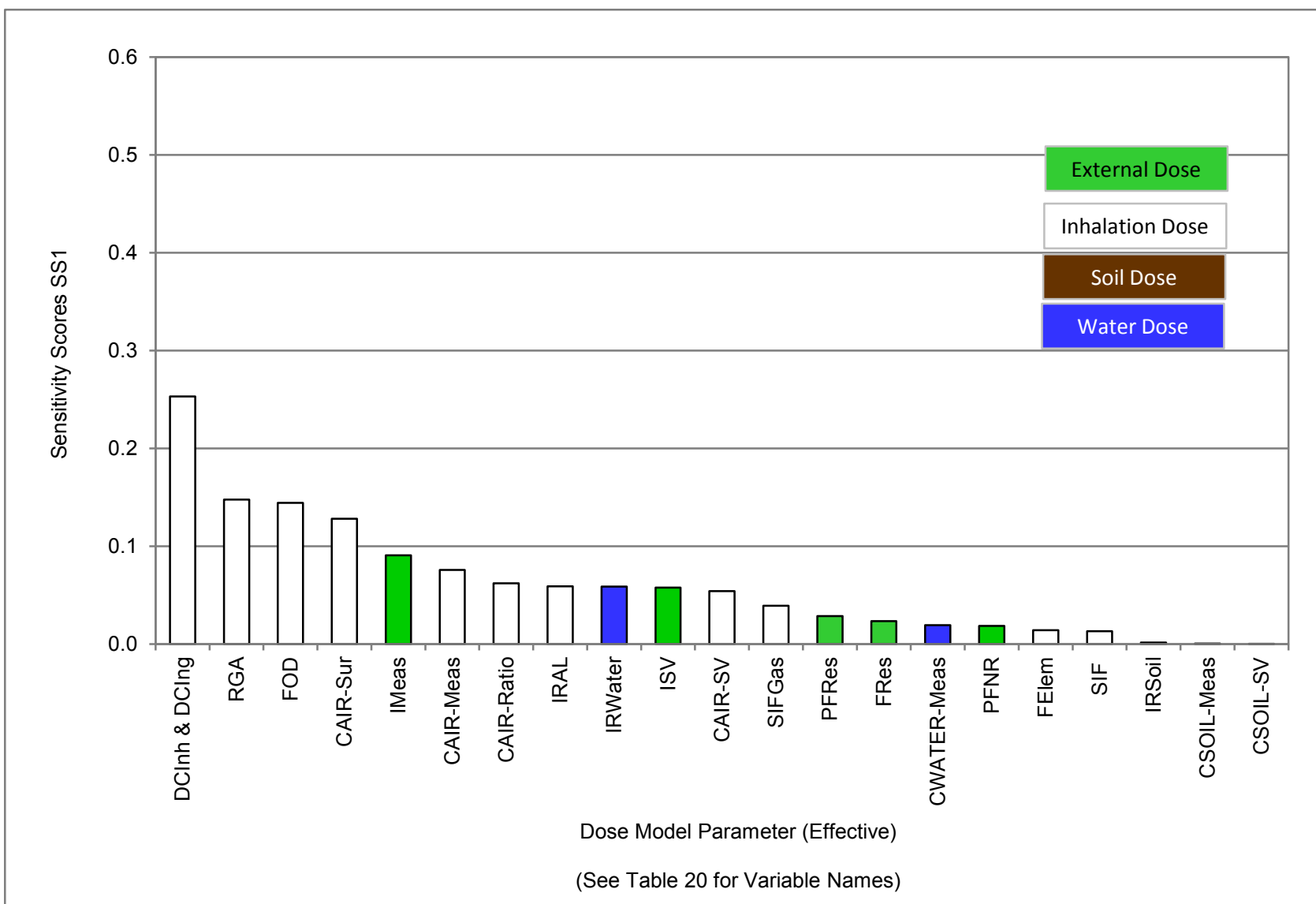


Figure 49. Sensitivity score SS1 for model parameters to total effective dose at Yokosuka Naval Base

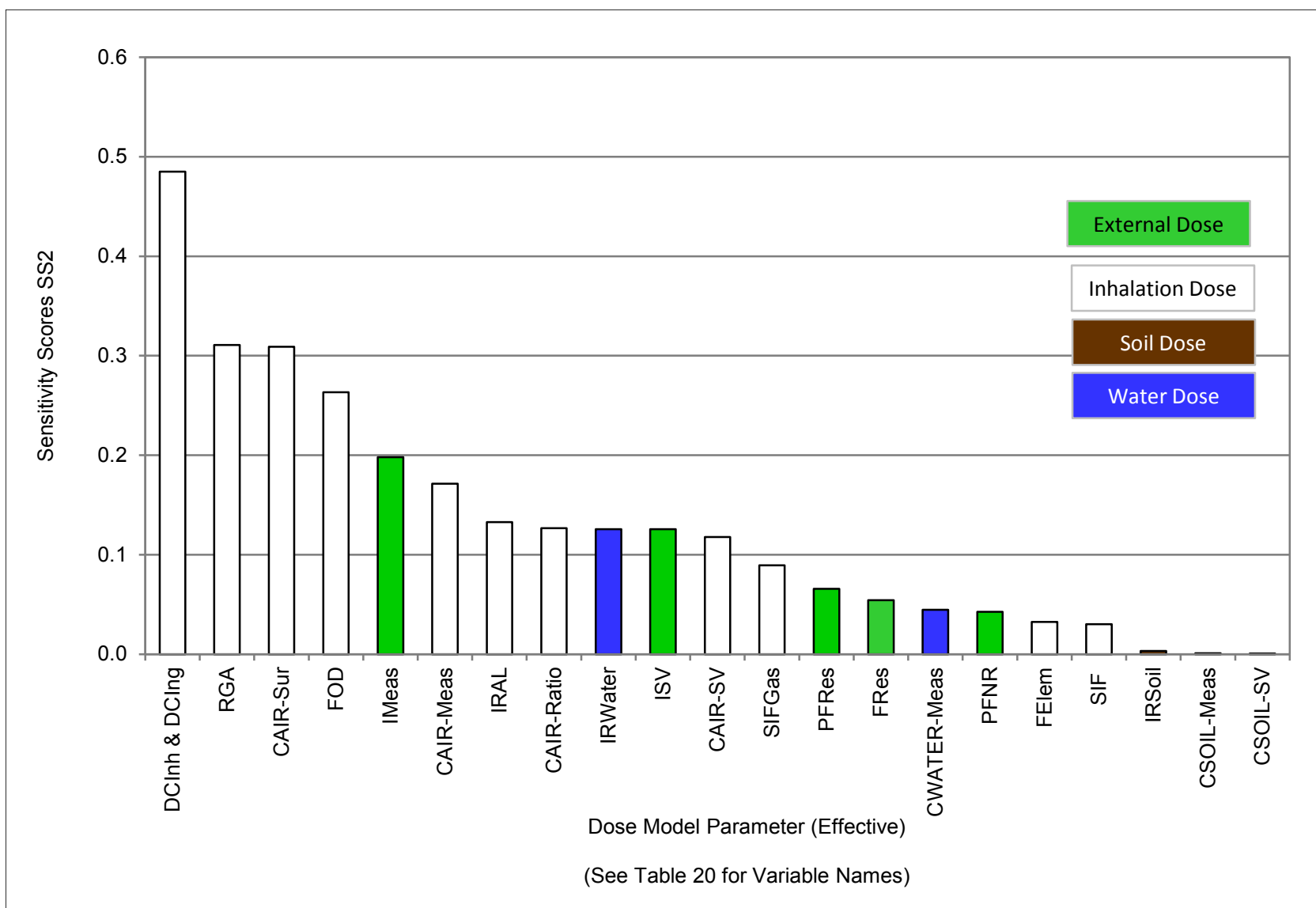


Figure 50. Sensitivity score SS2 for model parameters to total effective dose at Yokosuka Naval Base

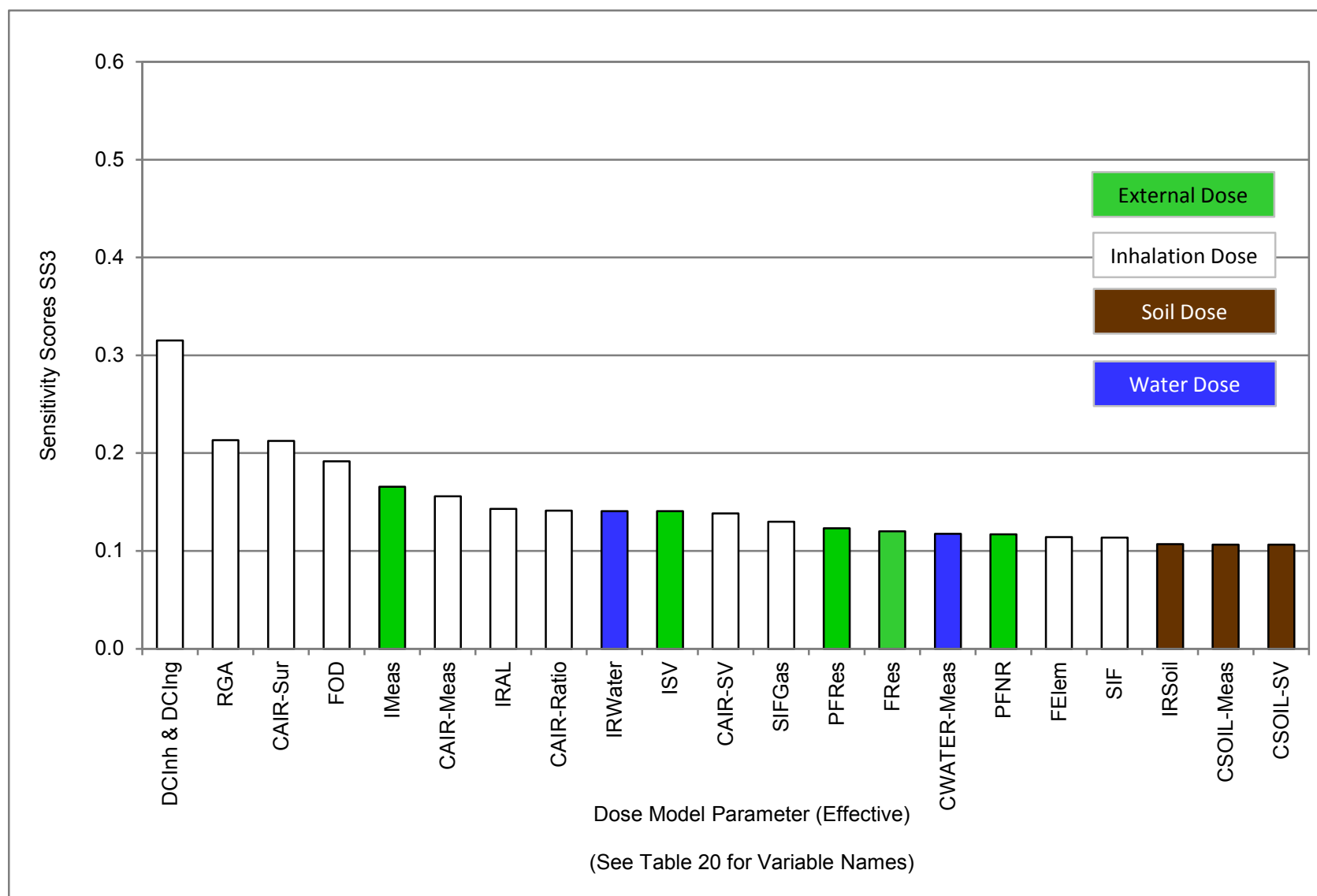


Figure 51. Sensitivity score SS3 for model parameters to total effective dose at Yokosuka Naval Base

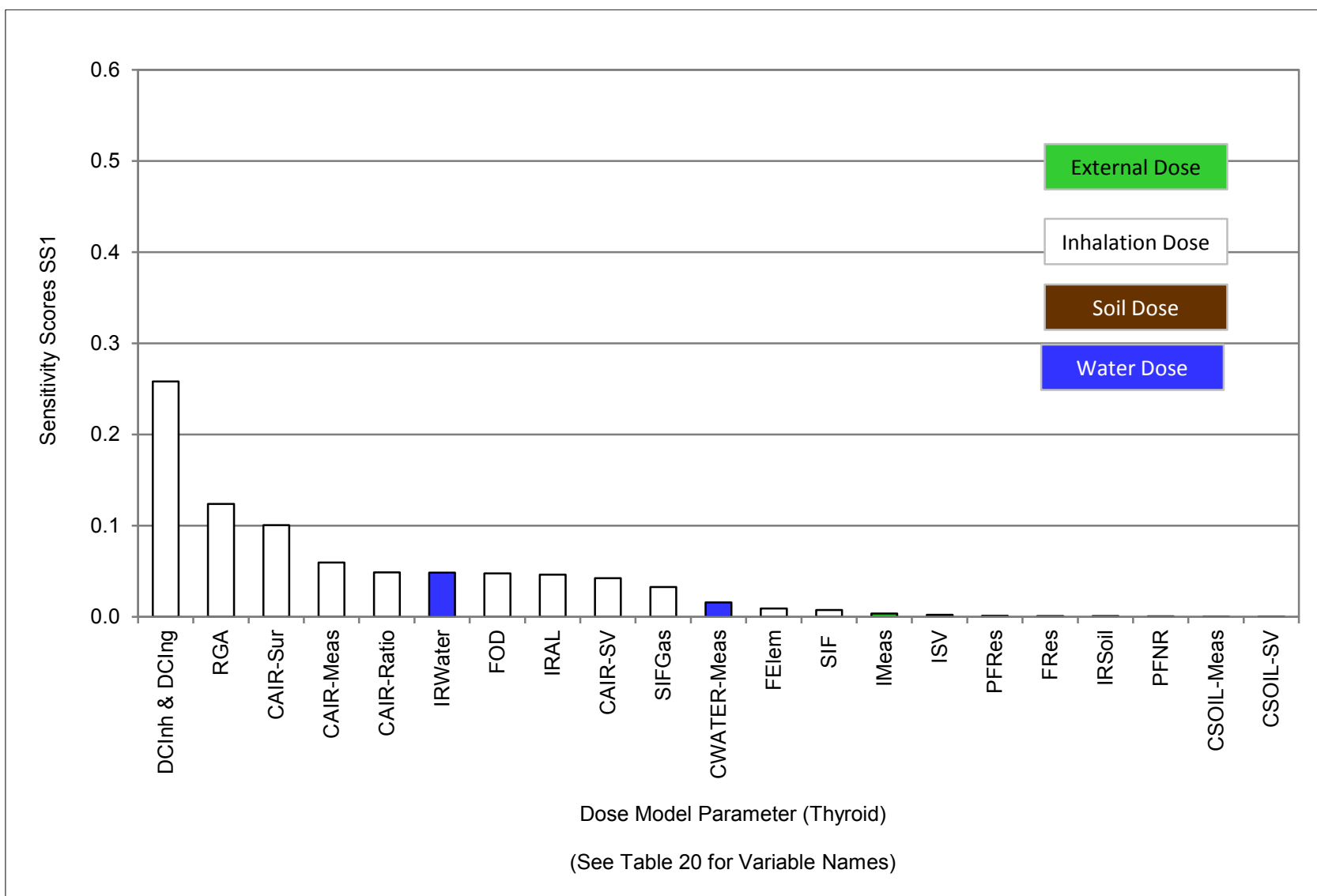


Figure 52. Sensitivity score SS1 for model parameters to total equivalent dose to the thyroid at Yokosuka Naval Base

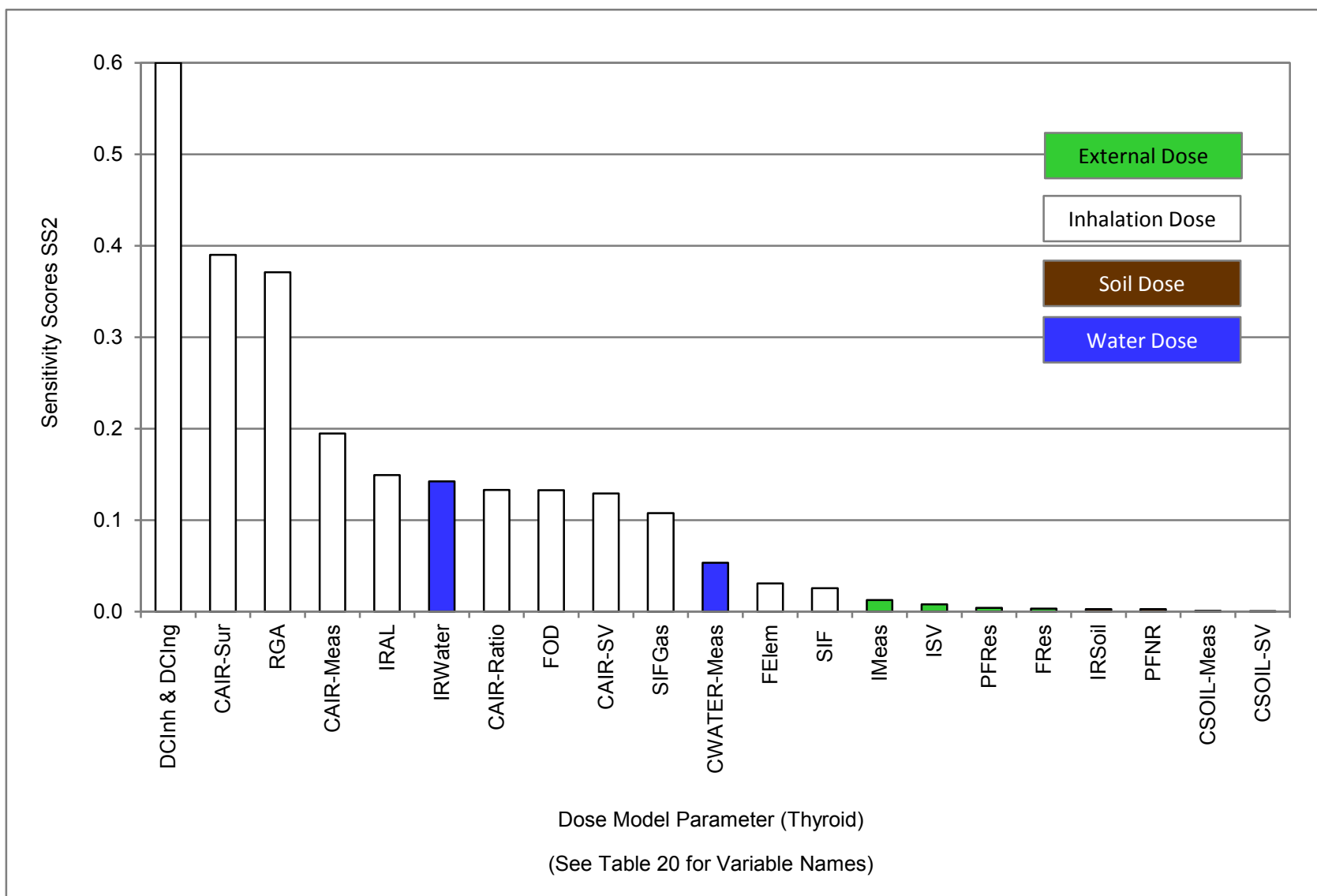


Figure 53. Sensitivity score SS2 for model parameters to total equivalent dose to the thyroid at Yokosuka Naval Base

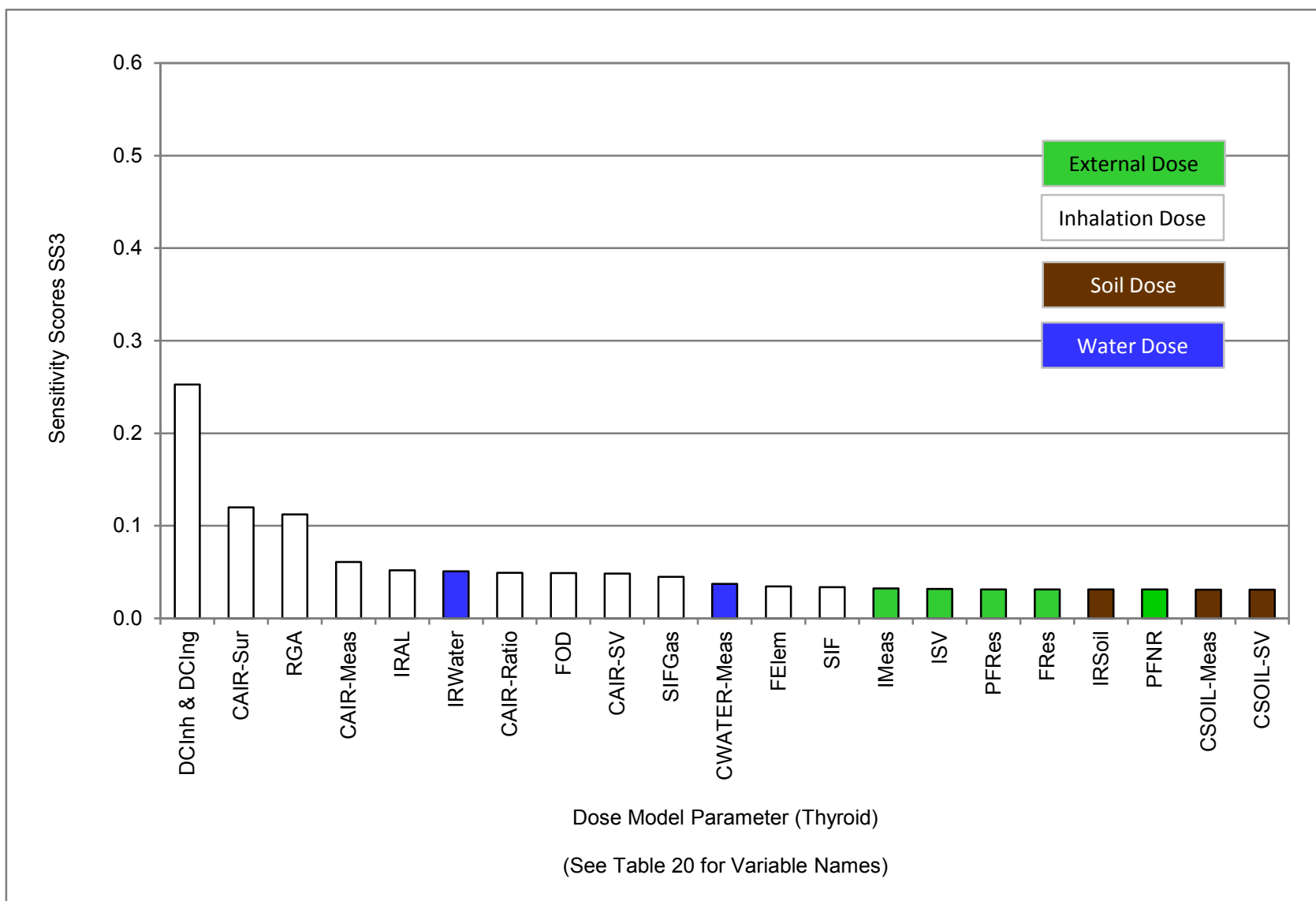


Figure 54. Sensitivity score SS3 for model parameters to total equivalent dose to the thyroid at Yokosuka Naval Base

Section 7.

Conclusions

The results of the radiation dose assessment reported in Cassata et al. (2012) covered 13 shore locations where DOD-affiliated persons were known to have lived, worked, or deployed. In that assessment, doses were estimated by deterministic methods and were intended to be high-sided and based on conservative assumptions. Doses were estimated for adults and several children's groups.

For this report, probabilistic analyses were performed to estimate total dose distributions using model input parameters with realistic central estimates and corresponding uncertainty distributions. The probabilistic analyses were completed for four selected locations including Yokosuka Naval Base, Yokota Air Base, Camp Sendai, and Sendai Airport. The doses were estimated for adults for the first three locations and for humanitarian field workers at Sendai Airport. Children aged 1-to-2 years-old were included for Yokota Air Base. The probabilistic dose models developed for these potentially exposed populations were applied for calculating total effective doses and total equivalent doses to the thyroid.

Model input parameters and uncertainty distributions were developed based on radiation exposure data collected from published sources, e.g., MEXT, DOD, DOE. In addition, recent exposure and radiation dose assessment literature was used as the basis for selected statistical data and models, including USEPA Exposure Factors Handbook (USEPA, 2011) and DTRA technical reports (Weitz et al., 2009; DTRA, 2010; Cassata et al., 2012). The correlations among all input parameters to the total dose models were evaluated and implemented in the probabilistic models.

Estimates of external and internal doses and uncertainty distributions were determined by Monte Carlo simulation. The results of the probabilistic analyses were compared with the doses estimated by deterministic methods reported in Cassata et al. (2012) to assess whether the latter are sufficiently conservative (high-sided). Finally, sensitivity analyses were carried out to assess the effects of parameter variations on the estimated dose. The geometric and arithmetic means of total effective doses and total equivalent doses to the thyroid as well as the corresponding 95th percentile values are summarized in Table 23. Also, shown in Table 23 are the doses estimated in Cassata et al. (2012) and corresponding percentile ranks within the probabilistic dose distributions. These comparisons show that in all the scenarios evaluated, the total effective doses and total equivalent doses to the thyroid estimated by deterministic methods lay much higher than the 95th percentile values determined using the probabilistic method. In fact, all the doses estimated by deterministic methods are higher than the 95.8th percentile values of the probabilistic analyses.

The results of the sensitivity analysis performed for the Yokosuka Naval Base location indicate that the model for the total effective dose is most sensitive to the uncertainty in inhalation and ingestion dose coefficients and least sensitive to uncertainties in parameters that are used in the calculation of the soil ingestion dose. The total effective doses showed an extremely low sensitivity to the ratio of strontium radionuclides to Cs-137. As expected, the dose model results are much more sensitive to input parameters that present broader uncertainty

distributions and are used in the calculation of dose components with larger contributions to total doses.

The sensitivity analysis carried out for the Yokosuka Naval Base location indicates that the model for the total equivalent dose to the thyroid is most sensitive to the uncertainty in inhalation and ingestion dose coefficients and least sensitive to uncertainties in parameters that are included in the calculation of the external dose or soil ingestion dose. The total equivalent doses to the thyroid showed an extremely low sensitivity to the ratio of strontium radionuclides to Cs-137. As expected, the dose model results are much more sensitive to input parameters that present broader uncertainty distributions and are used in the calculation of dose components with greater contributions to total doses.

Table 23. Summary and comparison of doses estimated using probabilistic analysis and by deterministic methods

Dose Type	Geometric Mean (mSv)	Arithmetic Mean Dose (mSv)	Dose Estimated by Deterministic Methods* (mSv)	Probabilistic 95th Percentile Dose (mSv)	Dose Estimated by Deterministic Methods as Percentile of the Probabilistic Distribution	Ratio of Deterministic Analysis to 95th Percentile Dose
Yokosuka Naval Base (Adults)						
Total effective dose	0.024	0.031	0.32	0.077	99.8	4.1
Total equivalent dose to thyroid	0.24	0.40	3.6	1.3	99.7	2.9
Yokota Air Base (Adults)						
Total effective dose	0.048	0.060	0.51	0.15	99.9	3.6
Total equivalent dose to thyroid	0.48	0.69	4.5	2.0	99.4	2.4
Yokota Air Base (1-to-2 Year-Old Children)						
Total effective dose	0.093	0.12	0.99	0.31	99.8	3.2
Total equivalent dose to thyroid	1.4	1.9	14	5.4	99.6	2.6
Camp Sendai (Adults)						
Total effective dose	0.074	0.12	1.0	0.36	99.6	2.9
Total equivalent dose to thyroid	0.87	1.8	9.8	6.3	98.6	1.6
Sendai Airport (Humanitarian Field Workers)						
Total effective dose	0.17	0.23	1.2	0.67	98.4	1.9
Total equivalent dose to thyroid	1.7	3.2	13	12	95.8	1.1

*Doses estimated by deterministic methods are those reported in Cassata et al. (2012).

Section 8.

References

- Air Force Housing, 2013. Welcome to Yokota AB Housing, Housing Management Office
<http://www.housing.af.mil/home> (Accessed February 25, 2013).
- Allen, M.J., 2012. E-mail to authors. Subject: Looking for Information About Operation Tomodachi and Camp Sendai. 3rd Marine Expeditionary Brigade. October 22.
- Averill, B.A. and Eldredge, P., 2011. General Chemistry: Principles, Patterns, and Applications, v. 1.0. Saylor.org, Washington, DC. December.
- Buddemeier, B.R., Dillon, M.B., 2009. Key Response Planning Factors for the Aftermath of Nuclear Terrorism. LLNL-TR-0410067, Lawrence Livermore National Laboratory, Livermore, CA. August.
- Bulmer, M.G., 1979. Principles of Statistics. Courier Dover Publications, New York, NY.
- Cassata, J., Falo, G., Rademacher, S., Alleman, L., Rosser, C., Dunavant, J., Case, D., Blake, P., 2012. Radiation Dose Assessment for Shore-Based Individuals in Operation Tomodachi, Revision 1. DTRA-TR-12-001(R1), Defense Threat Reduction Agency, Fort Belvoir, VA. December 31.
- CNIC (Commander, Navy Installations Command), 2013. Family and Unaccompanied Housing, COMMANDER FLEET ACTIVITIES YOKOSUKA, Yokosuka Naval Base, Japan.
<http://www.cnmc.navy.mil/Yokosuka/FleetAndFamilyReadiness/index.htm> (Accessed February 25, 2013).
- Doane, D.P. and Seward, L.E., 2009. Applied Statistics in Business and Economics, 2nd edition. McGraw Hill Irwin, Burr Ridge, IL.
- DOE (Department of Energy), 2013. *US DOE/NNSA and DoD Response to 2011 Fukushima Incident*. National Nuclear Security Agency, Washington, DC. <http://data.gov>. Accessed April 21, 2013.
- DOL (Department of Labor), 2011. American Time Use Survey User's Guide: Understanding ATUS 2003 to 2010. Bureau of Labor Statistics and U.S. Census Bureau, November. Data for 2003–2010. <http://www.bls.gov/tus/tables.htm>. Accessed December 1, 2011.
- DTRA (Defense Threat Reduction Agency), 2010. Standard Operating Procedures Manual for Radiation Dose Assessment, Revision 1.3/1.3a. DTRA-SOP-10-01, Defense Threat Reduction Agency, Fort Belvoir, VA. January 31/March 31.
- Finn, S. P., Simmons, G. L., and Spencer, L. V., 1979. Calculation of Fission Product Gamma Ray and Beta Spectra at Selected Times after Fast Fission of U238 and U235 and Thermal Fission of U235. SAI Report SAI-78-782-LJ/F, Science Applications, Inc., San Diego, CA.
- Glasstone, S. and P. J. Dolan, 1977. The Effects of Nuclear Weapons (third edition). Headquarters, Department of the Army, Washington, D.C. March.

- Hahn, G.J and Shapiro, S.S., 1967. Statistical Models in Engineering. John Wiley, New York, NY.
- Halbleib, J. A., Kensek, R. P., Mehlhorn, T. A., Valdez, G. D., Seltzer, S. M., and Berger, M. J., 1992. ITS Version 3.0: The Integrated TIGER Series of Coupled Electron/Photon Monte Carlo Transport Codes. SAND 91-1634, Sandia National Laboratories, Albuquerque, NM. March 1.
- Hoffman, F.O. and Gardner, R.H., 1983. Evaluation of Uncertainties in Radiological Assessment Models. Chapter 11 in Radiological Assessment, A Textbook on Environmental Dose Analysis, Till, J.E. and Meyer, H.R., Eds. NUREG/CR-3332; ORNL-5968 Oak Ridge National Laboratory, Oak Ridge, TN.
- IAEA (International Atomic Energy Agency), 2004. Methods for assessing occupational radiation doses due to intakes of radionuclides. Report No. 37, International Atomic Energy Agency, Vienna, Austria. July.
- ICRP (International Commission on Radiological Protection), 1994. "Dose Coefficients for Intakes of Radionuclides by Workers. ICRP Publication 68." Annals of the ICRP, 24(4), Elsevier Ltd., Oxford, UK.
- ICRP (International Commission on Radiological Protection), 1995a. "Age-dependent Doses to Members of the Public from Intake of Radionuclides - Part 4 Inhalation Dose Coefficients. ICRP Publication 71," Annals of the ICRP, 25(3-4), Elsevier Ltd., Oxford, UK.
- ICRP (International Commission on Radiological Protection), 1995b. "Age-dependent Doses to the Members of the Public from Intake of Radionuclides Part 5, Compilation of Ingestion and Inhalation Coefficients, ICRP Publication 72." Annals of the ICRP, 25(3-4), Elsevier Ltd., Oxford, UK.
- ICRP (International Commission on Radiological Protection), 2001. The ICRP Database of Dose Coefficients: Workers and Members of the Public. Compact Disc Version 2.01, Elsevier Ltd., Oxford, UK.
- ICRP (International Commission on Radiological Protection), 2007. "The 2007 Recommendations of the International Commission on Radiological Protection, ICRP Publication 103." Annals of the ICRP, 37(2-4), Elsevier Ltd., Oxford, UK.
- Kirchner, T.B., 2008. Estimating and Applying Uncertainty in Assessment Models, in Radiological Assessment and Environmental Analysis. Till, J. E. and Grogan, H. A., Editors, Oxford University Press, Oxford, New York.
- Kocher, D.C., Trabalka, J.R., and Apostolaei, A.I., 2009. Derivation of Effective Resuspension Factors in Scenarios for Inhalation Exposure Involving Resuspension of Previously Deposited Fallout by Nuclear Detonations at Nevada Test Site. DTRA-TR-09-15, Defense Threat Reduction Agency, Fort Belvoir, VA. November.
- MEXT (Ministry of Education, Culture, Sports, Science and Technology), 2011a. Results of Airborne Monitoring Survey by MEXT in Tokyo Metropolitan and Kanagawa Prefecture. Ministry of Education, Culture, Sports, Science and Technology, Tokyo, Japan. October 6.

- MEXT (Ministry of Education, Culture, Sports, Science and Technology), 2011b. Results of Airborne Monitoring Survey by MEXT and Miyagi Prefecture. Ministry of Education, Culture, Sports, Science and Technology, Tokyo, Japan. July 20.
- MEXT (Ministry of Education, Culture, Sports, Science and Technology), 2013. Monitoring Information of Environmental Radioactivity Level. Ministry of Education, Culture, Sports, Science and Technology. <http://radioactivity.nsr.go.jp/en/>. Accessed April 17, 2013.
- Misawa M. and Nagamori, F., 2008. “System for Predictions of Environmental Emergency Dose Information Network System” *Fujitsu Science and Technology Journal*. 44(4), pp. 377–399.
- Morgan, M.G. and Henrion, M., 1990. *Uncertainty: A Guide to Dealing with Uncertainty in Quantitative Risk and Policy Analysis*. Cambridge University Press, New York.
- National Bureau of Asian Research, 2011. “Chronology of Operation Tomodachi.” April 8.
- Nagaoka, K., Sato, S., Araki, S., Ohta, Y., Ikeuchi, Y., 2012. “Changes of Radionuclides in the Environment in Chiba, Japan, After the Fukushima Nuclear Power Plant Accident.” *Health Phys.* 102(4), pp. 437–442. April.
- Nair, S.K., Apostoaei, A.I., and Hoffman, F.O., 2000. “A Radioiodine Speciation, Deposition, and Dispersion Model with Uncertainty Propagation for the Oak Ridge Dose Reconstruction,” *Health Phys.* 78(4), pp. 396–414. April.
- NCRP (National Council on Radiological Protection and Measurements), 1996. *A Guide for Uncertainty Analysis in Dose and Risk Assessments Related to Environmental Contamination*. NCRP Commentary No. 14, National Council on Radiation Protection and Measurements, Bethesda, Maryland.
- NCRP (National Council on Radiological Protection and Measurements), 1998. *Evaluating the Reliability of Biokinetic and Dosimetric Models and Parameters Used to Assess Individual Doses for Risk Assessment Purposes*. NCRP Commentary 15, National Council on Radiological Protection and Measurements, Bethesda, Maryland.
- NCRP (National Council on Radiological Protection and Measurements), 2007. *Uncertainties in the Measurement and Dosimetry of External Radiation*. NCRP Report No. 158, National Council on Radiological Protection and Measurements, Bethesda, Maryland.
- NIST (National Institute of Standards and Technology), 2009. *NIST/SEMATECH e-Handbook of Statistical Methods*. National Institute of Standards and Technology, Gaithersburg, MD. <http://www.itl.nist.gov/div898/handbook/>. Accessed August, 2012
- NSTC (Nuclear Safety Technology Center), 2013. *Disaster Prevention and Nuclear Safety Network for Nuclear Environment*. Nuclear Regulatory Authority, Nuclear Safety Technology Center. <http://www.bousai.ne.jp/eng/index.html>. Accessed April 17, 2013.
- OSTP (Office of Science & Technology Policy), 2010. *National Planning Guidance for Response to a Nuclear Detonation (2nd Ed.)*, Office of Science & Technology Policy, Washington, DC. June. <http://www.usuhs.mil/afri/outreach/pdf/planning-guidance2010.pdf>. Accessed Feb 20, 2013.

- Robson, S. 2011. "U.S. Troops making Best of Situation at Sendai Airport," Stars and Stripes, Defense Media Activity, Fort Meade, MD. May 4.
- Saltelli, A., Ratto, M., Andres, T., Campolongo, F., Cariboni, J., Gatelli, D. Saisana, M., and Tarantola, S., 2008. Global Sensitivity Analysis, The Primer. John Wiley & Sons, Hoboken, NJ.
- Stevens, P. N., and Trubey, D. K., 1972. Weapons Radiation Shielding Handbook – Chapter 3: Methods for Calculating Neutron and Gamma-Ray Attenuation. DNA-1892-3, Defense Nuclear Agency, Washington, D.C. May.
- Stroad, M.W., 2011. "Services, JSDF unit during relief efforts," Okinawa Marine, III Marine Expeditionary Force and Marine Corps Bases Japan. <http://www.okinawa.usmc.mil>. Accessed August 20, 2012. April 8.
- Thatcher, T.L. and Layton, D.W., 1995. "Deposition, Resuspension, and Penetration of Particles within a Residence," Atmospheric Environment, 29(13), pp. 1487–1497.
- U.S. Air Force, 2011a. "Commander Discusses Yokota's Role in Operation Tomodachi," Tomodachi Times, 1(16):1. 374th Airlift Wing Commander, Yokota Air Base, Japan.
- U.S. Air Force, 2011b, "Yokota Airmen Central to Support Operation Tomodachi," 374th Airlift Wing Public Affairs, Yokota Air Base, March 30.
- U.S. Air Force, 2011c, "Yokota Comm Keeps Interagency Team Connected During Operation Tomodachi," 374th Airlift Wing Public Affairs, Yokota Air Base, April 8.
- USEPA (U.S. Environmental Protection Agency), 2009. Metabolically Derived Human Ventilation Rates: A Revised Approach Based Upon Oxygen Consumption Rates. EPA/600/R-06/129F, U.S. Environmental Protection Agency, Washington, D.C. May.
- USEPA (U.S. Environmental Protection Agency), 2011. Exposure Factors Handbook: 2011 Edition. EPA/600/R-09/052F, U.S. Environmental Protection Agency, Washington, D.C. September.
- USA Today, 2011, "Japan's Government Criticizes Nuke Plant Operator," USA Today, McLean, VA, March 26.
- VBDR (Veterans Advisory Board on Dose Reconstruction), 2013. Charter, VBDR, Arlington, VA. <http://www.vbdr.org/about/charter.php>. (accessed February 4, 2013).
- Vose, D., 2008. Risk Analysis: A Quantitative Guide. John Wiley, Chichester, England.
- Weitz, R.L., Case, D.R., Chehata, M., Egbert, S.D., Mason, C.L., Singer, H.A., Martinez, D.G., McKenzie-Carter M.A., Shaw. R.S., and Stiver J.S., 2009. A Probabilistic Approach to Uncertainty Analysis in NTPR Radiation Dose Assessments. DTRA-TR-09-13, Defense Threat Reduction Agency, Fort Belvoir, VA. November.
- Yocom, E.Y., 1982. "Indoor-Outdoor Air Quality Relationships," Journal of the Air Pollution Control Association, 32(5), pp. 500–520.

Appendix A.

Overview of Probability Distributions

The probability distributions used in this uncertainty analysis study are briefly described in this section. As used here, a cumulative probability distribution (cpd) is a function that gives the probability that the random variable of interest can take any real value less than or equal to some given value within a defined continuous range. The first derivative of the cpd with respect to its random variable is the probability density function (pdf). Thus, the pdf is a function that gives the probability that the random variable takes on a given value.

The references for Appendix A in its entirety are Bulmer (1979), Doane and Seward (2009), Hahn and Shapiro (1967), Kirchner (2008), NCRP (2007), NIST (2009), and Vose (2008); see also DTRA (2009).

A-1 Uniform Distribution

The uniform distribution applies if all values of random variable X between a minimum value a and a maximum value b have an equal probability of being sampled. For any value x , $a \leq x \leq b$ ($a < b$), the cpd is given by Equation A-1. The uniform distribution is shown in Figure A-1.

$$Prob(X \leq x) = \frac{x - a}{b - a} \quad (A-1)$$

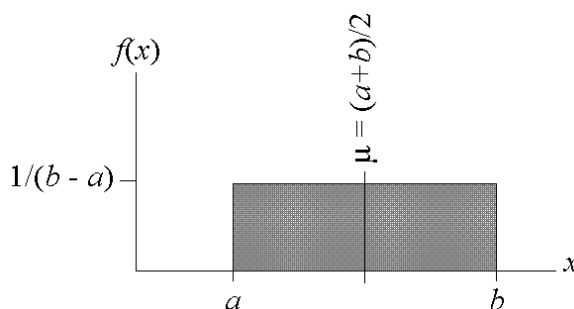


Figure A-1. Probability density function of a uniform distribution

The mean (which is also the median) μ and standard deviation σ of a uniform distribution are given in Equation A-2:

$$\mu = \frac{a+b}{2} \quad \sigma = \frac{b-a}{\sqrt{12}} \quad (\text{A-2})$$

Note that the uniform distribution has no mode (that is, all values are equally probable).

The uniform distribution is used as an approximate model when there are little or no available data and all values within a range are believed to have roughly equal probability. Rarely, a parameter may truly be uniformly distributed, as for rolling dice.

A-2 Gaussian Distribution

Also known as the normal distribution, the Gaussian distribution is defined by two parameters, the mean μ and the standard deviation σ . The Gaussian curve is shown in Figure A-2. The pdf and cpdf of the Gaussian distribution are given in Equations A-3 and A-4, respectively.

$$f(x) = \frac{1}{\sigma\sqrt{2\pi}} e^{-[(x-\mu)^2/2\sigma^2]} \quad (\text{A-3})$$

$$\text{Prob}(X \leq x) = \frac{1}{\sigma\sqrt{2\pi}} \int_{-\infty}^x e^{-[(x-\mu)^2/2\sigma^2]} dx \quad (\text{A-4})$$

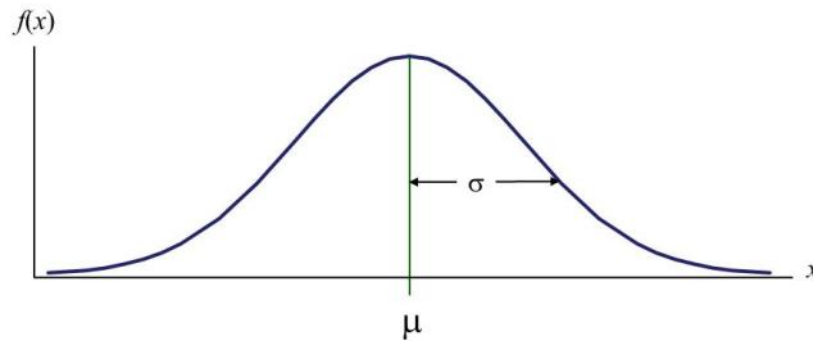


Figure A-2. Probability density function of a Gaussian distribution

A Gaussian can be “standardized” using Equation A-5 so that for any value x of the random variable of interest there is a corresponding value z such that:

$$z = \frac{x - \mu}{\sigma} \quad (\text{A-5})$$

There is only one standard Gaussian distribution which has been tabulated. Note that the standard normal variate Z has a mean 0, a standard deviation of 1, and is dimensionless. Although the Gaussian has an infinite range, as a practical matter the interval $\mu - 3\sigma < X < \mu + 3\sigma$ contains nearly all (99.73 percent) of the possible values of X .

Some of the input model parameters modeled herein with the Gaussian are not truly normal in that they show some amount of skewing. Even so, the Gaussian is a good approximation because of its robustness. Caution should be used when applying a Gaussian to model the uncertainty of a random variable that inherently has zero or positive values (e.g., dose), because the lower tail of the Gaussian may provide unphysical and meaningless negative values. A truncation rule that eliminates negative values or the use of another distribution (e.g., log-normal or triangular) may avoid this problem.

A-3 Log-normal Distribution

The random variable X is log-normally distributed if $Y = \ln(X)$ is normally distributed. The pdf of the log-normal is given in Equation A-6:

$$f(x) = \frac{1}{x\sigma\sqrt{2\pi}} e^{-[\ln(x)-\mu]^2/2\sigma^2} \quad (\text{A-6})$$

For $x > 0$ and where μ and σ are the mean and standard deviation of the variable's natural logarithm, that is, of Y . The log-normal distribution is right skewed.

If X is log-normally distributed, then its mean or expected value $E(X)$, standard deviation SD , geometric mean $GM(=median)$, and geometric standard deviation GSD are given in Equation A-7:

$$\begin{aligned} E(X) &= e^{\mu + \sigma^2/2}, \quad SD = e^{\mu + \sigma^2/2} \sqrt{e^{\sigma^2} - 1} \\ GM &= e^{\mu}, \quad GSD = e^{\sigma} \end{aligned} \quad (\text{A-7})$$

Log-normal pdf's for five values of σ , where $\mu = 0$, are presented in Figure A-3.

The log-normal distribution often provides a good representation of the distribution of the product of random variables as well as for physical quantities that take only positive values that range of several orders of magnitude. Many natural phenomena are well represented by log-normal distributions. Hence log-normal distributions are used extensively in radiation dose reconstruction, even to model the uncertainty in film badge dose readings (NRC, 1989). As used

is this report, the GM and GSD are the appropriate measures of central tendency and uncertainty, respectively.

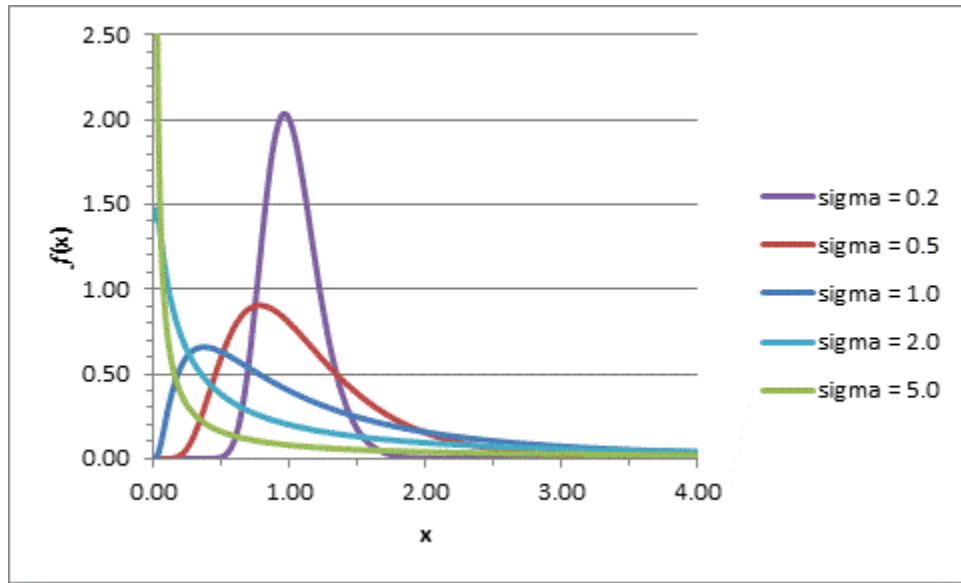


Figure A-3. Probability density functions of the log-normal distribution for various values of σ

A-4 Triangular Distribution

The triangular distribution is a simple distribution whose continuous random variable X can take on any value in the finite, fixed range from a to c such that $a < X < c$ with mode (or peak value) at b ($a \leq b \leq c$). Triangular distributions are shown in Figure A-4.

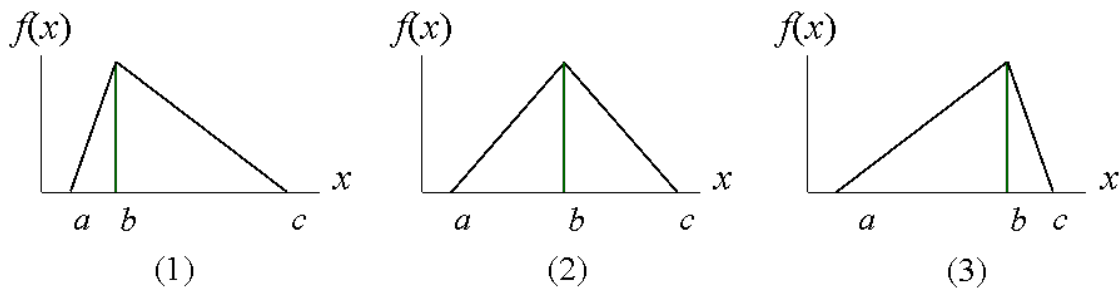


Figure A-4. Probability density functions of a triangular distribution (1) skewed right, (2) symmetric, and (3) skewed left

The cpd of the triangular distribution are given in Equation A-8:

$$Prob(X \leq x) = \begin{cases} \frac{(x-a)^2}{(b-a)(c-a)} & \text{for } a \leq x \leq b \\ \frac{(c-x)^2}{(c-a)(c-b)} & \text{for } b \leq x \leq c \end{cases} \quad (A-8)$$

The mean μ and standard deviation σ of X are given in Equation A-9:

$$\mu = \frac{a+b+c}{3} \quad \sigma = \sqrt{\frac{a^2 + b^2 + c^2 - ab - ac - bc}{18}} \quad (A-9)$$

The appeal of the triangular distribution is its great flexibility when there is limited to no data available. The triangular distribution is most often used when the true distribution is unknown but the extremes and the mean or mode of the distribution can be estimated and the intermediate values are more likely than the values on the extremes. A symmetric triangular distribution can be constructed to closely resemble a normal distribution; random samples from this symmetric triangular distribution will be similar to samples drawn from the normal distribution. Also, the finite range of the symmetric triangular is often preferred over the infinite range of the Gaussian.

A-5 Log-triangular Distribution

The log-triangular distribution is obtained when the distribution of the logarithms of the random variable is triangular. The cpd of the log-triangular distribution is given in Equation A-10:

$$Prob(X \leq x) = \begin{cases} \frac{2\ln(x/a)}{\ln(c/a)\ln(b/a)} & \text{for } a \leq x \leq b \\ \frac{2\ln(c/x)}{\ln(c/a)\ln(c/b)} & \text{for } b \leq x \leq c \end{cases} \quad (A-10)$$

with notation as for the triangular distribution. The mean and standard deviation of a log-triangular distribution are the logarithmic versions of the respective quantities in Equation (A-9). A severely right-skewed log-triangular distribution is shown in Figure A-5, in which values extend over nine orders of magnitude.

A triangular distribution of the values in log space can be used to represent the underlying exponential processes driving a random variable. The appeal of the log-triangular

distribution, like with the triangular distribution, is its great flexibility. Like the triangular distribution, it can be used to model a process in the absence or scarcity of data to represent uncertainty. The log-triangular distribution is most useful when the range of the possible values could cover several orders of magnitude (a property shared with the log-normal distribution), when intermediate values are more likely than values at the extremes, and when uncertainties are large.

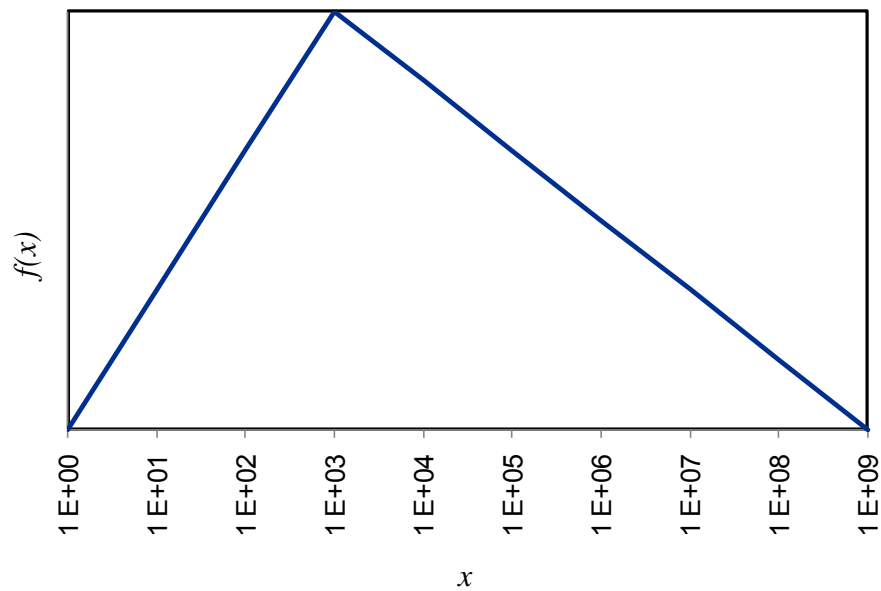


Figure A-5. A right-skewed log-triangular distribution

Appendix B.

Summary of Dose Parameters Values and Distributions

This appendix contains a listing of all parameters and uncertainty distributions used in the probabilistic analysis of the dose assessment for shore-based individuals during Operation Tomodachi described in Section 4.

Table B-1. Parameter values and distributions used in external and internal dose calculations

Parameter	Definition	Distribution	Nominal Value	Deterministic Value	Rationale for Probabilistic Values
Scenario Variables					
t_{start}	Start time of dose assessment	n/a	3-11-2011 0000		Based on selected scenario; no associated uncertainty
t_{end}	End time of dose assessment	n/a	5-11-2011 2359		Based on selected scenario; no associated uncertainty
External Dose Variables					
$I(t)$	Measured or modeled net dose rate measurement at time t (Gy hr ⁻¹)	See below	MEXT Measured minus background	DTRA-TR-12-001	Based on measured dose rates
Uncertainty modifier for spatial variability of external dose rates (unitless)	Yokosuka Naval Base	Uniform (0.7, 1.3)	1.0	n/a	Review of MEXT or SPEEDI data; based on average of the ranges of measured values at sites near location of interest
	Yokota Air Base	Uniform (0.9 1.1)	1.0		
	Camp Sendai Sendai Airport	Uniform (0.5, 1.5)	1.0		

Parameter	Definition		Distribution	Nominal Value	Deterministic Value	Rationale for Probabilistic Values
Uncertainty modifier for measurement and data reporting errors for external dose rates (unitless)	Yokosuka Naval Base		Normal Mean = 1.0 SD = 0.304	1.0	n/a	(Weitz et al., 2009)
	Yokota Air Base					
	Camp Sendai Sendai Airport					
<i>IDRF</i> (Calculated)	Based on time indoor and outdoor and shielding at Yokosuka Naval Base, Yokota Air Base and Camp Sendai		5th %ile = 0.17 Median = 0.27 95th %ile = 0.46	0.27 (mean of distribution)	1	Calculated using F_{OD} , F_{Res} , F_{NR} , PF_{Res} , PF_{NR}
	Based on time indoor and outdoor and shielding at Sendai Airport		5th %ile = 0.66 Median = 0.78 95th %ile = 0.88	0.78 (mean of distribution)		
F_{OD}	Fraction of time spent outdoors (unitless)	Adults (> 17 years)	Log-triangular Min = 0.001 (0.25 h) Mode = 0.04 (1 h) Max = 0.71 (17 h)	Mean value of F_{OD}	1.0	(USEPA, 2011)
		Humanitarian	Triangular Min = 0.25 (6 h) Mode = 0.42 (10 h) Max = 0.58 (14 h)			
		Children (1-2 year)	Log-triangular Min = 0.001 (0.1 h) Mode = 0.06 (1.5 h) Max = 0.56 (13.5 h)			
F_{IN} (Calculated)	Fraction of time spent indoors (unitless)		$1 - F_{OD}$	n/a	0	Calculated by difference ($1 - F_{OD}$)

Parameter	Definition		Distribution	Nominal Value	Deterministic Value	Rationale for Probabilistic Values
F_{Res}	Fraction of indoor time spent in a residence (unitless)	Adults (> 17 years)	Uniform, (0.4, 1.0)	0.7	n/a	Subjective estimate based on normal work day or child presence at home and day care.
		Humanitarian	Uniform (0.8, 1.0)	0.9		
		Children (1-2 year)	Uniform (0.8, 1.0)	0.9		
F_{NR} (Calculated)	Fraction of indoor time spent in a non-residence (unitless)		$1 - F_{Res}$	n/a	n/a	Calculated by difference ($1 - F_{Res}$)
PF_{Res}	Protection factor for residences (unitless)		Numerical Model 5th %ile = 3.7 Median = 4.6 95th %ile = 6.2	4.7 (mean of distribution)	n/a	(Weitz et al., 2009)
PF_{Tent}	Protection factor for tent (unitless)		Numerical Model 5th %ile = 1.2 Median = 1.5 95th %ile = 2	1.5 (mean of distribution)	n/a	(Weitz et al., 2009)
PF_{NR}	Protection factor for non-residential buildings (unitless)		Numerical Model 5th %ile = 4.8 Median = 9.2 95th %ile = 22	10.6 (mean of distribution)	n/a	(Weitz et al., 2009)
Internal Dose Variables						
IR_{AL}	Inhalation rate for each activity level (L min ⁻¹ or m ³ d ⁻¹)		See Table 7	See Table 7	DTRA-TR-12-001	Best fit to log-normal distribution using statistical data USEPA (2009, Table C-4)
F_{OD}	Fraction of each day spent outdoors (unitless)		See external dose above in this table	n/a	n/a	USEPA EFH (2011), Table 16-70
F_{ALout}	Fraction of outdoor time spent in each activity level (unitless)		See Appendix E	n/a	n/a	(USEPA, 2009; DOL 2011)
F_{ALin}	Fraction of indoor time spent in each activity level (unitless)		See Appendix E	n/a	n/a	Subjective based on USEPA EFH (2011)

Parameter	Definition	Distribution	Nominal Value	Deterministic Value	Rationale for Probabilistic Values
SIF	Structure infiltration factor for aerosols (unitless)	Triangular Min = 0.1 Mode = 0.3 Max = 0.5	0.3	0.5	Range of ratios for metals in aerosols (Yocom, 1982)
SIF_{Gas}	Structure infiltration factor for gas (unitless)	Triangular Min = 0.2 Mode = 0.5 Max = 0.8	0.5	1	Range of ratios for SO_x (Yocom, 1982)
$C_{Airj}(t)$	Measured air activity of aerosol radionuclide j ($Bq\ m^{-3}$)	Measured, modeled, or surrogate Section 4.2.1	Measured, modeled, or surrogate Section 4.2.1	DTRA-TR-12-001	
$C_{AIR-Ratio}$	Only for Yokosuka Naval Base The ratio of Yokosuka Naval Base air activity concentration to those at Yokota Air Base	Triangular Min = 0.45 Mode = 0.5 Max = 0.9	0.5	n/a	Range of ratios of daily external dose measurements at Yokosuka Naval Base to Yokota Air Base
Uncertainty modifier for spatial variability of air activity concentration (unitless)	Yokosuka Naval Base	Uniform (0.7, 1.3)	1.0	n/a	Based on external dose rate variability
	Yokota Air Base	Uniform (0.7, 1.3)	1.0		Range of daily values between Yokota Air Base and IMS measurements
	Camp Sendai Sendai Airport	Uniform (0.5, 1.5)	1.0		Variation of surface activity from aerial surveys referenced to June 30, 2011
Uncertainty modifier for measurement and data reporting errors for air activity concentration (unitless)	Yokosuka Naval Base	Normal Mean = 1.0 SD = 0.304	1.0	n/a	(Weitz et al., 2009)
	Yokota Air Base				
	Camp Sendai Sendai Airport				

Parameter	Definition	Distribution	Nominal Value	Deterministic Value	Rationale for Probabilistic Values
Uncertainty modifier for use of surrogate air activity concentration data	Yokosuka Naval Base only Yokota Air Base data is used adjusted by the ratio of total external doses	Normal Mean = 1.0 SD = 0.56	1.0	n/a	(Weitz et al., 2009)
Uncertainty modifier for use of modeled air activity concentration data	Sendai only Yokota Air Base and Sendai air activity concentration data and external dose rate data for Yokota Air Base and Sendai used to create model	Log-normal GM = 1.0 GSD = 1.95	1.0	n/a	(Weitz et al., 2009)
R_{CsSr}	Strontium radionuclides-to-cesium activity ratio for Sr-89 and Sr-90 (unitless)	Triangular Min = 0.0002 Mode = 0.00053 Max = 0.0015	0.00053	0.00053	GOJ soil analysis in Fukushima Prefecture
R_{GA}	Gaseous-to-aerosol concentration ratio for radioiodines (unitless)	Log-normal GM = 2.36 GSD = 1.87	2.6	2.5	U.S. Embassy (Tokyo) and Yokota Air Base air sampling data
F_{Elem}	Elemental fraction of gaseous iodine for radioiodines (unitless)	Triangular Min = 0.0 Mode = 0.5 Max = 1	0.5	0.33	DARWG judgment based on literature review (Cassata et al., 2012)
F_{Org}	Organic fraction of gaseous iodine for radioiodines (unitless)	$1 - F_{Elem}$	0.5	0.66	DARWG judgment based on literature review (Cassata et al., 2012)

Parameter	Definition		Distribution	Nominal Value	Deterministic Value	Rationale for Probabilistic Values
DC_{inhj}	Inhalation dose coefficient for either effective dose or equivalent dose to the thyroid for radionuclide j ($Sv\ Bq^{-1}$)		n/a	Published ICRP Dose Coefficients	Published ICRP Dose Coefficients	ICRP Database of Dose Coefficients (ICRP, 2011)
Uncertainty modifier for inhalation dose coefficients (unitless)			Log-normal GM = 1.0 GSD = 1.95	1.0	n/a	NCRP Commentary 15 (1998)
IR_{Water}	Ingestion rate of tap water ($L\ d^{-1}$)	Adults (> 17 years)	Log-normal GM = 1.1 GSD = 1.8	1.1 (geometric mean of distribution)	4	Individuals at Camp Sendai and Sendai Airport are assumed to have consumed bottled water
		Humanitarian	Log-normal GM = 1.1 GSD = 1.8	1.1 (geometric mean of distribution)	6	
		Children (1-2 year)	Log-normal GM = 0.3 GSD = 1.95	0.3 (geometric mean of distribution)	0.9	
$C_{Water\ j}(t)$	Water activity concentration of radionuclide j at time t ($Bq\ L^{-1}$)		Measured	Measured	DTRA-TR-12-001	
Uncertainty parameter for measurement and reporting errors in water activity concentrations (unitless)	Yokosuka Naval Base and Yokota Air Base only		Normal Mean = 1.0 SD = 0.304	n/a	n/a	DTRA (2009); DTRA (2010), SM UA01

Parameter	Definition		Distribution	Nominal Value	Deterministic Value	Rationale for Probabilistic Values
IR_{Soil}	Ingestion rate of soil and dust (g d^{-1})	Adults (> 17 years)	Triangular Min = 0.01 Mode = 0.05 Max = 0.2	0.087 (mean of distribution)	0.2	mode: Table 5-1 (USEPA, 2011) min/max: subjective, based on Table 5-1 (USEPA, 2011)
		Humanitarian	Triangular Min = 0.05 Mode = 0.2 Max = 0.5	0.25 (mean of distribution)	0.5	
		Children (1-2 year)	Triangular Min = 0.01 Mode = 0.1 Max = 1.0	0.37 (mean of distribution)	1.0	
DC_{Ingi}	Ingestion dose coefficient for either effective dose or equivalent dose to the thyroid for radionuclide j (Sv Bq^{-1})		n/a	Published ICRP Dose Coefficients	Published ICRP Dose Coefficients	ICRP Database of Dose Coefficients (ICRP, 2011)
$C_{Soil j}(t)$	Soil and dust activity concentration of radionuclide j at time t (Bq g^{-1})		Modeled based on measurements (Section 4.2.2)	Modeled based on measurements (Section 4.2.2)	DTRA-TR-12-001	
Uncertainty modifier for spatial variability of soil/dust activity concentration (unitless)	Yokosuka Naval Base		Uniform (0.7, 1.3)	1.0	n/a	Based on external dose rate variability
	Yokota Air Base		Uniform (0.9, 1.1)	1.0		Review of MEXT data; based on average of the ranges of measured values at sites near location of interest
	Camp Sendai Sendai Airport		Uniform (0.5, 1.5)	1.0		Variation of surface activity from aerial surveys referenced to June 30, 2011

Parameter	Definition	Distribution	Nominal Value	Deterministic Value	Rationale for Probabilistic Values
Uncertainty modifier for measurement and data reporting errors for soil/dust activity concentration (unitless)		Normal Mean = 1.0 SD = 0.304	1.0	n/a	(Weitz et al., 2009)
Uncertainty modifier for ingestion dose coefficients (unitless)		Log-normal GM = 1.0 GSD = 1.95	1.0	n/a	NCRP Commentary 15 (1998)

Appendix C.

Correlations and Dependencies

This appendix contains a description of the dependencies and correlations among the major input parameters used in the probabilistic analysis of the dose assessment for shore-based individuals during Operation Tomodachi described in Section 4.

Table C-1. Correlations and dependencies among dose model input parameters

Parameter and Definition *	Correlation	Basis/Comments
All parameters are correlated in time		
All parameters used for effective dose and thyroid dose		
External Dose		
$I(t)$: Net dose rate at time (t)	Partially correlated with air activity concentration, soil activity concentration. Uncorrelated with all other parameters	All hourly dose rates are modified by the same two factors for measurement uncertainty and spatial uncertainty. The same modifier is used for spatial uncertainty for net dose rate, air activity concentration, and soil activity concentration since the modifier was derived from external dose rate measurements.
F_{OD} : Fraction of time spent outdoors	Uncorrelated with all other parameters	The same F_{OD} is used to calculate external dose and inhalation dose.
F_{IN} : Fraction of time spent indoors	Calculated	$F_{IN} = 1 - F_{OD}$
F_{Res} : Fraction of time spend inside a residential structure	Uncorrelated with all other parameters	
F_{NR} : Fraction of time spend inside a non-residential structure	Calculated	$F_{NR} = 1 - F_{Res}$
PF_{Res} : Protection factor for a residential structure	Uncorrelated with all other parameters	
PF_{NR} : Protection factor for a non-residential structure	Uncorrelated with all other parameters	

Parameter and Definition *	Correlation	Basis/Comments
PF_{Tent} : Protection factor for a non-residential structure	Uncorrelated with all other parameters	
Inhalation Pathway		
$C_{Air,j}(t)$: Measured air activity concentration at time t	Correlated for all isotopes. Partially correlated with net dose rate and soil activity concentration. Uncorrelated with all other parameters.	The isotopic air activity concentration results derive from the same air filters and were analyzed using the same instruments. All isotopic air activity concentrations are modified by the same two factors for spatial variation and measurement uncertainty. Yokosuka Naval Base isotopic air activity concentrations were modified with a factor for surrogate data uncertainty. The same modifier is used for spatial uncertainty for net dose rate, air activity concentration, and soil activity concentration since the modifier was derived from external dose rate measurements.
R_{GA} : Gas-to-aerosol ratio for radioiodines	Correlated for all isotopes of iodine. Uncorrelated with all other parameters.	All isotopes of iodine are assumed to behave the same chemically. (Averill and Eldredge, 2011)
F_{Elem} : Elemental fraction of gaseous iodine for radioiodines	Correlated for all isotopes of iodine. Uncorrelated with all other parameters.	All isotopes of iodine are assumed to behave the same chemically. (Averill and Eldredge, 2011)
R_{CsSr} : Strontium radionuclides-to-cesium activity ratio for Sr-89, Sr-90	Correlated for all isotopes of strontium. Uncorrelated with all other parameters.	The percentage fission yields and thus the activity ratios for Sr-89 and Sr-90 are similar (Cassata et al., 2012).
$IR_{AL,k}$: Inhalation rate for activity level k	Partially corrected across activity levels. Uncorrelated with all other parameters.	Inhalation rates for each activity level are based on two different probabilistic distributions and the two distributions are partially correlated. A correlation factor, CC, (0.5 for this analysis) determines amount of correlation between activity levels.
SIF : Structure infiltration factor for aerosols	Correlated for all isotopes. Uncorrelated with all other parameters	Aerosols are assumed to have the same physical characteristics dependent on size and independent of radioisotope attached.

Parameter and Definition *	Correlation	Basis/Comments
SIF_{Gas} : Structure infiltration factor for gases	Correlated for all isotopes. Uncorrelated with all other parameters.	Elemental and methyl iodide gas form of all isotopes of iodine are assumed to have the same chemical and physical properties. (Averill and Eldredge, 2011)
$DC_{Inh j}$: Inhalation dose coefficients for radionuclide j	Correlated for all isotopes and with $DC_{Ing j}$ Uncorrelated with all other parameters.	Dose coefficients are assumed correlated for all isotopes and with the dose coefficients for ingestion since an individual's variations in bio-kinetic and dosimetric parameters are more correlated than uncorrelated. (IAEA Safety Report Series No. 37, 2004)
Water Ingestion Pathway		
$C_{Water j}(t)$: Water activity concentration of radionuclide j at time t	Correlated for all isotopes. Uncorrelated with all other parameters	The isotopic water activity concentration results came from the same water samples and were analyzed using the same instruments. All concentrations are modified by the same factors for measurement uncertainty.
IR_{Water} : Ingestion Rate of contaminated water ingested per day	Uncorrelated with all parameters	
$DC_{Ing j}$: Ingestion dose coefficient for radionuclide j	Correlated with $DC_{Inh j}$ for air inhalation and $DC_{Ing j}$ for soil ingestion and for all isotopes Uncorrelated with all parameters.	An individual would ingest radioactive materials in soil and water simultaneously. Dose coefficients are assumed correlated for all isotopes and with the dose coefficients for inhalation since an individual's variations in bio-kinetic and dosimetric parameters are more correlated than uncorrelated. (IAEA Safety Report Series No. 37, 2004)
Soil Ingestion Pathway		
$C_{Soil j}(t)$: Measured soil activity concentration at time t	Correlated for all isotopes. Partially correlated with net dose rate and air activity concentration. Uncorrelated with all other parameters.	The isotopic soil activity concentration results came from the same soil samples and were analyzed using the same instruments. All concentrations are modified by the same two factors for spatial variation and measurement uncertainty. The same modifier is used for spatial uncertainty for net dose rate, air activity concentration, and soil activity concentration since the modifier was derived from external dose rate measurements.
IR_{Soil} : Ingestion rate of contaminated soil and dust	Uncorrelated with all parameters	

Parameter and Definition *	Correlation	Basis/Comments
DC_{Ingj} : Ingestion dose coefficient for radionuclide j		See water ingestion above

*Each probabilistic run is presumed to be for the same person doing approximately the same activities for the full 60 days of the dose assessment.

Appendix D.

Air Activity Concentration Model for Sendai Locations

Due to the sparseness of air monitoring conducted at or near Camp Sendai and Sendai Airport, modeled air activity concentrations were developed and used in the probabilistic analysis estimation of inhalation doses. The model uses the available air activity concentration measurements made in or near Sendai, the external radiation dose rates at Sendai, and the 60-day air activity concentration and external dose rate measurements for Yokota Air Base. All mentioned data is presented in Section 4. A separate model was developed for I-131, Cs-137 and Cs-134 in three steps as follows:

- Step 1: create a model that relates the air activity concentration to the external dose rates for Yokota Air Base where complete sets of measurements are available for the 60-day assessment period from March 11 to May 11, 2011.
- Step 2: apply the Yokota air activity concentration model parameters determined in Step 1 to create a model of the Sendai air activity concentration using the measured and filled-in dose rate data and the mean air activity concentration from the limited number of field measurements at or near Sendai. This model is ultimately used for the “early period” from March 11 to March 21, 2011.
- Step 3: Use the Yokota Air Base measured air activity concentration data adjusted by a multiplying factor to model air activity concentration for Sendai during the “late period” from March 21 to May 11, 2011.

D-1 Step 1: Air Activity Concentration Model for Yokota Air Base

An exponential model is developed to relate external daily dose rate data for Tokyo (used for Yokota Air base) and continuous 24-h air activity concentration measurements made at Yokota Air Base reported in Cassata et al. (2012). A review of this data showed that while daily air activity concentration results vary exponentially, the daily external doses vary by less than an order of magnitude. The review also showed that the relationship between air activity concentration and external dose rate changes once radioactive materials starts depositing on the ground. The time before significant ground deposition is referred to as the “early period” and runs from March 11 to March 21, 2011. The time after significant ground deposition occurred is referred to as the “late period.” Equations D-1 and D-2 are used to model the air activity concentration for Yokota Air Base for both periods. The daily dose rates for two reference days are used in the early and late period models as calibration points to best reproduce the two measured peak air activity concentrations at Yokota Air Base.

$$C_E(d) = C_{E_0} A^{\frac{I(d)}{I_{E_0}}} \quad (D-1)$$

$$C_L(d) = C_{L_0} B^{\frac{I(d)}{I_{L_0}}} \quad (D-2)$$

where:

d	=	day of estimate
$I(d)$	=	External daily dose rate on day d (μSv)
$C_E(d)$	=	Modeled air activity concentration on day d during the early period (Bq m^{-3})
C_{E_0}	=	Measured air activity concentration on the early period calibration day (Bq m^{-3})
I_{E_0}	=	External daily dose rate on the early period calibration day (μSv)
A	=	Base of the exponential function during the early period
$C_L(d)$	=	Modeled air activity concentration on day d during the late period (Bq m^{-3})
C_{L_0}	=	Measured air activity concentration on the late period calibration day (Bq m^{-3})
I_{L_0}	=	External daily dose rate on the late period calibration day (μSv)
B	=	Base of the exponential function during the late period

To determine the bases and the calibration days for Equations D-1 and D-2 that best fit the Yokota Air Base measurement data, an iterative process is used. The iterative process varied the exponential functions bases A and B and calibration days so that the model reproduced the total 60-day integrated activity and the two peaks of the model in the early period matched the measured peak data. The resulting parameters are reported in Table D-1 for I-131, Cs-134 and Cs-137. The model created in this step for I-131 is shown in Figure D-1.

D-2 Step 2: Model for Sendai Locations during the “Early Period” (March 11-21, 2011)

In this step, the values of exponential function bases A and B determined using the Yokota Air Base measurements are applied to the Sendai daily external doses to estimate the air activity concentration at Sendai using the mean of the activity concentration of the Sendai field measurements as a calibration point. For this, the air activity concentration measurements at Sendai collected from March 21 to April 11, 2011 were averaged with a result of 0.8 Bq m^{-3} . This mean value was assigned to March 31, 2011, which is the mid-point day for all the field measurements taken at Sendai. The parameters used for the Sendai model for the early period are

shown in Table D-2 for I-131, Cs-134 and Cs-137. The model created in this step for I-131 is shown in Figure D-2.

Table D-1. Air activity concentration model parameters for Yokota Air Base

Parameter Name	Unit	I-131	Cs-134	Cs-137
A	n/a	2.6	3.7	3.6
C_{E_o}	Bq m ⁻³	0.123	0.0065	0.0066
I_{E_o}	mrem	0.0.028	0.028	0.028
Early calibration day	n/a	March 20, 2011	March 20, 2011	March 20, 2011
B	n/a	10	10	10
C_{L_o}	Bq m ⁻³	0.011	0.0098	0.012
I_{L_o}	mrem	0.152	0.152	0.152
Late calibration day	n/a	April 1, 2011	April 1, 2011	April 1, 2011

Table D-2. Air activity concentration model parameters for Sendai (early period)

Parameter Name	Unit	I-131	Cs-134	Cs-137
A	n/a	2.6	3.7	3.6
C_{E_o}	Bq m ⁻³	0.8	0.50	0.46
I_{E_o}	mrem	0.132	0.132	0.132
Early calibration day	n/a	March 31, 2011	March 31, 2011	March 31, 2011
B	n/a	10	10	10
C_{L_o}	Bq m ⁻³	0.8	0.50	0.46
I_{L_o}	mrem	0.132	0.132	0.132
Late calibration day	n/a	March 31, 2011	March 31, 2011	March 31, 2011

D-3 Step 3: Model for Sendai Locations during the “Late Period” (March 21 to May 11, 2011)

Figure D-2 shows that the air activity concentration at Sendai for the late period following March 21 does not reflect the decreasing concentrations seen in the Yokota Air Base measurement data. The model results show the air activity concentration remaining stable over the last 40 days whereas the Yokota Air Base air activity concentration measurement results show a decrease by several orders of magnitude as seen in Figure D-1. This overestimate in the Sendai model is due to the external radiation dose rates in the late period being dominated by radiation from radioactive materials deposited on the ground after the end of significant releases from the FDNPS in late March.

An alternative method that provided a reasonable model for Sendai late period was to use Yokota Air Base air activity concentration measurements for the time period between March 21 and May 11 as surrogate data. The Yokota measurement data for this late period was adjusted by a multiplying factor that is a function of the ratio of the 60-day external doses for Sendai and Yokota Air base as shown in Equation D-3 as follows:

$$C_S(d) = C_Y(d) (Dext_{ratio})^F \quad (D-3)$$

where:

$C_S(d)$	=	Modeled air activity concentration on day d at Sendai (Bq m ⁻³)
$C_Y(d)$	=	Measured air activity concentration on day d at Yokota Air Base (Bq m ⁻³)
$Dext_{ratio}$	=	Ratio of the 60-day external doses at Sendai and Yokota Air Base (unitless)
F	=	Power of the exponential function (unitless)

The exponent F is explicitly determined by requiring continuity between the early and late period air activity concentration models for Sendai on March 21, 2011. $Dext_{ratio}$ is estimated by using the ratio of the 60-day total external dose at Sendai (7.8 mrem) to Yokota Air Base (6.7 mrem). The parameter values used in Equation D-3 are found in Table D-3. The Sendai air activity concentration model for the late period is shown in Figure D-3. The full Sendai air activity concentration model that combines the early and late period models is shown in Figure D-4. The results for the final models for I-131, Cs-134, and Cs-137 are shown in Figure D-5.

Table D-3. Air activity concentration model parameters for Sendai (late period)

Parameter Name	Unit	I-131	Cs-134	Cs-137
$Dext_{ratio}$	n/a	1.16	1.16	1.16
F	n/a	7	11	9
$C_S(Mar\ 21)$	Bq m ⁻³	42	28	25
$C_Y(Mar\ 21)$	Bq m ⁻³	4.4	1.8	2.0
Calibration day	n/a	March 21, 2011	March 21, 2011	March 21, 2011

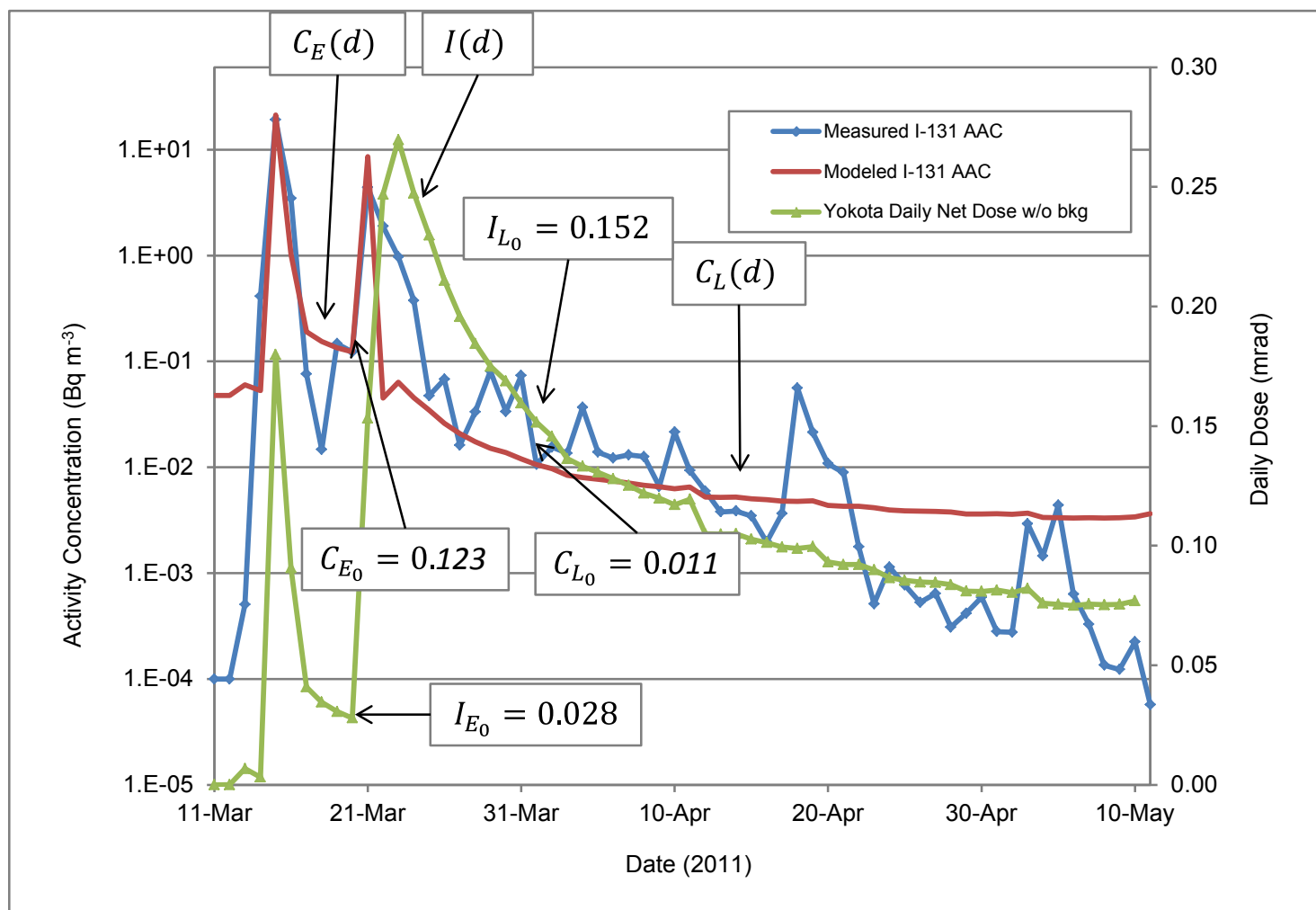


Figure D-1. I-131 air activity concentration model for Yokota Air Base

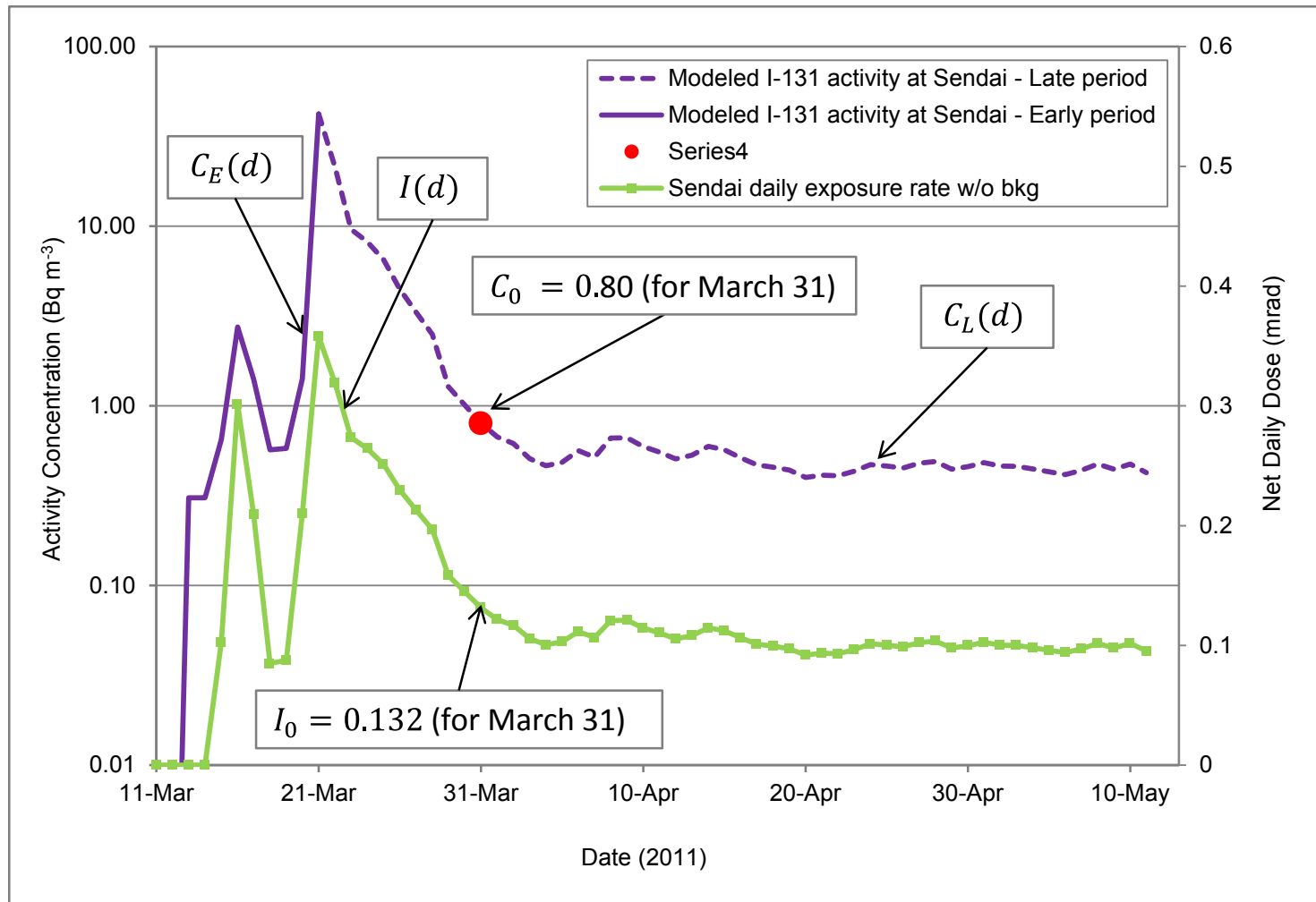


Figure D-2. I-131 air activity concentration model for Sendai (early period)

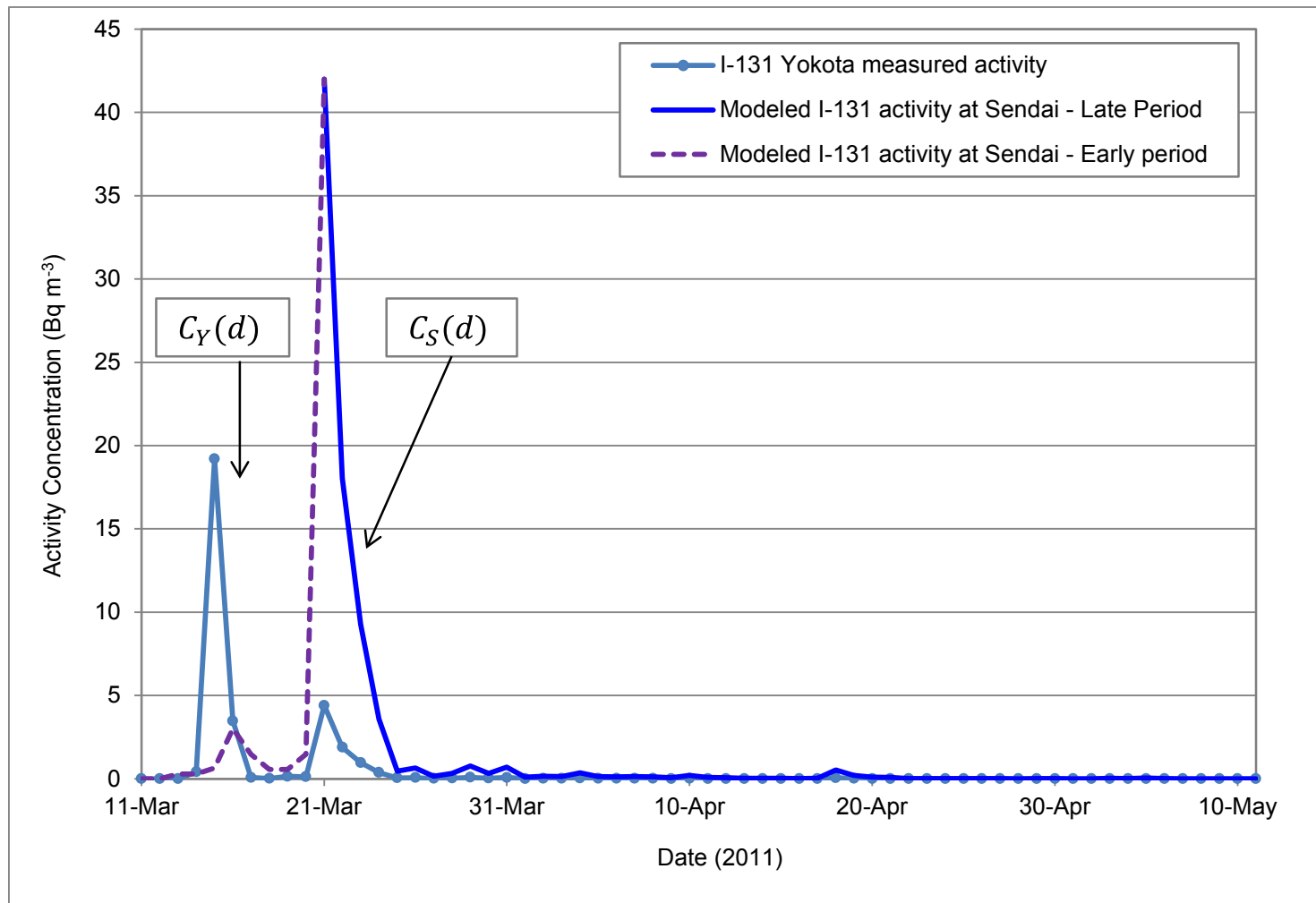


Figure D-3. I-131 air activity concentration model for Sendai (late period)

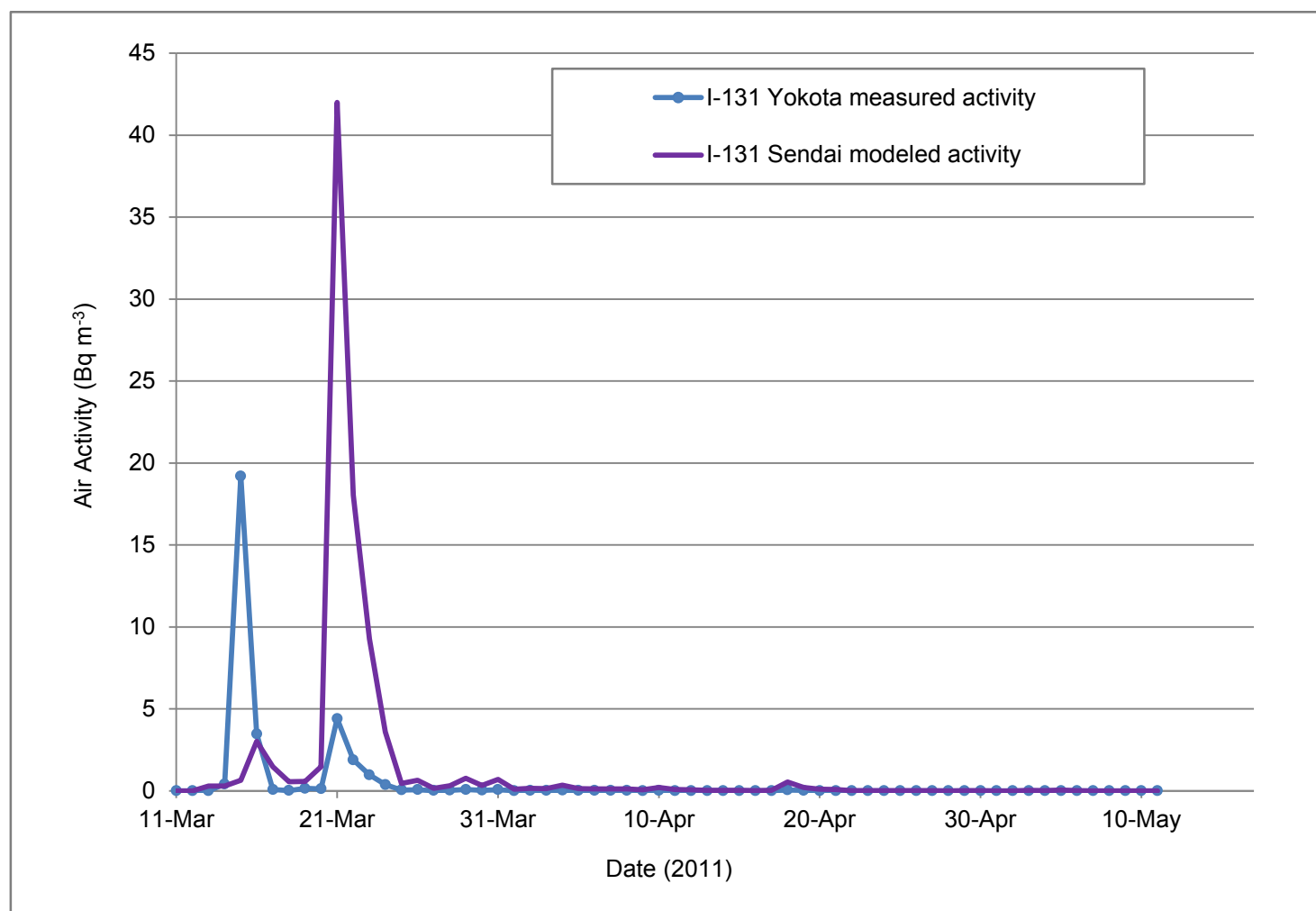


Figure D-4. I-131 combined air activity concentration model for Sendai

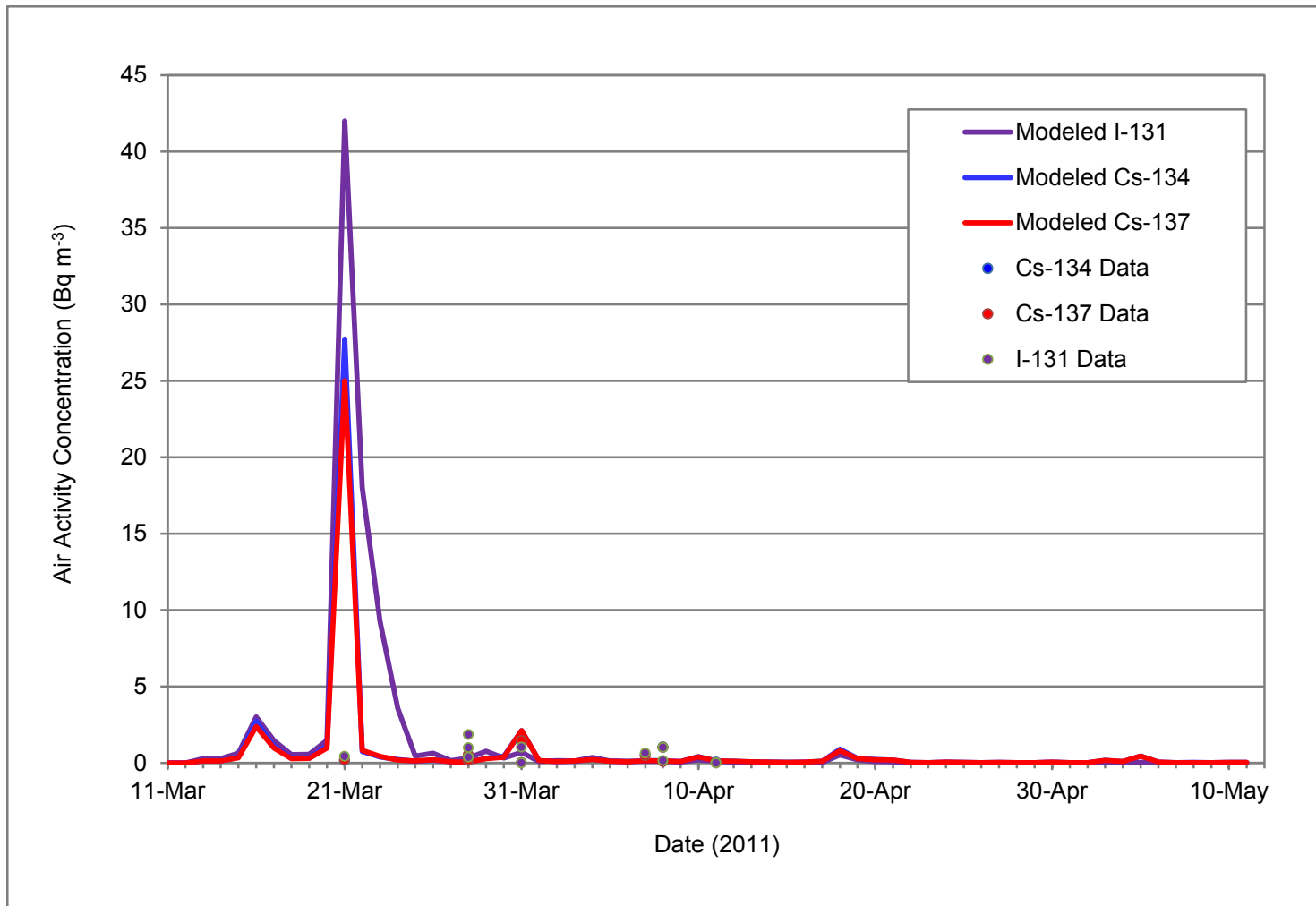


Figure D-5. I-131, Cs-134, and Cs-137 air activity concentration models for Sendai

Appendix E.

Time-Activity Patterns

The time-activity patterns used in the Operation Tomodachi probabilistic analyses were determined using a combination of statistical data and subjective judgment. Statistical data for time spent in various activities are available from several sources and in multiple formats, and the data are available using a variety of human activity categories. Representative time-use data were first obtained, and then subjective judgment was used to apportion the data into exertion levels and indoor/outdoor time fractions.

For this analysis, statistical data were obtained from the American Time Use Survey (ATUS). The ATUS is a time-use survey conducted annually by the U.S. Census Bureau and sponsored by the Bureau of Labor Statistics that measures the amount of time people spend doing various activities, such as work, childcare, housework, watching television, volunteering, and socializing (DOL, 2011). The ATUS data are compiled and summarized using 10 primary activity categories, each with sub-activities. For this analysis, four primary ATUS activities and associated hours were identified as the most significant, based on the number of hours per day in the categories. The activity categories used are those with more than one hour per day or greater; one category (see below) is represented by combining hours from several similar categories. Based on data averaged over the years 2003–2010 (DOL, 2011), the following hours were assigned to the four primary activity categories:

- Personal care (sleep, grooming, health-related care, personal activities): 9.4 h d^{-1}
- Eating and drinking: 1.2 h d^{-1}
- Work or household activities¹: 8 h d^{-1}
- Leisure and sports²: 5.4 h d^{-1}

Following the assignment of daily hours into the four primary activity categories used, the time spent in each activity category was assigned to one or more activity (exertion) levels. As described in Section 4 of the main report, four activity levels were used to determine an average daily inhalation rate: sedentary, light, moderate, and high. The assignment of time-use hours into the activity level categories was done using subjective judgment or according to the time-activity pattern definitions for outdoor and indoor workers (i.e., sedentary/light, light/moderate, moderate/high—see below). For example, all time spent in personal care and eating/drinking categories (10.6 h d^{-1}) was assigned to the “sedentary” activity level. Time spent in the work or household activities category was divided into three groupings based on the time-activity pattern definitions. For sedentary/light workers, 30 percent of the work/household time was assigned to sedentary and 70 percent to light. For light/moderate workers, 50 percent of the work/household time was assigned to both light and moderate levels. For moderate/high workers, 25 percent of

¹ “Household” comprises hours from categories Household, Purchasing Goods and Services, and Caring for others.

² The hours assigned to “Leisure and Sports” were adjusted slightly in order for all activities to sum to 24 hours.

the work/household time was assigned to light, 70 percent to moderate, and 5 percent to high levels. Finally, assignment of time spent in leisure and sports was done subjectively according to the category level of leisure/recreation time (i.e., sedentary/light, light/moderate, moderate/high).

Indoor/outdoor time fractions for each activity category were assigned in a similar subjective manner as activity levels. All time spent in personal care and eating/drinking was assumed to be spent indoors. All time in spent in work/household was assigned based on the type of worker (i.e., all work/household time is assumed to be spent outdoors or indoors for an outdoor worker or indoor worker, respectively). The time spent in leisure and sports was assigned to outdoor or indoor time such that overall outdoor and Indoor time fell on either side of the average daily outdoor fraction of 0.20 for individuals aged 18 to <64 years (USEPA, 2011). Overall daily outdoor fractions of approximately 0.45 and 0.14 were thus obtained for outdoor workers and indoor workers, respectively.

Using combinations of the four activity levels (sedentary, light, moderate, and high), nine time-activity level categories were subjectively defined for use in the analysis. These categories are based on the activity levels of work and leisure/recreation periods. These were defined by combining two of the activity levels at a time, and assigning one each to work time and leisure/recreation time. Each of these nine levels was used for both “indoor workers” and “outdoor workers,” for a sub-total of 18 categories. An additional category was defined based on national averages for time spent in various activity categories, and was used for both “indoor workers” and “outdoor workers,” for a total of 20 time-activity level categories. The nine basic categories are as follows:

- Sedentary/light level of work and sedentary/light level of leisure/recreation (S/L - S/L).
- Sedentary/light level of work and light/moderate level of leisure/recreation (S/L - L/M).
- Sedentary/light level of work and moderate/high level of leisure/recreation (S/L - M/H).
- Light/moderate level of work and sedentary/light level of leisure/recreation (L/M - S/L).
- Light/moderate level of work and light/moderate level of leisure/recreation (L/M - L/M).
- Light/moderate level of work and moderate/high level of leisure/recreation (L/M - M/H).
- Moderate/high level of work and sedentary/light level of leisure/recreation (M/H - S/L).
- Moderate/high level of work and light/moderate level of leisure/recreation (M/H - L/M).
- Moderate/high level of work and moderate/high level of leisure/recreation (M/H - M/H).

The time in each activity (exertion) level for all time-activity level categories was converted to percentage of outdoor time and percentage of indoor time in each activity level. These values are displayed for outdoor workers and indoor workers in Table E-1.

For the five age groups of children, the mean daily time spent in seven major activity categories was found in Tables 16-8 and 16-25 of USEPA (2011). The seven major activity levels include sleep, personal care, eating, household activities, education, passive leisure, and active leisure. Children in these age groups are assumed to spend varying amounts of time outdoors, ranging from four percent of each day for ages less than 2 years, eight percent for 2 year-old children, 12 percent for ages 3–10, to 13 percent for ages 11–16 (USEPA, 2011).

The time spent in each activity category was assigned to one or more of the four activity (exertion) levels that were previously described; sedentary, light, moderate, and high; based on the MET value associated with that activity (USEPA, 2009). MET values lower than 0.5 were associated with sedentary activities, 1.5–3 with low activity, 3–6 with moderate activity, and above 6 with a high level of activity. The time in each activity (exertion) level for all time-activity level categories was converted to percentage of outdoor time and percentage of indoor time in each activity level. These values are displayed for each age group in Table E-2.

Table E-1. Fraction of time indoor and outdoor workers spend in each inhalation activity level

	Fractions of Outdoor Time in Each Activity Level (%)				Fractions of Indoor Time in Each Activity Level (%)				Definitions
	Sedentary	Light	Moderate	High	Sedentary	Light	Moderate	High	
Outdoor Worker									
Average Male	0	4	90	6	64	31	5	0	National "averages" for activity levels and indoor/outdoor fractions
S/L - S/L	32	59	9	0	85	15	0	0	Sedentary/light work activity, Sedentary/light leisure & recreation time
S/L - L/M	27	55	18	0	90	2	8	0	Sedentary /light work activity, Light/mod leisure & recreation time
S/L - M/H	26	44	26	4	84	0	16	0	Sedentary /light work activity, Moderate/high leisure & recreation time
L/M - S/L	9	55	36	0	92	8	0	0	Light/mod work activity, Sedentary /light leisure & recreation time
L/M - L/M	0	46	54	0	85	11	5	0	Light/mod work activity Light/mod leisure & recreation time
L/M - M/H	0	35	61	4	84	4	12	0	Light/mod work activity, Moderate/high leisure & recreation time
M/H - S/L	0	45	46	9	85	15	0	0	Moderate/high work activity Sedentary /light leisure & recreation time
M/H - L/M	0	37	50	13	81	15	4	0	Moderate/high work activity Light/moderate leisure & recreation time
M/H - M/H	0	17	61	22	85	0	15	0	Moderate/high work activity, Moderate/high leisure & recreation time

	Fractions of Outdoor Time in Each Activity Level (%)				Fractions of Indoor Time in Each Activity Level (%)				Definitions
	Sedentary	Light	Moderate	High	Sedentary	Light	Moderate	High	
Indoor Worker									
Average Male	0	5	89	6	64	31	5	0	National "averages" for activity levels and indoor/outdoor fractions
S/L - S/L	17	83	0	0	65	35	0	0	Sedentary/light work activity, Sedentary/light leisure & recreation time
S/L - L/M	0	43	57	0	64	31	5	0	Sedentary /light work activity, Light/mod leisure & recreation time
S/L - M/H	0	0	88	12	64	26	10	0	Sedentary /light work activity, Moderate/high leisure & recreation time
L/M - S/L	32	68	0	0	58	22	20	0	Light/mod work activity, Sedentary /light leisure & recreation time
L/M - L/M	0	44	56	0	54	24	22	0	Light/mod work activity Light/mod leisure & recreation time
L/M - M/H	0	0	88	12	51	22	27	0	Light/mod work activity, Moderate/high leisure & recreation time
M/H - S/L	0	100	0	0	54	17	27	2	Moderate/high work activity Sedentary /light leisure & recreation time
M/H - L/M	0	74	15	12	51	17	30	2	Moderate/high work activity Light/moderate leisure & recreation time
M/H - M/H	0	0	59	41	52	10	36	2	Moderate/high work activity, Moderate/high leisure & recreation time

**Table E-2. Fraction of time indoor and outdoor children spend
in each inhalation activity level**

Age Group	Fractions of Outdoor Time in Each Activity Level (%)				Fractions of Indoor Time in Each Activity Level (%)			
	Sedentary	Light	Moderate	High	Sedentary	Light	Moderate	High
3 months	0	14	43	43	61	36	03	
1 year	0	33	50	17	59	29	08	
5 years	0	54	27	19	57	31	09	
10 years	0	47	30	23	54	37	08	
15 years	0	62	19	19	50	49	01	

Appendix F.

Inhalation and Ingestion Dose Coefficients

Dose coefficients for adults and for all age groups of children were found in the ICRP Database of Dose Coefficients: Workers and Members of the Public (ICRP, 2001). The database contains dose coefficients from ICRP Publication 68 “Dose Coefficients for Intakes of Radionuclides by Workers” and ICRP 72 “ICRP Publication 72: Age-dependent Doses to the Members of the Public from Intake of Radionuclides Part 5, Compilation of Ingestion and Inhalation Coefficients.” The inhalation dose coefficients are committed effective dose and committed equivalent dose for the thyroid (50-year for adults and to age 70 for children), for absorption Type F, and for a particle size distribution of one micrometer activity median aerodynamic diameter. The values used for adults are in Table F-1 and Table F-2. The values used for 1-to-2 year-old children are in Table F-3 and Table F-4.

Table F-1. Inhalation 50-year committed dose coefficients for adults

Isotope	Effective Dose (Sv Bq⁻¹)	Equivalent Thyroid Dose (Sv Bq⁻¹)
Cs-134	6.6×10^{-9}	6.3×10^{-9}
Cs-136	1.2×10^{-9}	1.0×10^{-9}
Cs-137	4.6×10^{-9}	4.4×10^{-9}
I-131 aerosol	7.4×10^{-9}	1.5×10^{-7}
I-131 organic gas	1.5×10^{-8}	3.1×10^{-7}
I-131 elemental gas	2.0×10^{-8}	3.9×10^{-7}
I-132 aerosol	9.4×10^{-11}	1.4×10^{-9}
I-132 organic gas	1.9×10^{-10}	3.2×10^{-9}
I-132 elemental gas	3.1×10^{-10}	3.6×10^{-9}
I-133 aerosol	1.5×10^{-9}	2.8×10^{-8}
I-133 organic gas	3.1×10^{-9}	6.0×10^{-8}
I-133 elemental gas	4.0×10^{-9}	7.6×10^{-8}
La-140	5.7×10^{-10}	9.0×10^{-11}
Mo-99	2.2×10^{-10}	8.4×10^{-11}
Tc-99m	1.2×10^{-11}	3.9×10^{-11}
Te-129	1.6×10^{-11}	2.4×10^{-12}
Te-129m	1.3×10^{-9}	4.1×10^{-9}
Te-131m	8.6×10^{-10}	1.3×10^{-8}
Te-132	1.8×10^{-9}	2.5×10^{-8}
Sr-89	1.0×10^{-9}	1.8×10^{-10}
Sr-90	2.4×10^{-8}	5.9×10^{-10}

Table F-2. Ingestion 50-year committed dose coefficients for adults

Isotope	Effective Dose (Sv Bq⁻¹)	Equivalent Thyroid Dose (Sv Bq⁻¹)
I-131	2.2×10^{-8}	4.3×10^{-7}
Cs-134	1.9×10^{-8}	1.8×10^{-8}
Cs-137	1.3×10^{-8}	1.3×10^{-8}
Mo-99	6.0×10^{-10}	2.5×10^{-10}
Cs-136	3.0×10^{-9}	2.9×10^{-9}
La-140	2.0×10^{-9}	5.2×10^{-12}
Tc-99m	2.2×10^{-11}	4.7×10^{-11}
Te-132	3.8×10^{-9}	3.1×10^{-8}

**Table F-3. Inhalation committed dose coefficients to age 70
for 1 year-old children**

Isotope	Effective Dose (Sv Bq⁻¹)	Equivalent Thyroid Dose (Sv Bq⁻¹)
Cs-134	7.3×10^{-9}	6.3×10^{-9}
Cs-136	5.2×10^{-9}	3.9×10^{-9}
Cs-137	5.4×10^{-9}	4.4×10^{-9}
I-131 aerosol	1.7×10^{-8}	1.4×10^{-6}
I-131 organic gas	7.2×10^{-8}	2.5×10^{-6}
I-131 elemental gas	1.3×10^{-7}	3.2×10^{-6}
I-132 aerosol	1.6×10^{-7}	1.6×10^{-8}
I-132 organic gas	9.6×10^{-10}	3.3×10^{-8}
I-132 elemental gas	1.8×10^{-9}	3.8×10^{-8}
I-133 aerosol	2.3×10^{-9}	3.5×10^{-7}
I-133 organic gas	1.8×10^{-8}	6.3×10^{-7}
I-133 elemental gas	3.2×10^{-8}	8.0×10^{-7}
La-140	4.2×10^{-9}	4.8×10^{-10}
Mo-99	1.7×10^{-9}	6.3×10^{-10}
Tc-99m	8.7×10^{-11}	4.4×10^{-10}
Te-129	1.2×10^{-10}	2.1×10^{-11}
Te-129m	1.3×10^{-8}	5.1×10^{-8}
Te-131m	7.6×10^{-9}	1.2×10^{-7}
Te-132	1.80×10^{-8}	2.9×10^{-7}
Sr-89	7.30×10^{-9}	1.3×10^{-9}
Sr-90	5.20×10^{-8}	4.3×10^{-9}

**Table F-4. Ingestion committed dose coefficients to age 70
for 1 year-old children**

Isotope	Effective Dose (Sv Bq⁻¹)	Equivalent Thyroid Dose (Sv Bq⁻¹)
I-131	1.8×10^{-7}	3.6×10^{-6}
Cs-134	1.6×10^{-8}	1.6×10^{-8}
Cs-137	1.2×10^{-8}	1.1×10^{-8}
Mo-99	3.5×10^{-9}	1.7×10^{-9}
Cs-136	9.5×10^{-9}	9.6×10^{-9}
La-140	1.3×10^{-8}	7.8×10^{-11}
Tc-99m	1.3×10^{-10}	4.7×10^{-10}
Te-132	3.0×10^{-8}	3.2×10^{-7}

Data Compendium

All data, either processed from measurements or modeled, which are used to calculate internal doses from inhalation of airborne radioactive materials, ingestion of contaminated water, or incidental ingestion of contaminated soil are compiled in this data compendium. All time periods and isotopes where data are not available are labeled with an en dash (–). All measurements reported as below detectable limits are labeled as not detected (ND). All times are in JST.

Note: data used to calculate external doses are available at the websites cited in Section 4 and listed in the references section.

DC-1 Air Activity Concentration

Table DC-1 includes air activity concentration data from measurements performed at Yokota Air Base. These data are also used in the calculation of inhalation doses for Yokosuka Naval Base with appropriate adjustment (see Section 4 for details). Table DC-2 contains modeled air activity concentration data used to calculate inhalation doses for individuals at Sendai Airport and Camp Sendai (see Section 4).

Table DC-1. Air activity concentration measurement data at Yokota Air Base

Date	Cs-134	Cs-136	Cs-137	I-131	I-132	La-140	Mo-99	Te-129	Te-129m	Te-132
(Bq m ⁻³)										
3/11/2011	–	–	–	–	–	–	–	–	–	–
3/12/2011	1.97E-04	4.66E-05	2.15E-04	5.06E-04	1.46E-03	–	–	1.35E-04	2.85E-04	2.47E-03
3/13/2011	1.41E-01	3.76E-02	1.45E-01	4.11E-01	8.05E-01	9.56E-03	–	7.65E-02	4.69E-01	1.02E+00
3/14/2011	6.59E+00	1.46E+00	6.34E+00	1.92E+01	4.45E+01	3.59E-01	5.63E-01	–	6.41E+00	4.82E+01
3/15/2011	9.61E-01	2.08E-01	9.84E-01	3.47E+00	4.90E+00	4.95E-02	5.38E-02	–	9.30E-01	5.76E+00
3/16/2011	1.40E-02	3.44E-03	1.98E-02	7.59E-02	6.33E-02	1.38E-03	–	1.39E-02	2.42E-02	8.86E-02
3/17/2011	5.19E-03	9.44E-04	6.06E-03	1.47E-02	1.30E-02	–	–	3.05E-03	6.61E-03	1.80E-02
3/18/2011	8.05E-03	1.52E-03	9.13E-03	1.08E-01	2.66E-02	2.75E-04	4.92E-04	3.05E-03	9.21E-03	3.37E-02
3/19/2011	6.22E-03	1.10E-03	6.56E-03	1.13E-01	1.05E-02	1.66E-03	5.60E-04	2.45E-03	4.71E-03	1.23E-02
3/20/2011	1.21E+00	2.12E-01	1.26E+00	2.53E+00	2.05E+00	8.37E-03	7.48E-02	6.05E-01	9.64E-01	2.32E+00
3/21/2011	4.84E-02	3.48E-02	6.52E-02	1.89E+00	2.65E-01	–	–	1.09E-01	1.97E-01	3.13E-01
3/22/2011	2.60E-02	4.57E-03	3.34E-02	9.71E-01	6.99E-02	–	–	3.04E-03	5.65E-02	8.19E-02
3/23/2011	1.42E-02	1.82E-03	1.56E-02	3.76E-01	2.71E-02	–	–	8.19E-03	1.65E-02	1.81E-02
3/24/2011	7.95E-03	1.16E-03	1.09E-02	4.74E-02	2.06E-02	–	–	5.41E-03	1.08E-02	8.90E-03
3/25/2011	1.23E-02	1.66E-02	1.69E-01	6.77E-01	1.72E-01	–	–	8.14E-02	1.51E-01	1.11E-01
3/26/2011	4.46E-03	5.32E-03	5.84E-02	1.61E-01	2.87E-02	–	–	2.55E-02	3.98E-02	3.20E-02
3/27/2011	4.45E-03	4.04E-03	5.36E-02	3.33E-01	1.63E-02	–	–	2.91E-02	5.49E-02	3.26E-02
3/28/2011	1.66E-02	1.11E-02	1.89E-01	6.78E-01	5.71E-02	–	1.68E-02	5.42E-02	9.30E-02	3.97E-02
3/29/2011	2.78E-02	2.02E-02	2.95E-01	3.36E-01	2.62E-02	–	–	4.46E-02	9.40E-02	2.94E-02
3/30/2011	7.92E-02	4.78E-02	9.53E-01	5.22E-01	8.09E-02	4.29E-01	5.36E-02	1.14E-01	2.08E-01	6.43E-02
3/31/2011	8.12E-03	6.00E-03	9.78E-02	1.10E-01	1.51E-02	–	–	2.35E-02	5.02E-02	1.08E-02
4/1/2011	4.99E-03	3.93E-03	6.05E-02	1.54E-01	1.33E-02	–	–	2.28E-02	4.50E-02	8.29E-03
4/2/2011	6.29E-03	4.96E-03	7.68E-02	1.46E-01	1.34E-02	–	–	3.09E-02	4.78E-02	9.14E-03
4/3/2011	8.43E-03	5.02E-03	9.82E-02	1.96E-01	1.25E-02	–	–	3.47E-02	6.63E-02	9.50E-03
4/4/2011	6.27E-03	4.37E-03	7.67E-02	1.11E-01	8.47E-03	–	–	2.63E-02	4.96E-02	6.27E-03

Date	Cs-134	Cs-136	Cs-137	I-131	I-132	La-140	Mo-99	Te-129	Te-129m	Te-132
(Bq m ⁻³)										
4/5/2011	4.23E-03	2.98E-03	5.26E-02	1.09E-01	8.40E-03	–	–	1.76E-02	3.65E-02	3.38E-03
4/6/2011	8.06E-03	4.12E-03	9.49E-02	1.34E-01	6.88E-03	–	–	2.71E-02	5.31E-02	3.78E-03
4/7/2011	8.77E-03	4.38E-03	1.03E-01	6.65E-02	4.96E-03	–	–	2.69E-02	5.46E-02	3.39E-03
4/8/2011	4.35E-03	2.57E-03	5.37E-02	5.11E-02	2.36E-03	–	–	1.90E-02	3.58E-02	1.81E-03
4/9/2011	1.45E-02	5.33E-03	1.63E-01	1.88E-01	–	–	–	2.80E-02	5.87E-02	2.62E-03
4/10/2011	7.70E-03	3.12E-03	8.90E-02	7.77E-02	2.14E-03	–	–	2.18E-02	4.52E-02	1.55E-03
4/11/2011	6.40E-03	3.09E-03	7.71E-02	5.74E-02	2.80E-03	–	–	1.89E-02	3.73E-02	1.15E-03
4/12/2011	3.83E-03	1.96E-03	4.84E-02	3.65E-02	–	–	–	1.29E-02	2.33E-02	2.82E-04
4/13/2011	3.05E-03	1.46E-03	3.75E-02	3.46E-02	–	–	–	9.96E-03	2.36E-02	3.23E-04
4/14/2011	2.68E-03	1.27E-03	3.40E-02	3.64E-02	–	–	–	1.04E-02	2.41E-02	–
4/15/2011	2.91E-03	1.22E-03	3.56E-02	1.65E-02	–	–	–	9.89E-03	2.25E-02	–
4/16/2011	5.63E-03	2.26E-03	6.89E-02	2.80E-02	–	–	–	1.78E-02	3.64E-02	–
4/17/2011	4.69E-02	1.19E-02	5.17E-01	4.62E-01	–	8.55E-03	–	5.45E-02	1.10E-01	9.66E-04
4/18/2011	1.41E-02	3.64E-03	1.60E-01	1.42E-01	–	4.99E-03	–	2.10E-02	3.93E-02	–
4/19/2011	1.48E-02	3.43E-03	1.70E-01	1.08E-01	–	2.70E-03	–	1.59E-02	3.01E-02	–
4/20/2011	1.27E-02	2.70E-03	1.45E-01	8.92E-02	–	1.79E-03	–	1.20E-02	2.60E-02	–
4/21/2011	3.24E-03	7.85E-04	3.73E-02	1.77E-02	–	4.34E-04	–	7.49E-03	1.19E-02	–
4/22/2011	1.34E-03	4.02E-04	1.71E-02	5.12E-03	–	–	–	4.03E-03	9.05E-03	–
4/23/2011	3.69E-03	8.57E-04	4.34E-02	1.14E-02	–	–	–	6.07E-03	1.27E-02	–
4/24/2011	2.44E-03	5.39E-04	3.10E-02	7.72E-03	–	–	–	5.47E-03	1.14E-02	–
4/25/2011	1.54E-03	3.91E-04	1.93E-02	5.28E-03	–	–	–	4.22E-03	1.05E-02	–
4/26/2011	3.00E-03	7.58E-04	3.58E-02	6.41E-03	–	–	–	8.85E-03	1.64E-02	–
4/27/2011	1.78E-03	3.78E-04	2.08E-02	3.09E-03	–	3.52E-04	–	4.63E-03	1.08E-02	–
4/28/2011	1.96E-03	4.17E-04	2.26E-02	4.17E-03	–	–	–	4.65E-03	6.67E-03	–
4/29/2011	3.41E-03	6.01E-04	3.98E-02	5.91E-03	–	–	–	5.49E-03	1.18E-02	–
4/30/2011	1.94E-03	3.49E-04	2.24E-02	2.81E-03	–	–	–	9.34E-03	1.59E-02	–

Date	Cs-134	Cs-136	Cs-137	I-131	I-132	La-140	Mo-99	Te-129	Te-129m	Te-132
(Bq m ⁻³)										
5/1/2011	1.51E-03	3.35E-04	1.71E-02	2.76E-03	—	—	—	3.72E-03	7.18E-03	—
5/2/2011	1.09E-02	1.34E-03	1.30E-01	2.92E-02	—	—	—	1.20E-02	1.48E-02	—
5/3/2011	6.38E-03	9.14E-04	7.44E-02	1.45E-02	—	—	—	5.15E-03	1.26E-02	—
5/4/2011	2.89E-02	3.44E-03	3.47E-01	4.38E-02	—	1.77E-03	—	1.48E-02	2.57E-02	—
5/5/2011	3.73E-03	4.96E-04	4.34E-02	6.31E-03	—	—	—	0.00E+00	8.54E-03	—
5/6/2011	1.78E-03	1.94E-04	2.07E-02	3.28E-03	—	—	—	7.32E-03	1.14E-02	—
5/7/2011	2.09E-03	2.49E-04	2.45E-02	1.35E-03	—	—	—	5.34E-03	7.85E-03	—
5/8/2011	1.81E-03	—	2.14E-02	1.23E-03	—	—	—	1.31E-02	2.48E-02	—
5/9/2011	2.31E-03	1.93E-04	2.71E-02	2.24E-03	—	—	—	4.01E-03	9.04E-03	—
5/10/2011	2.92E-03	2.02E-04	3.41E-02	2.35E-03	—	—	—	2.76E-03	6.90E-03	—
5/11/2011	9.93E-04	—	1.13E-02	5.73E-04	—	—	—	3.50E-03	7.15E-03	—

Table DC-2. Modeled air activity concentrations used for Sendai Airport and Camp Sendai

Date	Cs-134	Cs-136	Cs-137	I-131	I-133	La-140	Mo-99	Tc-99m	Te-129	Te-129m	Te-131m	Te-132
(Bq m ⁻³)												
3/11/2011	0.00E+00	0.00E+00	1.00E-02	0.00E+00	0.00E+00	0.00E+00	0.00E+00	3.00E-02	0.00E+00	1.00E-02	0.00E+00	1.00E-02
3/12/2011	0.00E+00	0.00E+00	1.00E-02	0.00E+00	0.00E+00	0.00E+00	0.00E+00	3.00E-02	0.00E+00	1.00E-02	0.00E+00	1.00E-02
3/13/2011	1.40E-01	1.00E-02	1.30E-01	2.90E-01	4.00E-02	1.00E-02	1.00E-02	3.70E-01	4.00E-02	9.00E-02	1.00E-02	1.80E-01
3/14/2011	1.40E-01	1.00E-02	1.30E-01	2.90E-01	4.00E-02	1.00E-02	1.00E-02	3.70E-01	4.00E-02	9.00E-02	1.00E-02	1.80E-01
3/15/2011	3.80E-01	2.00E-02	3.50E-01	6.40E-01	1.10E-01	2.00E-02	2.00E-02	9.90E-01	1.10E-01	2.40E-01	3.00E-02	4.90E-01
3/16/2011	2.73E+00	1.60E-01	2.38E+00	3.02E+00	7.50E-01	1.10E-01	1.60E-01	6.86E+00	7.60E-01	1.64E+00	2.00E-01	3.41E+00
3/17/2011	1.09E+00	6.00E-02	9.70E-01	1.47E+00	3.10E-01	4.00E-02	7.00E-02	2.80E+00	3.10E-01	6.70E-01	8.00E-02	1.39E+00
3/18/2011	3.20E-01	2.00E-02	2.90E-01	5.60E-01	9.00E-02	1.00E-02	2.00E-02	8.30E-01	9.00E-02	2.00E-01	–	4.10E-01
3/19/2011	3.30E-01	2.00E-02	3.00E-01	5.70E-01	9.00E-02	1.00E-02	2.00E-02	8.60E-01	1.00E-01	2.00E-01	–	4.30E-01
3/20/2011	1.10E+00	6.00E-02	9.80E-01	1.48E+00	3.10E-01	4.00E-02	7.00E-02	2.82E+00	3.10E-01	6.70E-01	–	1.40E+00
3/21/2011	2.77E+01	1.65E+00	2.50E+01	4.20E+01	7.85E+00	1.13E+00	1.71E+00	7.20E+01	8.01E+00	1.72E+01	–	3.58E+01
3/22/2011	7.50E-01	6.00E-02	8.40E-01	1.80E+01	2.60E-01	4.00E-02	–	–	2.70E-01	5.70E-01	–	1.20E+00
3/23/2011	4.10E-01	3.00E-02	4.30E-01	9.27E+00	1.30E-01	2.00E-02	–	–	1.40E-01	2.90E-01	–	6.10E-01
3/24/2011	2.20E-01	1.00E-02	2.00E-01	3.59E+00	6.00E-02	1.00E-02	–	–	6.00E-02	1.40E-01	–	2.90E-01
3/25/2011	1.20E-01	1.00E-02	1.40E-01	4.50E-01	4.00E-02	1.00E-02	–	–	4.00E-02	1.00E-01	–	2.00E-01
3/26/2011	1.90E-01	1.00E-02	2.20E-01	6.50E-01	7.00E-02	1.00E-02	–	–	7.00E-02	1.50E-01	–	3.10E-01
3/27/2011	7.00E-02	0.00E+00	7.00E-02	1.50E-01	2.00E-02	0.00E+00	–	–	2.00E-02	5.00E-02	–	1.10E-01
3/28/2011	7.00E-02	0.00E+00	7.00E-02	3.20E-01	–	0.00E+00	–	–	2.00E-02	5.00E-02	–	1.00E-01
3/29/2011	3.10E-01	2.00E-02	2.90E-01	7.70E-01	–	1.00E-02	–	–	9.00E-02	2.00E-01	–	4.20E-01
3/30/2011	4.30E-01	2.00E-02	3.80E-01	3.20E-01	–	2.00E-02	–	–	1.20E-01	2.60E-01	–	5.40E-01
3/31/2011	2.12E+00	1.40E-01	2.12E+00	7.00E-01	–	1.00E-01	–	–	6.80E-01	1.45E+00	–	3.03E+00
4/1/2011	1.50E-01	1.00E-02	1.50E-01	1.00E-01	–	1.00E-02	–	–	5.00E-02	1.00E-01	–	2.20E-01
4/2/2011	1.00E-01	1.00E-02	1.00E-01	1.50E-01	–	0.00E+00	–	–	3.00E-02	7.00E-02	–	1.50E-01
4/3/2011	1.30E-01	1.00E-02	1.30E-01	1.30E-01	–	1.00E-02	–	–	4.00E-02	9.00E-02	–	1.80E-01
4/4/2011	2.40E-01	1.00E-02	2.20E-01	3.50E-01	–	1.00E-02	–	–	7.00E-02	1.50E-01	–	3.10E-01
4/5/2011	1.20E-01	1.00E-02	1.20E-01	1.30E-01	–	1.00E-02	–	–	4.00E-02	8.00E-02	–	1.70E-01

Date	Cs-134	Cs-136	Cs-137	I-131	I-133	La-140	Mo-99	Tc-99m	Te-129	Te-129m	Te-131m	Te-132
(Bq m ⁻³)												
4/6/2011	8.00E-02	1.00E-02	8.00E-02	1.20E-01	—	0.00E+00	—	—	3.00E-02	6.00E-02	—	1.20E-01
4/7/2011	1.50E-01	1.00E-02	1.40E-01	1.30E-01	—	1.00E-02	—	—	5.00E-02	1.00E-01	—	2.10E-01
4/8/2011	1.50E-01	1.00E-02	1.40E-01	1.20E-01	—	1.00E-02	—	—	5.00E-02	1.00E-01	—	2.10E-01
4/9/2011	9.00E-02	1.00E-02	9.00E-02	6.00E-02	—	0.00E+00	—	—	3.00E-02	6.00E-02	—	1.30E-01
4/10/2011	4.20E-01	3.00E-02	4.00E-01	2.10E-01	—	2.00E-02	—	—	1.30E-01	2.80E-01	—	5.70E-01
4/11/2011	1.40E-01	1.00E-02	1.30E-01	9.00E-02	—	1.00E-02	—	—	4.00E-02	9.00E-02	—	1.90E-01
4/12/2011	1.20E-01	1.00E-02	1.20E-01	6.00E-02	—	1.00E-02	—	—	4.00E-02	8.00E-02	—	1.70E-01
4/13/2011	8.00E-02	1.00E-02	8.00E-02	4.00E-02	—	0.00E+00	—	—	3.00E-02	6.00E-02	—	1.20E-01
4/14/2011	5.00E-02	0.00E+00	5.00E-02	4.00E-02	—	0.00E+00	—	—	2.00E-02	4.00E-02	—	8.00E-02
4/15/2011	4.00E-02	0.00E+00	5.00E-02	3.00E-02	—	0.00E+00	—	—	1.00E-02	3.00E-02	—	7.00E-02
4/16/2011	5.00E-02	0.00E+00	5.00E-02	2.00E-02	—	0.00E+00	—	—	2.00E-02	4.00E-02	—	8.00E-02
4/17/2011	1.20E-01	1.00E-02	1.20E-01	3.00E-02	—	1.00E-02	—	—	4.00E-02	8.00E-02	—	1.70E-01
4/18/2011	9.00E-01	5.00E-02	8.10E-01	5.30E-01	—	4.00E-02	—	—	2.60E-01	5.60E-01	—	1.16E+00
4/19/2011	3.10E-01	2.00E-02	2.90E-01	2.00E-01	—	1.00E-02	—	—	9.00E-02	2.00E-01	—	4.10E-01
4/20/2011	2.30E-01	1.00E-02	2.20E-01	1.00E-01	—	1.00E-02	—	—	7.00E-02	1.50E-01	—	3.10E-01
4/21/2011	2.00E-01	1.00E-02	1.90E-01	9.00E-02	—	1.00E-02	—	—	6.00E-02	1.30E-01	—	2.70E-01
4/22/2011	5.00E-02	0.00E+00	5.00E-02	2.00E-02	—	0.00E+00	—	—	2.00E-02	3.00E-02	—	—
4/23/2011	2.00E-02	0.00E+00	2.00E-02	0.00E+00	—	0.00E+00	—	—	1.00E-02	2.00E-02	—	—
4/24/2011	6.00E-02	0.00E+00	6.00E-02	1.00E-02	—	0.00E+00	—	—	2.00E-02	4.00E-02	—	—
4/25/2011	4.00E-02	0.00E+00	4.00E-02	1.00E-02	—	0.00E+00	—	—	1.00E-02	3.00E-02	—	—
4/26/2011	2.00E-02	0.00E+00	2.00E-02	1.00E-02	—	0.00E+00	—	—	1.00E-02	2.00E-02	—	—
4/27/2011	5.00E-02	0.00E+00	5.00E-02	1.00E-02	—	0.00E+00	—	—	1.00E-02	3.00E-02	—	—
4/28/2011	3.00E-02	0.00E+00	3.00E-02	0.00E+00	—	0.00E+00	—	—	1.00E-02	2.00E-02	—	—
4/29/2011	3.00E-02	0.00E+00	3.00E-02	0.00E+00	—	0.00E+00	—	—	1.00E-02	2.00E-02	—	—
4/30/2011	5.00E-02	0.00E+00	5.00E-02	1.00E-02	—	0.00E+00	—	—	2.00E-02	4.00E-02	—	—
5/1/2011	3.00E-02	0.00E+00	3.00E-02	0.00E+00	—	0.00E+00	—	—	1.00E-02	2.00E-02	—	—

Date	Cs-134	Cs-136	Cs-137	I-131	I-133	La-140	Mo-99	Tc-99m	Te-129	Te-129m	Te-131m	Te-132
(Bq m ⁻³)												
5/2/2011	2.00E-02	0.00E+00	2.00E-02	0.00E+00	–	0.00E+00	–	–	1.00E-02	2.00E-02	–	–
5/3/2011	1.70E-01	1.00E-02	1.70E-01	3.00E-02	–	1.00E-02	–	–	5.00E-02	1.10E-01	–	–
5/4/2011	1.00E-01	1.00E-02	1.00E-01	1.00E-02	–	0.00E+00	–	–	3.00E-02	7.00E-02	–	–
5/5/2011	4.50E-01	3.00E-02	4.40E-01	4.00E-02	–	2.00E-02	–	–	1.40E-01	3.10E-01	–	–
5/6/2011	6.00E-02	0.00E+00	6.00E-02	1.00E-02	–	0.00E+00	–	–	2.00E-02	4.00E-02	–	–
5/7/2011	3.00E-02	0.00E+00	3.00E-02	0.00E+00	–	0.00E+00	–	–	1.00E-02	2.00E-02	–	–
5/8/2011	3.00E-02	0.00E+00	3.00E-02	0.00E+00	–	0.00E+00	–	–	1.00E-02	2.00E-02	–	–
5/9/2011	3.00E-02	0.00E+00	3.00E-02	0.00E+00	–	0.00E+00	–	–	1.00E-02	2.00E-02	–	–
5/10/2011	4.00E-02	0.00E+00	3.00E-02	0.00E+00	–	0.00E+00	–	–	1.00E-02	2.00E-02	–	–
5/11/2011	5.00E-02	0.00E+00	3.00E-02	0.00E+00	–	0.00E+00	–	–	1.00E-02	2.00E-02	–	–

DC-2 Water Activity Concentration

Table DC-3 and Table DC-4 include water activity concentration data from measurements performed at Yokosuka Naval Base and Yokota Air Base, respectively. These tables contain data used for water ingestion dose calculations carried out for this report. However, as of April 2013, some data entries available through the MEXT website have been updated to generally lower values with no discernible change to the doses. Also, a value of 0 was used in the dose calculations for data reported as non-detectable (ND).

**Table DC-3. Water activity concentration measurement data
at Yokosuka Naval Base**

Date	I-131	Cs-134	Cs-137
(Bq L ⁻¹)			
3/11/2011	–	–	–
3/12/2011	–	–	–
3/13/2011	–	–	–
3/14/2011	–	–	–
3/15/2011	–	–	–
3/16/2011	–	–	–
3/17/2011	–	–	–
3/18/2011	–	–	–
3/19/2011	4.30E-01	ND	ND
3/20/2011	4.60E-01	ND	ND
3/21/2011	5.80E-01	ND	ND
3/22/2011	9.30E-01	ND	ND
3/23/2011	7.50E-01	ND	ND
3/24/2011	1.00E+00	ND	ND
3/25/2011	4.90E+00	ND	ND
3/26/2011	7.40E+00	ND	ND
3/27/2011	9.20E+00	ND	ND
3/28/2011	9.60E+00	ND	ND
3/29/2011	9.90E+00	ND	ND
3/30/2011	8.60E+00	ND	ND
3/31/2011	6.30E+00	ND	ND
4/1/2011	4.50E+00	ND	ND
4/2/2011	3.30E+00	ND	ND
4/3/2011	2.70E+00	ND	ND
4/4/2011	2.30E+00	ND	ND
4/5/2011	1.90E+00	ND	ND
4/6/2011	1.20E+00	ND	ND

Date	I-131	Cs-134	Cs-137
(Bq L ⁻¹)			
4/7/2011	1.10E+00	ND	ND
4/8/2011	5.30E-01	ND	ND
4/9/2011	5.40E-01	ND	ND
4/10/2011	6.50E-01	ND	ND
4/11/2011	ND	ND	ND
4/12/2011	5.20E-01	ND	ND
4/13/2011	ND	ND	ND
4/14/2011	ND	ND	ND
4/15/2011	ND	ND	ND
4/16/2011	ND	ND	ND
4/17/2011	ND	ND	ND
4/18/2011	ND	ND	ND
4/19/2011	ND	ND	ND
4/20/2011	ND	ND	ND
4/21/2011	ND	ND	ND
4/22/2011	ND	ND	ND
4/23/2011	ND	ND	ND
4/24/2011	ND	ND	ND
4/25/2011	ND	ND	ND
4/26/2011	ND	ND	ND
4/27/2011	ND	ND	ND
4/28/2011	ND	ND	ND
4/29/2011	ND	ND	ND
4/30/2011	ND	ND	ND
5/1/2011	ND	ND	ND
5/2/2011	ND	ND	ND
5/3/2011	ND	ND	ND
5/4/2011	ND	ND	ND
5/5/2011	ND	ND	ND
5/6/2011	ND	ND	ND
5/7/2011	ND	ND	ND
5/8/2011	ND	ND	ND
5/9/2011	ND	ND	ND
5/10/2011	ND	ND	ND
5/11/2011	ND	ND	ND

**Table DC-4. Water activity concentration measurement data
at Yokota Air Base**

Date	I-131	Cs-134	Cs-137
(Bq L⁻¹)			
3/11/2011	—	—	—
3/12/2011	—	—	—
3/13/2011	—	—	—
3/14/2011	—	—	—
3/15/2011	—	—	—
3/16/2011	—	—	—
3/17/2011	—	—	—
3/18/2011	1.50E+00	ND	ND
3/19/2011	2.90E+00	1.89E-01	2.10E-01
3/20/2011	2.90E+00	0.00E+00	0.00E+00
3/21/2011	5.30E+00	1.98E-01	2.20E-01
3/22/2011	1.90E+01	2.79E-01	3.10E-01
3/23/2011	2.60E+01	1.35E+00	1.50E+00
3/24/2011	2.60E+01	2.16E+00	2.40E+00
3/25/2011	3.20E+01	1.89E+00	2.10E+00
3/26/2011	3.70E+01	1.62E+00	1.80E+00
3/27/2011	2.00E+01	1.08E+00	1.20E+00
3/28/2011	9.80E+00	7.38E-01	8.20E-01
3/29/2011	5.60E+00	4.59E-01	5.10E-01
3/30/2011	5.10E+00	8.10E-01	9.00E-01
3/31/2011	3.40E+00	7.92E-01	8.80E-01
4/1/2011	2.10E+00	4.05E-01	4.50E-01
4/2/2011	2.00E+00	4.05E-01	4.50E-01
4/3/2011	2.90E+00	4.50E-01	5.00E-01
4/4/2011	3.80E+00	5.31E-01	5.90E-01
4/5/2011	2.60E+00	5.76E-01	6.40E-01
4/6/2011	1.63E+00	4.50E-01	5.00E-01
4/7/2011	1.40E+00	5.40E-01	6.00E-01
4/8/2011	7.90E-01	ND	ND
4/9/2011	1.00E+00	2.34E-01	2.60E-01
4/10/2011	7.10E-01	ND	ND
4/11/2011	6.00E-01	2.43E-01	2.70E-01
4/12/2011	5.70E-01	ND	ND
4/13/2011	4.10E-01	2.34E-01	2.60E-01
4/14/2011	4.10E-01	ND	ND

Date	I-131	Cs-134	Cs-137
(Bq L ⁻¹)			
4/15/2011	3.00E-01	ND	ND
4/16/2011	3.00E-01	ND	ND
4/17/2011	2.00E-01	ND	ND
4/18/2011	2.20E-01	1.89E-01	2.10E-01
4/19/2011	2.90E-01	ND	ND
4/20/2011	1.90E-01	ND	ND
4/21/2011	2.60E-01	ND	ND
4/22/2011	3.60E-01	3.69E-01	4.10E-01
4/23/2011	3.00E-01	1.80E-01	2.00E-01
4/24/2011	3.60E-01	ND	ND
4/25/2011	2.40E-01	2.88E-01	3.20E-01
4/26/2011	0.00E+00	ND	ND
4/27/2011	2.90E-01	ND	ND
4/28/2011	1.40E-01	ND	ND
4/29/2011	2.20E-01	ND	ND
4/30/2011	1.00E-01	ND	ND
5/1/2011	ND	ND	ND
5/2/2011	1.00E-01	ND	ND
5/3/2011	1.00E-01	ND	ND
5/4/2011	ND	ND	ND
5/5/2011	ND	ND	ND
5/6/2011	ND	ND	ND
5/7/2011	ND	ND	ND
5/8/2011	ND	ND	ND
5/9/2011	ND	ND	ND
5/10/2011	ND	ND	ND
5/11/2011	ND	ND	ND

DC-3 Soil Activity Concentration

Table DC-5, Table DC-6, and Table DC-7 include modeled soil activity concentration data used to calculate soil ingestion doses for Yokosuka Naval Base, Yokota Air Base, and Sendai, respectively. These tables contain data used for soil and dust ingestion dose calculations carried out for this report. A value of 0 was used in the dose calculations for data reported as non-detectable (ND).

Table DC-5. Modeled soil activity concentrations used for Yokosuka Naval Base

Date	I-131	Cs-134	Cs-137	Cs-136	Te-132
(pCi g ⁻¹)					
3/11/2011	0.00E+00	0.00E+00	0.00E+00	0.00E+00	0.00E+00
3/12/2011	0.00E+00	0.00E+00	0.00E+00	0.00E+00	0.00E+00
3/13/2011	0.00E+00	0.00E+00	0.00E+00	0.00E+00	0.00E+00
3/14/2011	0.00E+00	0.00E+00	0.00E+00	0.00E+00	0.00E+00
3/15/2011	0.00E+00	0.00E+00	0.00E+00	0.00E+00	0.00E+00
3/16/2011	0.00E+00	0.00E+00	0.00E+00	0.00E+00	0.00E+00
3/17/2011	0.00E+00	0.00E+00	0.00E+00	0.00E+00	0.00E+00
3/18/2011	0.00E+00	0.00E+00	0.00E+00	0.00E+00	0.00E+00
3/19/2011	0.00E+00	0.00E+00	0.00E+00	0.00E+00	0.00E+00
3/20/2011	3.65E+01	2.44E+00	2.79E+00	5.28E-01	3.23E+00
3/21/2011	7.30E+01	4.89E+00	5.59E+00	1.06E+00	6.45E+00
3/22/2011	6.70E+01	4.89E+00	5.59E+00	1.00E+00	5.21E+00
3/23/2011	6.15E+01	4.89E+00	5.59E+00	9.55E-01	4.21E+00
3/24/2011	5.64E+01	4.89E+00	5.59E+00	9.08E-01	3.40E+00
3/25/2011	5.17E+01	4.89E+00	5.59E+00	8.63E-01	2.75E+00
3/26/2011	4.75E+01	4.89E+00	5.59E+00	8.20E-01	2.22E+00
3/27/2011	4.35E+01	4.89E+00	5.59E+00	7.80E-01	1.80E+00
3/28/2011	4.00E+01	4.89E+00	5.59E+00	7.41E-01	1.45E+00
3/29/2011	3.67E+01	4.89E+00	5.59E+00	7.05E-01	1.17E+00
3/30/2011	3.36E+01	4.89E+00	5.59E+00	6.70E-01	9.47E-01
3/31/2011	3.08E+01	4.89E+00	5.59E+00	6.37E-01	7.65E-01
4/1/2011	2.83E+01	4.89E+00	5.59E+00	6.06E-01	6.18E-01
4/2/2011	2.60E+01	4.89E+00	5.59E+00	5.76E-01	4.99E-01
4/3/2011	2.38E+01	4.89E+00	5.59E+00	5.47E-01	4.04E-01
4/4/2011	2.19E+01	4.89E+00	5.59E+00	5.20E-01	3.26E-01
4/5/2011	2.00E+01	4.89E+00	5.59E+00	4.95E-01	2.63E-01
4/6/2011	1.84E+01	4.89E+00	5.59E+00	4.70E-01	2.13E-01
4/7/2011	1.69E+01	4.89E+00	5.59E+00	4.47E-01	1.72E-01
4/8/2011	1.55E+01	4.89E+00	5.59E+00	4.25E-01	1.39E-01
4/9/2011	1.42E+01	4.89E+00	5.59E+00	4.04E-01	1.12E-01

Date	I-131	Cs-134	Cs-137	Cs-136	Te-132
(pCi g ⁻¹)					
4/10/2011	1.30E+01	4.89E+00	5.59E+00	3.84E-01	9.07E-02
4/11/2011	1.20E+01	4.89E+00	5.59E+00	3.65E-01	7.33E-02
4/12/2011	1.10E+01	4.89E+00	5.59E+00	3.47E-01	5.92E-02
4/13/2011	1.01E+01	4.89E+00	5.59E+00	3.30E-01	4.78E-02
4/14/2011	9.23E+00	4.89E+00	5.59E+00	3.14E-01	3.87E-02
4/15/2011	8.47E+00	4.89E+00	5.59E+00	2.98E-01	3.12E-02
4/16/2011	7.77E+00	4.89E+00	5.59E+00	2.84E-01	2.52E-02
4/17/2011	7.13E+00	4.89E+00	5.59E+00	2.70E-01	2.04E-02
4/18/2011	6.54E+00	4.89E+00	5.59E+00	2.56E-01	1.65E-02
4/19/2011	6.00E+00	4.89E+00	5.59E+00	2.44E-01	1.33E-02
4/20/2011	5.50E+00	4.89E+00	5.59E+00	2.32E-01	1.08E-02
4/21/2011	5.05E+00	4.89E+00	5.59E+00	2.20E-01	8.69E-03
4/22/2011	4.63E+00	4.89E+00	5.59E+00	2.09E-01	7.02E-03
4/23/2011	4.25E+00	4.89E+00	5.59E+00	1.99E-01	5.67E-03
4/24/2011	3.90E+00	4.89E+00	5.59E+00	1.89E-01	4.58E-03
4/25/2011	3.58E+00	4.89E+00	5.59E+00	1.80E-01	3.70E-03
4/26/2011	3.28E+00	4.89E+00	5.59E+00	1.71E-01	2.99E-03
4/27/2011	3.01E+00	4.89E+00	5.59E+00	1.63E-01	2.42E-03
4/28/2011	2.76E+00	4.89E+00	5.59E+00	1.55E-01	1.95E-03
4/29/2011	2.53E+00	4.89E+00	5.59E+00	1.47E-01	1.58E-03
4/30/2011	2.32E+00	4.89E+00	5.59E+00	1.40E-01	1.28E-03
5/1/2011	2.13E+00	4.89E+00	5.59E+00	1.33E-01	1.03E-03
5/2/2011	1.96E+00	4.89E+00	5.59E+00	1.26E-01	8.32E-04
5/3/2011	1.79E+00	4.89E+00	5.59E+00	1.20E-01	6.73E-04
5/4/2011	1.65E+00	4.89E+00	5.59E+00	1.14E-01	5.43E-04
5/5/2011	1.51E+00	4.89E+00	5.59E+00	1.08E-01	4.39E-04
5/6/2011	1.39E+00	4.89E+00	5.59E+00	1.03E-01	3.55E-04
5/7/2011	1.27E+00	4.89E+00	5.59E+00	9.80E-02	2.87E-04
5/8/2011	1.17E+00	4.89E+00	5.59E+00	9.32E-02	2.32E-04
5/9/2011	1.07E+00	4.89E+00	5.59E+00	8.86E-02	1.87E-04
5/10/2011	9.82E-01	4.89E+00	5.59E+00	8.42E-02	1.51E-04
5/11/2011	9.00E-01	4.89E+00	5.59E+00	8.01E-02	1.22E-04

Table DC-6. Modeled soil activity concentrations used for Yokota Air Base

Date	I-131	Cs-134	Cs-137	Cs-136	Te-132
(pCi g ⁻¹)					
3/11/2011	0.00E+00	0.00E+00	0.00E+00	0.00E+00	0.00E+00
3/12/2011	0.00E+00	0.00E+00	0.00E+00	0.00E+00	0.00E+00
3/13/2011	0.00E+00	0.00E+00	0.00E+00	0.00E+00	0.00E+00
3/14/2011	0.00E+00	0.00E+00	0.00E+00	0.00E+00	0.00E+00
3/15/2011	0.00E+00	0.00E+00	0.00E+00	0.00E+00	0.00E+00
3/16/2011	0.00E+00	0.00E+00	0.00E+00	0.00E+00	0.00E+00
3/17/2011	0.00E+00	0.00E+00	0.00E+00	0.00E+00	0.00E+00
3/18/2011	0.00E+00	0.00E+00	0.00E+00	0.00E+00	0.00E+00
3/19/2011	0.00E+00	0.00E+00	0.00E+00	0.00E+00	0.00E+00
3/20/2011	2.67E+01	1.66E+00	1.94E+00	4.28E-01	1.00E+01
3/21/2011	5.33E+01	3.32E+00	3.88E+00	8.56E-01	8.11E+00
3/22/2011	4.90E+01	3.32E+00	3.88E+00	8.14E-01	6.56E+00
3/23/2011	4.50E+01	3.32E+00	3.88E+00	7.74E-01	5.30E+00
3/24/2011	4.14E+01	3.32E+00	3.88E+00	7.36E-01	4.28E+00
3/25/2011	3.80E+01	3.32E+00	3.88E+00	6.99E-01	3.46E+00
3/26/2011	3.49E+01	3.32E+00	3.88E+00	6.65E-01	2.79E+00
3/27/2011	3.21E+01	3.32E+00	3.88E+00	6.32E-01	2.26E+00
3/28/2011	2.95E+01	3.32E+00	3.88E+00	6.01E-01	1.82E+00
3/29/2011	2.71E+01	3.32E+00	3.88E+00	5.71E-01	1.47E+00
3/30/2011	2.49E+01	3.32E+00	3.88E+00	5.43E-01	1.19E+00
3/31/2011	2.29E+01	3.32E+00	3.88E+00	5.16E-01	9.62E-01
4/1/2011	2.10E+01	3.32E+00	3.88E+00	4.91E-01	7.77E-01
4/2/2011	1.93E+01	3.32E+00	3.88E+00	4.67E-01	6.28E-01
4/3/2011	1.78E+01	3.32E+00	3.88E+00	4.44E-01	5.07E-01
4/4/2011	1.63E+01	3.32E+00	3.88E+00	4.22E-01	4.10E-01
4/5/2011	1.50E+01	3.32E+00	3.88E+00	4.01E-01	3.31E-01
4/6/2011	1.38E+01	3.32E+00	3.88E+00	3.81E-01	2.68E-01
4/7/2011	1.27E+01	3.32E+00	3.88E+00	3.62E-01	2.16E-01
4/8/2011	1.16E+01	3.32E+00	3.88E+00	1.70E-01	1.75E-01
4/9/2011	1.07E+01	3.32E+00	3.88E+00	1.61E-01	1.41E-01
4/10/2011	9.83E+00	3.32E+00	3.88E+00	1.53E-01	1.14E-01
4/11/2011	9.04E+00	3.32E+00	3.88E+00	1.46E-01	9.22E-02
4/12/2011	8.30E+00	3.32E+00	3.88E+00	1.39E-01	7.45E-02
4/13/2011	7.63E+00	3.32E+00	3.88E+00	1.32E-01	6.02E-02
4/14/2011	7.01E+00	3.32E+00	3.88E+00	1.25E-01	4.86E-02
4/15/2011	6.44E+00	3.32E+00	3.88E+00	1.19E-01	3.93E-02

Date	I-131	Cs-134	Cs-137	Cs-136	Te-132
(pCi g ⁻¹)					
4/16/2011	5.92E+00	3.32E+00	3.88E+00	1.13E-01	3.17E-02
4/17/2011	5.44E+00	3.32E+00	3.88E+00	1.08E-01	2.56E-02
4/18/2011	5.00E+00	3.32E+00	3.88E+00	1.02E-01	2.07E-02
4/19/2011	4.60E+00	3.32E+00	3.88E+00	9.73E-02	1.67E-02
4/20/2011	4.22E+00	3.32E+00	3.88E+00	9.25E-02	1.35E-02
4/21/2011	3.88E+00	3.32E+00	3.88E+00	8.79E-02	1.09E-02
4/22/2011	3.57E+00	3.32E+00	3.88E+00	8.36E-02	8.83E-03
4/23/2011	3.28E+00	3.32E+00	3.88E+00	7.95E-02	7.13E-03
4/24/2011	3.01E+00	3.32E+00	3.88E+00	7.55E-02	5.76E-03
4/25/2011	2.77E+00	3.32E+00	3.88E+00	7.18E-02	4.66E-03
4/26/2011	2.54E+00	3.32E+00	3.88E+00	6.83E-02	3.76E-03
4/27/2011	2.34E+00	3.32E+00	3.88E+00	6.49E-02	3.04E-03
4/28/2011	2.15E+00	3.32E+00	3.88E+00	6.17E-02	2.46E-03
4/29/2011	1.97E+00	3.32E+00	3.88E+00	5.87E-02	1.98E-03
4/30/2011	1.81E+00	3.32E+00	3.88E+00	5.58E-02	1.60E-03
5/1/2011	1.67E+00	3.32E+00	3.88E+00	5.30E-02	1.30E-03
5/2/2011	1.53E+00	3.32E+00	3.88E+00	5.04E-02	1.05E-03
5/3/2011	1.41E+00	3.32E+00	3.88E+00	4.79E-02	8.46E-04
5/4/2011	1.29E+00	3.32E+00	3.88E+00	4.55E-02	6.83E-04
5/5/2011	1.19E+00	3.32E+00	3.88E+00	4.33E-02	5.52E-04
5/6/2011	1.09E+00	3.32E+00	3.88E+00	4.12E-02	4.46E-04
5/7/2011	1.00E+00	3.32E+00	3.88E+00	3.91E-02	3.60E-04
5/8/2011	9.23E-01	3.32E+00	3.88E+00	3.72E-02	2.91E-04
5/9/2011	8.48E-01	3.32E+00	3.88E+00	3.54E-02	2.35E-04
5/10/2011	7.79E-01	3.32E+00	3.88E+00	3.36E-02	1.90E-04
5/11/2011	7.16E-01	3.32E+00	3.88E+00	3.20E-02	1.54E-04

Table DC-7. Modeled soil activity concentrations used for Sendai locations

Date	I-131	Cs-134	Cs-137	Cs-136	Te-132 ¹
(pCi g ⁻¹)					
3/11/2011	0.00E+00	0.00E+00	0.00E+00	0.00E+00	0.00E+00
3/12/2011	0.00E+00	0.00E+00	0.00E+00	0.00E+00	0.00E+00
3/13/2011	0.00E+00	0.00E+00	0.00E+00	0.00E+00	0.00E+00
3/14/2011	0.00E+00	0.00E+00	0.00E+00	0.00E+00	0.00E+00
3/15/2011	0.00E+00	0.00E+00	0.00E+00	0.00E+00	0.00E+00
3/16/2011	0.00E+00	0.00E+00	0.00E+00	0.00E+00	0.00E+00
3/17/2011	0.00E+00	0.00E+00	0.00E+00	0.00E+00	0.00E+00
3/18/2011	0.00E+00	0.00E+00	0.00E+00	0.00E+00	0.00E+00
3/19/2011	0.00E+00	0.00E+00	0.00E+00	0.00E+00	0.00E+00
3/20/2011	1.86E+01	2.22E+00	2.21E+00	1.70E+00	4.32E+00
3/21/2011	3.72E+01	4.43E+00	4.41E+00	3.40E+00	8.64E+00
3/22/2011	3.41E+01	4.43E+00	4.41E+00	3.23E+00	6.98E+00
3/23/2011	3.14E+01	4.43E+00	4.41E+00	3.07E+00	5.64E+00
3/24/2011	2.88E+01	4.43E+00	4.41E+00	2.92E+00	4.56E+00
3/25/2011	2.65E+01	4.43E+00	4.41E+00	2.78E+00	3.68E+00
3/26/2011	2.44E+01	4.43E+00	4.41E+00	2.64E+00	2.97E+00
3/27/2011	2.24E+01	4.43E+00	4.41E+00	2.51E+00	2.40E+00
3/28/2011	2.06E+01	4.43E+00	4.41E+00	2.39E+00	1.94E+00
3/29/2011	1.89E+01	4.43E+00	4.41E+00	2.27E+00	1.57E+00
3/30/2011	1.74E+01	4.43E+00	4.41E+00	2.16E+00	1.27E+00
3/31/2011	1.60E+01	4.43E+00	4.41E+00	2.05E+00	1.02E+00
4/1/2011	1.47E+01	4.43E+00	4.41E+00	1.95E+00	8.28E-01
4/2/2011	1.35E+01	4.43E+00	4.41E+00	1.85E+00	6.69E-01
4/3/2011	1.24E+01	4.43E+00	4.41E+00	1.76E+00	5.40E-01
4/4/2011	1.14E+01	4.43E+00	4.41E+00	1.67E+00	4.36E-01
4/5/2011	1.05E+01	4.43E+00	4.41E+00	1.59E+00	3.53E-01
4/6/2011	9.61E+00	4.43E+00	4.41E+00	1.51E+00	2.85E-01
4/7/2011	8.83E+00	4.43E+00	4.41E+00	1.44E+00	2.30E-01
4/8/2011	8.12E+00	4.43E+00	4.41E+00	1.37E+00	1.86E-01
4/9/2011	7.46E+00	4.43E+00	4.41E+00	1.30E+00	1.50E-01
4/10/2011	6.86E+00	4.43E+00	4.41E+00	1.24E+00	1.21E-01
4/11/2011	6.30E+00	4.43E+00	4.41E+00	1.17E+00	9.81E-02
4/12/2011	5.79E+00	4.43E+00	4.41E+00	1.12E+00	7.93E-02
4/13/2011	5.32E+00	4.43E+00	4.41E+00	1.06E+00	6.41E-02
4/14/2011	4.89E+00	4.43E+00	4.41E+00	1.01E+00	5.18E-02
4/15/2011	4.49E+00	4.43E+00	4.41E+00	9.60E-01	4.18E-02
4/16/2011	4.13E+00	4.43E+00	4.41E+00	9.12E-01	3.38E-02
4/17/2011	3.79E+00	4.43E+00	4.41E+00	8.67E-01	2.73E-02

Date	I-131	Cs-134	Cs-137	Cs-136	Te-132¹
(pCi g⁻¹)					
4/18/2011	3.49E+00	4.43E+00	4.41E+00	8.25E-01	2.21E-02
4/19/2011	3.20E+00	4.43E+00	4.41E+00	7.84E-01	1.78E-02
4/20/2011	2.94E+00	4.43E+00	4.41E+00	7.45E-01	1.44E-02
4/21/2011	2.71E+00	4.43E+00	4.41E+00	7.08E-01	1.16E-02
4/22/2011	2.49E+00	4.43E+00	4.41E+00	6.73E-01	9.40E-03
4/23/2011	2.28E+00	4.43E+00	4.41E+00	6.40E-01	7.59E-03
4/24/2011	2.10E+00	4.43E+00	4.41E+00	6.09E-01	6.14E-03
4/25/2011	1.93E+00	4.43E+00	4.41E+00	5.79E-01	4.96E-03
4/26/2011	1.77E+00	4.43E+00	4.41E+00	5.50E-01	4.01E-03
4/27/2011	1.63E+00	4.43E+00	4.41E+00	5.23E-01	3.24E-03
4/28/2011	1.50E+00	4.43E+00	4.41E+00	4.97E-01	2.61E-03
4/29/2011	1.38E+00	4.43E+00	4.41E+00	4.73E-01	2.11E-03
4/30/2011	1.26E+00	4.43E+00	4.41E+00	4.49E-01	1.71E-03
5/1/2011	1.16E+00	4.43E+00	4.41E+00	4.27E-01	1.38E-03
5/2/2011	1.07E+00	4.43E+00	4.41E+00	4.06E-01	1.11E-03
5/3/2011	9.81E-01	4.43E+00	4.41E+00	3.86E-01	9.00E-04
5/4/2011	9.02E-01	4.43E+00	4.41E+00	3.67E-01	7.27E-04
5/5/2011	8.29E-01	4.43E+00	4.41E+00	3.49E-01	5.88E-04
5/6/2011	7.62E-01	4.43E+00	4.41E+00	3.32E-01	4.75E-04
5/7/2011	7.00E-01	4.43E+00	4.41E+00	3.15E-01	3.84E-04
5/8/2011	6.43E-01	4.43E+00	4.41E+00	3.00E-01	3.10E-04
5/9/2011	5.91E-01	4.43E+00	4.41E+00	2.85E-01	2.50E-04
5/10/2011	5.43E-01	4.43E+00	4.41E+00	2.71E-01	2.02E-04
5/11/2011	4.99E-01	4.43E+00	4.41E+00	2.58E-01	1.64E-04

Abbreviations, Acronyms, and Unit Symbols

AB	air base
AIPH	Army Institute of Public Health
AMAD	activity median aerodynamic diameter
ATUS	American Time Use Survey
Ba	barium
Bq	becquerel
CHAD	Consolidated Human Activity Database
cpd	cumulative probability distribution
Cs	cesium
d	day
DARWG	DOD Dose Assessment and Recording Working Group
DC	dose coefficient
DOD	Department of Defense
DOE	Department of Energy
DOL	Department of Labor
DTRA	Defense Threat Reduction Agency
EFH	Exposure Factors Handbook
FDNPS	Fukushima Daiichi Nuclear Power Station
ft	feet
g	gram
GM	geometric mean
GOJ	Government of Japan
GSD	geometric standard deviation
Gy	gray
h	hour
I	iodine
ICRP	International Commission on Radiological Protection
IDRF	indoor dose reduction factor
IMS	International Monitoring Station
JGDSF	Japanese Ground Self-Defense Forces

JST	Japan Standard Time
km	kilometer
L	liter
La	Lanthanum
LCE	Logistics Combat Element
ln	natural logarithm
MEXT	Ministry of Education, Culture, Sports, Science & Technology
m	meter
MDA	minimum detectable activity
mi	mile
min	minute
Mo	molybdenum
mSv	millisievert
NAF	naval air facility
NB	naval base
NCRP	National Council on Radiation Protection and Measurements
ND	not detected
nGy	nanogray
NIST	National Institute of Standards and Technology
NTPR	Nuclear Test Personnel Review
OTR	Operation Tomodachi Registry
pdf	probability density function
PEP	potentially exposed population
POI	population of interest
Rh	rhodium
Ru	ruthenium
SD	standard deviation
SIF	structure infiltration factor
SM	standard method
SOP	standard operating procedure
SO _x	sulfur oxides
SPEEDI	System for Prediction of Environment Emergency Dose Information
Sr	strontium
Sv	sievert
Tc	technetium

Te	tellurium
UA	uncertainty analysis
USEPA	U.S. Environmental Protection Agency

**DISTRIBUTION LIST
DTRA-TR-12-2**

DEPARTMENT OF DEFENSE

DEFENSE TECHNICAL
INFORMATION CENTER
8725 JOHN J. KINGMAN ROAD,
SUITE 0944
FT. BELVOIR, VA 22060-6201
ATTN: DTIC/OCA

DEFENSE THREAT REDUCTION
AGENCY
8725 JOHN J. KINGMAN ROAD
STOP 6201
FT. BELVOIR, VA 22060-6201
ATTN: P. BLAKE

**DEPARTMENT OF DEFENSE
CONTRACTORS**

EXELIS, INC.
1680 TEXAS STREET, SE
KIRTLAND AFB, NM 87117-5669
ATTN: DTRIAC